Arthropod Structure & Development 85 (2025) 101409

Contents lists available at ScienceDirect

Arthropod Structure & Development

journal homepage: www.elsevier.com/locate/asd

The first detailed morphological treatment of a Cretaceous psocid and the character evolution of Trogiomorpha (Insecta: Psocodea)

Michael Weingardt [a, *], Feiyang Liang [b], Brendon E. Boudinot [a, c, d], Jörg U. Hammel [e], Bernhard L. Bock [a], Kazunori Yoshizawa [f], Rolf G. Beutel [a]

[a] Friedrich-Schiller-Universität Jena. Institute of Zoology and Evolutionary Research, Entomology Group, Erbertstraße 1, 07743, Jena, Germany
[b] Key Laboratory of Economic Crops Genetic Improvement and Integrated Utilization, School of Life Science, Hunan University of Science and Technology, Xiangtan, 411201, China
[c] Senckenberg Naturmuseum Frankfurt, Senckenberganlage 25, 60325, Frankfurt, Germany
[d] National Museum of Natural History, Smithsonian Institution, 10th & Constitution Ave. NW, Washington, DC, USA
[e] Institute of Materials Physics, Helmholtz-Zentrum Hereon, Max-Planck-Straße 1, 21502, Geesthacht, Germany
[f] Systematic Entomology, School of Agriculture, Hokkaido University, Sapporo, Japan

ARTICLE INFO

Article history:
Received 23 October 2024
Received in revised form
1 January 2025
Accepted 2 January 2025
Available online 19 February 2025

Handling Editor: B. Beltz

Keywords:
Ancestral state estimation
Burmese amber
Character evolution
Cybertype
Micro computed tomography (μCT)
Phylogeny

ABSTRACT

While new fossil psocid taxa are described every year, the morphology is generally not studied and documented in sufficient detail, limiting our understanding of the character evolution in this order. A new fossil species of the genus *Psyllipsocus* from mid-Cretaceous Kachin amber is described and its morphology reconstructed in detail using synchrotron-radiation micro-computed tomography (SR-μ-CT). We present the first cybertype of a Cretaceous fossil psocid. We also describe and discuss the putative evolution of previously unrecognized and underestimated exoskeletal characters for the suborder Trogiomorpha. Additionally, using our new observations, we critically evaluate the phylogeny of Trogiomorpha and the character evolution in this group. We also present a modified character matrix which we analyze using Bayesian inference and parsimony. Based on our results and previous studies we propose monophyletic Trogiomorpha *s.l.* (incl. †*Brachyantennum*) and Trogiomorpha *s. str.* (possibly incl. †Cormopsocidae), the latter comprising Prionoglarididae and monophyletic Spinaprocta. Spinaprocta contain Atropetae and Psyllipsocetae (incl. *Psyllipsocus*) as sister taxa. Some relationships on the genus level in Trogiomorpha are still strongly disputed and unclear. Here, we synonymize the extinct monotypic genus †*Khatangia* with *Psyllipsocus* and discuss the systematic position of †*Sinopsyllipsocus*, †*Parapsyllipsocus*, †*Empheriopsis* and †*Concavapsocus*. A key for all extinct species of Psyllipsocidae is provided.

1. Introduction

Whereas extant species of "Psocoptera", the non-parasitic grade of the order Psocodea, are presently only investigated by few researchers, fossils of the group have long fascinated palaeoentomologists (e.g., Pictet, 1854; Hagen, 1865; Enderlein, 1911; Roesler, 1943; Vishnyakova, 1975; Yoshizawa and Lienhard, 2020). Even the writer, poet, and naturalist Hermann Loens was perplexed by small psocids in amber with wings covered with scales (Amphientomidae) and also by tiny beetle-like species (Sphaeropsocidae). He called them a turntable of insects, potentially reducing the insect systematists studying them to tears (Löns, 1911). Recently, the understudied Psocodea came into the focus of insect systematics, as they are either the sister group of the Condylognatha (Thysanoptera+Hemiptera) or of the megadiverse Holometabola (Misof et al., 2014; Johnson et al., 2018). This key position in the insect tree of life inspired insect systematists to study their phylogeny (e.g., de Moya et al., 2021), anatomy (e.g., Cheng and Yoshizawa, 2022; Cheng et al., 2023), and behavior (e.g., Yoshizawa et al., 2014, 2018) using modern methods. Until now, micro-computed tomography (μ-CT) has only been applied to one (sub-) fossil species of this phylogenetically important order,

* Corresponding author.
E-mail addresses: michael.weingardt@uni-jena.de, michael.weingardt@gmx.net (M. Weingardt).

https://doi.org/10.1016/j.asd.2025.101409

‡*Amphientomum knorrei* Weingardt, Bock & Boudinot, 2024 (in Boudinot et al., 2024). More broadly, μ-CT technology is now becoming a standard tool of palaeontology, revealing previously unconceivable details of anatomy (e.g., Pohl et al., 2010; Solórzano-Kraemer et al., 2014; Richter et al., 2022) or the biology (e.g., Boudinot et al., 2022) of extinct insects.

The study of fossils greatly enhances the reconstruction of character evolution, as they are the only direct evidence of evolutionary changes on the phenotypic level in the dimension of time. Of special importance are fossil psocids of the mid-Cretaceous period due to their frequent exceptional preservation and old age. Only recently a new psocodean family, the †Cormopsocidae (Yoshizawa and Lienhard, 2020), was described from Cretaceous Kachin amber. The authors suggested that this extinct group has preserved the maximum number of plesiomorphies among all families in Psocodea. As our current understanding of the early psocodean evolution is fragmentary at best, it is important to study the morphology of fossils in greater detail. This applies especially to species of families with many apparent plesiomorphies, such as the †Cormopsocidae and Prionoglarididae, but also the Psyllipsocidae, the only family of Psocodea with a genus (*Psyllipsocus*) surviving as a diagnostic unit since the mid-Cretaceous (minimum age of 99 million years) (Mockford et al., 2013; Álvarez-Parra et al., 2020; Lienhard et al., 2022). Studying the morphology of fossils of these "ancestral" groups and comparisons with extant taxa will greatly contribute to reconstruct the groundplan and character evolution of Psocodea.

The Psyllipsocidae themselves are a relatively species-poor family of trogiomorphan psocids (barklice) with approximately 90 described species (Mockford, 2018; Lienhard et al., 2022). Four extant genera are currently known, *Psyllipsocus* Selys-Longchamps, 1872, *Dorypteryx* Aaron, 1883, *Pseudorypteryx* García-Aldrete, 1984, and *Psocathropos* Ribaga, 1899. The genus *Pseudopsyllispsocus* Li, 2002, previously placed in Psyllipsocidae (Li, 2002), likely belongs to the Lepidopsocidae (Mockford, 2011), a family of trogiomorphan barklice in the infraorder Atropetae, usually characterized by a vestiture of scales. Additionally, four extinct genera are recognized, †*Annulipsyllipsocus* Hakim, Azar, Maksoud, Huang & Azar, 2018, †*Concavapsocus* Wang, Li, Ren & Yao, 2019 (and by extension also †*Globopsocus* Azar & Engel, 2008), †*Khatangia* Vishnyakova, 1975 and †*Sinopsyllipsocus* Zhang, Nel, Azar & Wang, 2016 (Liang and Liu, 2021; Hopkins et al., 2024). These fossil representatives of Psyllipsocidae are known from different Cretaceous deposits, including Lebanese amber (Grimaldi and Engel, 2005; Mockford et al., 2013), Burmese amber (=Burmite) (Hakim et al., 2018; Álvarez-Parra et al., 2020; Jouault et al., 2021; Liang and Liu, 2021), and amber from Siberia (Vishnyakova, 1975). They also occur in amber of the French (Nel et al., 2005) and Chinese Eocene (Zhang et al., 2016), and further in Mexican (Mockford, 1969) and Dominican Miocene amber (Mockford, 2011). Surprisingly, no species of *Psyllipsocus* is known from Baltic amber, which is the best studied and most species-rich Eocene deposit for Psocodea (Enderlein, 1911; see Psocodea Species File: Hopkins et al., 2024). Several problematic fossils placed in Psyllipsocidae likely belong to other families or their placement is unclear. Examples are †*Libanopsyllipsocus alexanderasnitsyni* Azar & Nel, 2011 (Mockford et al., 2013) as a member of the troctomorphan family Pachytroctidae and †*Parapsyllipsocus vergereaui* Perrichot, Azar, Néraudeau & Nel, 2003 with an uncertain position in Trogiomorpha.

We examined four specimens of a new fossil species of *Psyllipsocus* from Cretaceous Kachin amber and two extant species of Trogiomorpha using photomicrographs, synchrotron radiation μ-CT scans, and 3D reconstructions. Our goal was to study the external morphology in as much detail as possible using these methods, especially the morphology of the thorax. This tagma is often neglected in descriptions but possibly contains a plethora of characters with phylogenetical signal. Additionally, we reworked the character matrix assembled by Li et al. (2022) and added more characters for future phylogenetic analyses on Trogiomorpha. This allowed us to discuss the character evolution in Trogiomorpha in more detail, estimate a phylogeny based only on these characters using Bayesian inference and parsimony, and identify large gaps of information that have to be filled in future morphological investigations.

2. Material and methods

2.1. Preparation and origin of amber material

Four individual amber pieces were used for this study. The holotype **PMJ Pa 6101** and paratype **SMF Be 14667**; the holotype specimen is currently stored in the Phyletisches Museum Jena (Thuringia, Germany). The paratype **SMF Be 14667** will be deposited in the collection of the Section Amber Research in the Senckenberg Research and Natural History Museum Frankfurt am Main (Hesse, Germany). The paratypes **CAU-BA-LFY-24001** and **CAU-BA-LFY-24002** are currently stored in Hunan University of Science and Technology (Xiangtan; China) and will eventually be deposited in the Entomological Museum of the China Agricultural University (CAU) in Beijing, China.

The amber piece containing the holotype **PMJ Pa 6101** and the paratype **SMF Be 14667** were ground using quadratic pieces of sand paper with decreasing granularity of 150, 400, 1200, 2000, 3000 and 5000. For the final step, we used a piece of cloth and Colgate® toothpaste for polishing.

Burmese amber (Kachin amber, Burmite) is based on fossilized resin of Cretaceous origin from mines of northern Myanmar (Shi et al., 2012). They have been dated to the Cenomanian age of ca. 98.8 mya (Shi et al., 2012). The exact locality of where the amber pieces **PMJ Pa 6101** and **SMF Be 14667** came from is unknown and verified as Kachin amber by comparing them to the specimens **CAU-BA-LFY-24001** and **CAU-BA-LFY-24002** and performing FR-IR analysis (see below and supplementary file S1).

To obtain additional information on the amber, we sent small fractions of the amber piece (**PMJ Pa 6101**) to the "International Amber Association" in Gdansk, Poland for IR-spectroscopy (see Boudinot et al., 2024 for details). The results of this analysis confirm that it is Cretaceous burmite (see supplementary file S1).

2.2. Extant taxa

Two specimens of trogiomorphan barklice were collected by the first author. Both species were determined using keys in Lienhard (1998). A single male of *Dorypteryx domestica* (Smithers, 1958) (Psyllipsocetae: Psyllipsocidae) was collected on the 05.X.2023 inside of the Phyletisches Museum (Jena, Germany). The specimen was stored in 70 % Ethanol and transferred to 100 % Ethanol via a stepwise ethanol series. One single female of *Cerobasis guestfalica* (Kolbe, 1880) (Atropetae: Trogiidae) was collected in Thuringia (Germany) in the vicinity of Kunitz by beating it from a shrub of the genus *Crataegus* sp. on the 27.VI.2021. The specimen was also stored in 70 % Ethanol and transferred to 100 % Ethanol via a stepwise ethanol series. No collection permit was necessary. Both specimens are stored in the Phyletisches Museum (Jena, Germany).

2.3. Microphotography

The amber pieces were mounted on a microscope slide and fixed with putty. On the upper surface a small droplet of distilled water was pipetted, and a thin cover glass was placed on top. Improved illumination was achieved with an Euromex LE.5211-230 cold light

source (Euromex, Papenkamp, Netherlands) attached with three gooseneck lamps.

Manual photographs in the z-axis were taken at the Museum für Naturkunde Berlin (Germany) using a Zeiss Axioscope 5 with a Zeiss Achromat S 1,0 FWD 63 (Carl Zeiss AG, Oberkochen, Germany) and a mounted Canon EOS 80D (Canon, Krefeld, Germany) via a T2-T2 1.6x SLR tube. As the holotype specimen was too large for a single overview shot, the photograph was stitched using four single stacked shots in the xy-axes using Photoshop (v.24.1.0) (Adobe, San Jose, USA).

For **CAU-BA-LFY-24001** and **CAU-BA-LFY-24002** photographs were taken using a Sony Alpha 7III (Sony Corp., Tokyo, Japan) digital camera mounted on an Olympus CX-33 (Olympus, Tokyo, Japan).

Photographs were processed in Adobe Lightroom Classic (v. 11.5) (Adobe in San Jose, USA) as tif stacks. Individual photos underwent denoising using the standard option through Topaz DeNoize AI (Topaz Labs in Dallas, USA), and were afterwards merged using Zerene Stacker (v. 1.04) (Zerene System LLC in Richland, USA). The final plates were created using Adobe Photoshop (v. 24.1.0) and Adobe Illustrator (v. 27.2) (both Adobe, San Jose, USA).

2.4. SR-μCT scan

The holotype of †*Psyllipsocus mili* **sp. nov.** Weingardt, Liang & Yoshizawa **sp. nov.** was scanned at the imaging beamline P05 of storage ring PETRA III (Haibel et al., 2010; Greving et al., 2014; Wilde et al., 2016) at DESY (Hamburg, Germany) with the ID "fsu_122_d_174 (CASENT0753247)" on 19.X.2022. The parameters of the scan were as follows: effective pixel size (binned) 0.913 μm, photon energy of ca. 18 keV, sample to detector distances of 50 mm, using a 50 MP CMOS camera system, 4001 projections, exposure time of 350 ms.

Two additional trogiomorphan species: *D. domestica* (FSU_240_MW_Pso_18_1_10_2023) and *C. guestfalica* (FSU_258_MW_Pso_26_22_10_2023) were scanned on the 11.X.2023 at the same facility. The parameters for both scans are as follows: effective pixel size (binned) 1.285 μm, photon energy of ca. 18 keV, sample to detector distance of 100 mm, using a 20 MP CMOS camera system (Lytaev et al., 2014), 3501 projections, exposure time of 250 ms.

2.5. Computer-based 3D reconstruction

Before segmentation, the scans were cropped, sampled, and transformed to 8 bit using Fiji (Schindelin et al., 2012) and Dragonfly (Object Research Systems, Montreal, Quebec, Canada). The segmentation was performed using Amira Ver. 6.0.1 and 6.1.1 (Thermo Fisher Scientific, Hillsboro, USA). After segmentation, the materials were exported as tif stacks using the Amira macro "Multi Export" (Engelkes et al., 2018). For 3D Phong rendering, we used VGStudio Max Ver. 3.4 (Volume Graphics, Germany). The final renders are presented in central perspective (24°), while renders in parallel perspective were used to create scale bars.

2.6. Plates

The final plates (including the phylogenetic trees) were created using Adobe Photoshop (v. 24.1.0) (preparation of image plates) and Adobe Illustrator (v. 27.2) (for lettering and finalizing) (both Adobe Systems Incorporated, San Jose, CA, USA).

2.7. Interactive 3D Model

The Amira macro "Multi Export" (Engelkes et al., 2018) was used to create isosurfaces for each segmented material, which were then imported into Blender 3.6.5 (Amsterdam, Netherlands). The created models were uploaded to Sketchfab (New York, USA; Paris, France). Important characters were visualized using the annotation function of Sketchfab. The interactive 3D model of †*P. mili* **sp. nov.** (**PMJ Pa 6101**) represents its official cybertype (see Akkari et al., 2015).

2.8. Measurements and microscopy

Measurements of the holotype were done using 3D renders prepared with VGStudio Max Ver. 3.4 (Volume Graphics, Germany) in parallel perspective or with the micrographs. Measurements of the paratypes were taken with the micrographs or by using a compound microscope Zeiss Stemi SV 11 (maximum magnification of 40×). Specimens were examined with the previously listed stereo microscope and the light microscope Zeiss Axioscope (maximum magnification of 200×).

2.9. Terminology

The interpretation of head structures is based on the studies of Badonnel (1934), Yoshizawa (2005) and Boudinot et al. (2024). Yoshizawa (2005) was the main reference for the interpretation and homology hypotheses of the sclerotized thoracic areas. Our interpretation of male and female external genital structures is based on Yoshizawa (2005) and Mockford (2011). We consider any external line that corresponds with an internal ridge as a sulcus (= strengthening line), and a line without ridge as a suture (= line of weakness) (see Girón et al., 2023).

The use of taxonomic names for Psocodea and Psyllipsocidae is based on the database of the "Psocodea Species File" (Hopkins et al., 2024, based on the world catalogue by Lienhard and Smithers, 2002) and Smithers (1972), Lienhard and Yoshizawa (2019), and Liang and Liu (2021). For the age of the amber and copal material we used the Paleobiology Database (2024) and Boudinot et al. (2024).

2.10. Phylogenetic inference for Trogiomorpha

To explore the phylogenetic information content of psocodean morphological features, we first extracted characters from the literature that had been previously discussed as putative apomorphies occurring in Trogiomorpha (e.g., Yoshizawa et al., 2006; Mockford, 2011; Li et al., 2022). Based on this we compiled a character matrix (supplementary files S2 and S3) with 59 characters (58 were used) for 2 outgroups and 22 ingroups, including †*Brachyantennum*. We also included †*Paralellopsocus elongatus* Hakim, Huang & Azar, 2024 from the matrix of Álvarez-Parra et al. (2024) and added the missing character states. Of these 59 characters, 15 are new in our study (38 are modified from Li et al., 2022 and 6 from Yoshizawa, 2002); 24 characters apply to the wings (chars. 24–46; 58 contains information on both wings and body) and the remainder are from various structures of the head, thorax, legs, and terminalia. The most complete terminal was *Stenopsocus stigmaticus* (Imhoff & Labram, 1842) and †*P. mili* with ca. 2 % missing data including inapplicable characters; the least complete was †*Empheriopsis vulnerata* Vishnyakova, 1975 with 66 % missing data. Most of the missing data ("?") were distributed among the characters of mouthparts and thorax (especially in fossil species), underscoring the importance of careful anatomical documentation in future studies.

The data were evaluated with three approaches. As a first step we synthesized possible character transitions based on our experience with character state distribution across the Psocodea. Afterwards, we used TNT 1.6 (Goloboff and Morales, 2023) to infer the phylogeny using the maximum parsimony criterion (Wagner trees, Traditional search: random seed = 1, replications = 1000, trees to

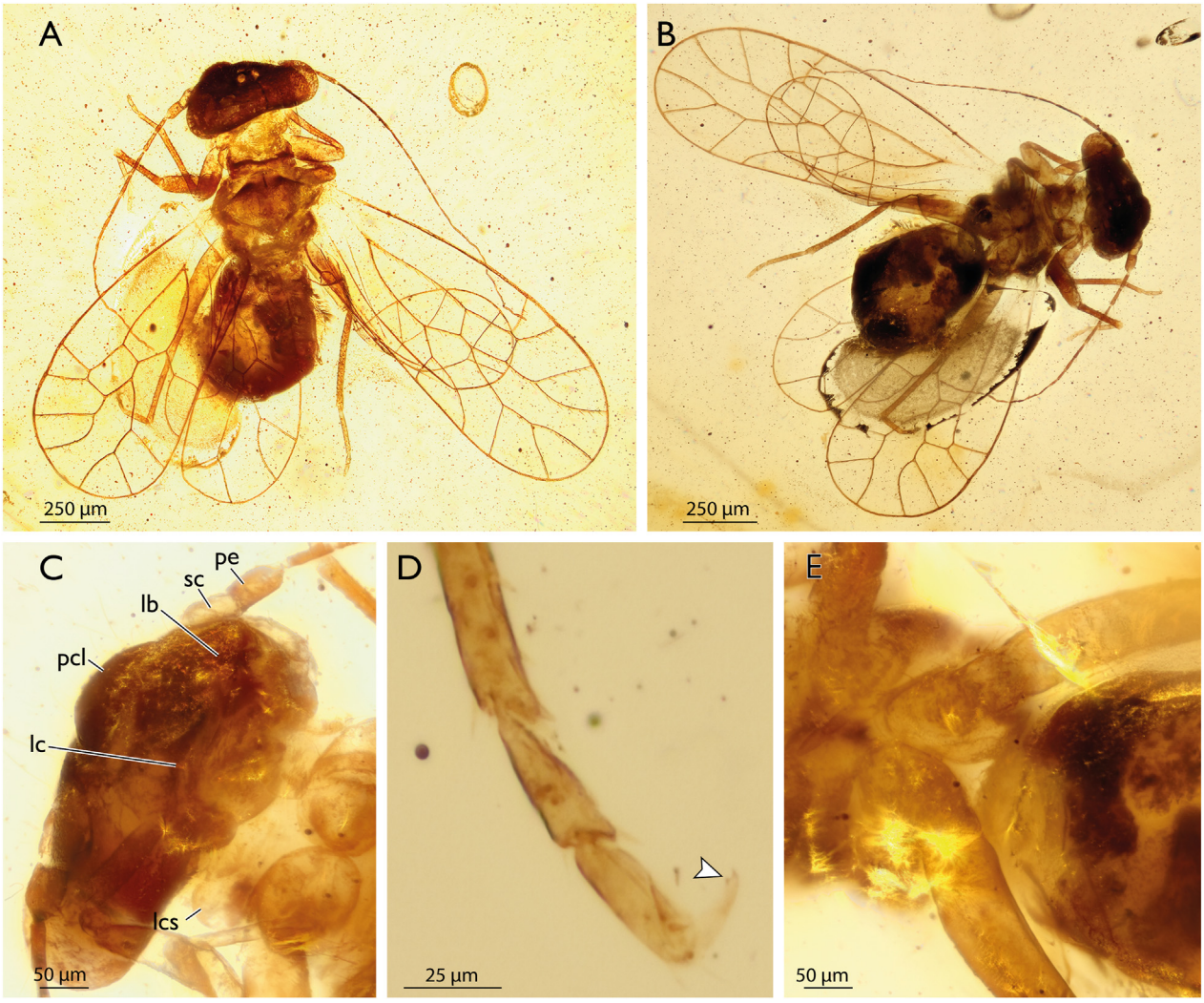

Fig. 1. Micrographs of holotype **PMJ Pa 6101** (female?) of †*Psyllipsocus mili* **sp. nov. A** Habitus in dorsal view; **B** Habitus in ventral view; **C** Details of head in ventral view; **D** Details of right hindleg claw; **E** Details of hindcoxae. Abbreviations: lb, labrum; lc, lacinia; lcs, laterocervical sclerite; pcl, postclypeus; pe, pedicellus; sc, scapus.

save per replication = 100, TBR algorithm, using implied weighting, weight with default function, K = 3.0). As the first taxon in the matrix *S. stigmaticus* is treated as outgroup terminal. To create the tree and to trace the character transformations we used WinClada 1.00.08 (Nixon, 2002) (we added +1 to each character for the final tree as the character list started with the number "0" instead of "1" in WinClada). Bremer support values (hold 10000, bsupport 10) were calculated with NONA 2.0 (Goloboff, 1994). Subsequently we applied Bayesian inference using the program MrBayes 3.2.7a (Ronquist et al., 2012). We converted all polymorphisms to uncertains and included all of the data in a single partition. To this partition, we applied the Mk model (Lewis, 2001) with +Γ to account for among-character rate variation (ACRV) (Yang, 1994). We also provided a backbone scaffold based on the topology of Yoshizawa et al. (2006) and Yoshizawa and Johnson (2014) by implementing partial ("soft") constraints on the extant taxa; these constraints simplify treespace searches while allowing the unconstrained taxa (namely, the fossils) to move freely about the topology. Each Bayesian analysis was performed for a minimum of 1 million generations, sampling every 1000th, with two runs of four chains, with one cold chain each and a temp of 0.01. A relative burnin of 0.25 was used for diagnosis at checkpoints, where convergence was assessed by ensuring that the average standard deviation of split frequencies (ASDSF) was <0.01. The performance of sampling was further diagnosed in Tracer 1.7.2 (Rambaut et al., 2018). The tree was summarized using a conservative 50 % Bayesian posterior probability (BPP) cutoff value and was visualized using FigTree 1.2.2 (Rambaut, 2010). Additionally, we performed analyses each without constraints, with wing venation characters excluded ("body only", char. 1–23, 47–58) and with body characters excluded ("wing only", char. 24–46). All analyses took 2 million MCMC generations.

To estimate ancestral states using MrBayes, we constrained all of the nodes for which we wanted character state probabilities to be reported. After the analyses were completed, we used a custom script (Supplemental file S4) to summarize the detected state transitions across the tree. We then manually plotted the results on the constrained topology.

2.11. Data availability

The complete SR-μCT scan (.tif format) of †*P. mili* **sp. nov.** used for segmentation is available at MorphoBank (O'Leary and Kaufman, 2012): https://www.morphobank.org/index.php/Projects/ProjectOverview/project_id/5274.

As the SR-μCT scans for the segmentation of *D. domestica* and

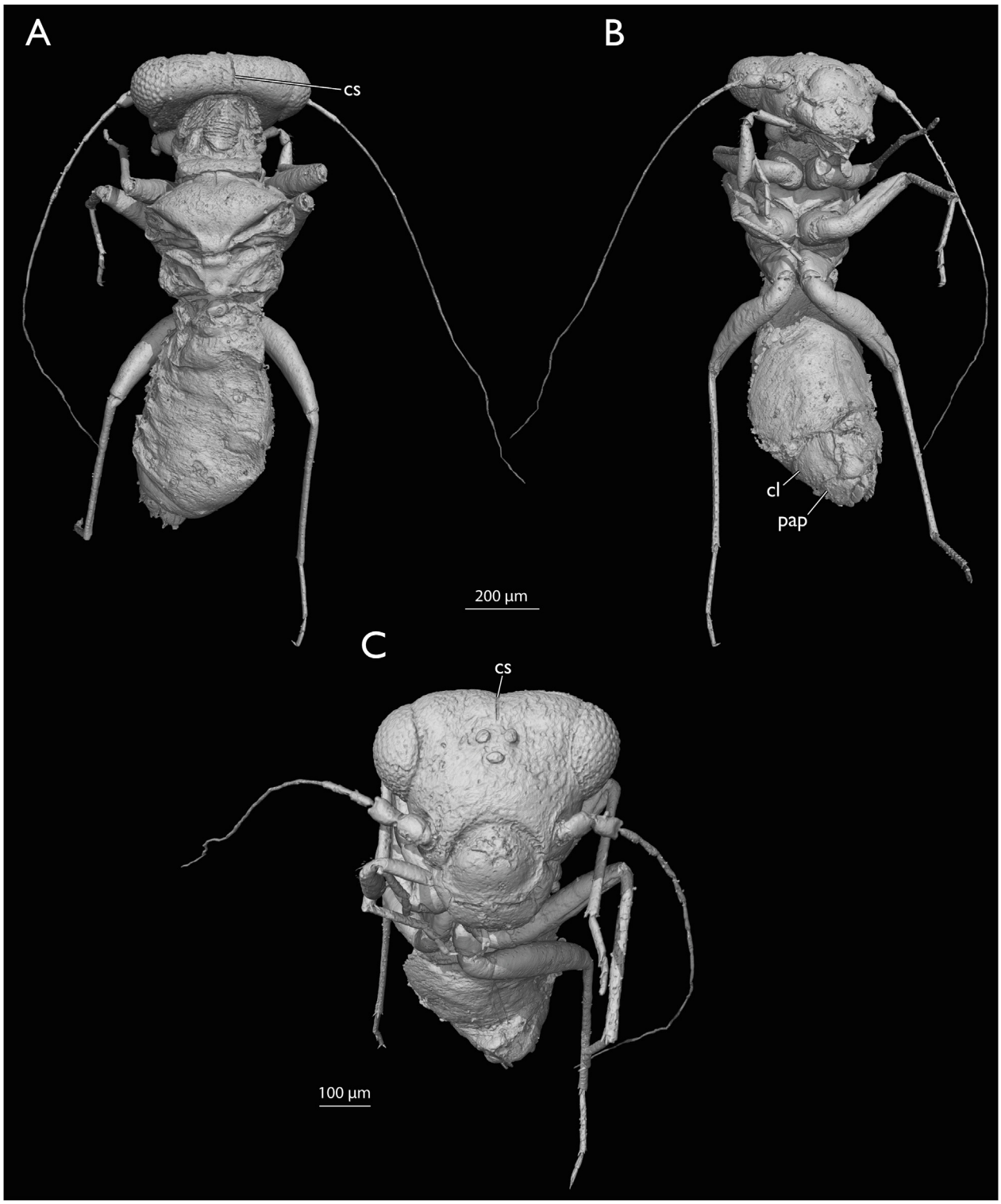

Fig. 2. 3D renders based on SR-µCT of the holotype (female?) of †*P. mili* **sp. nov.**, fore- and hindwings removed. **A** Habitus in dorsal view; **B** Habitus in ventral view, same scale as A; **C** Habitus in frontal view. Abbreviations: cl, clunium; cs, coronal sulcus; pap, paraproct.

C. guestfalica will be used in future studies (and then also made publicly available via the same project in MorphoBank), we will make the files privately available upon request.

The morphological data matrix is available in the supplementary file S3 and from MorphoBank (O'Leary and Kaufman, 2012): https://www.morphobank.org/index.php/Projects/ProjectOverview/project_id/5274.

3. Results

3.1. Systematic palaeontology

3.1.1. Synopsis of fossil Psyllipsocidae

Order Psocodea Hennig, 1966.

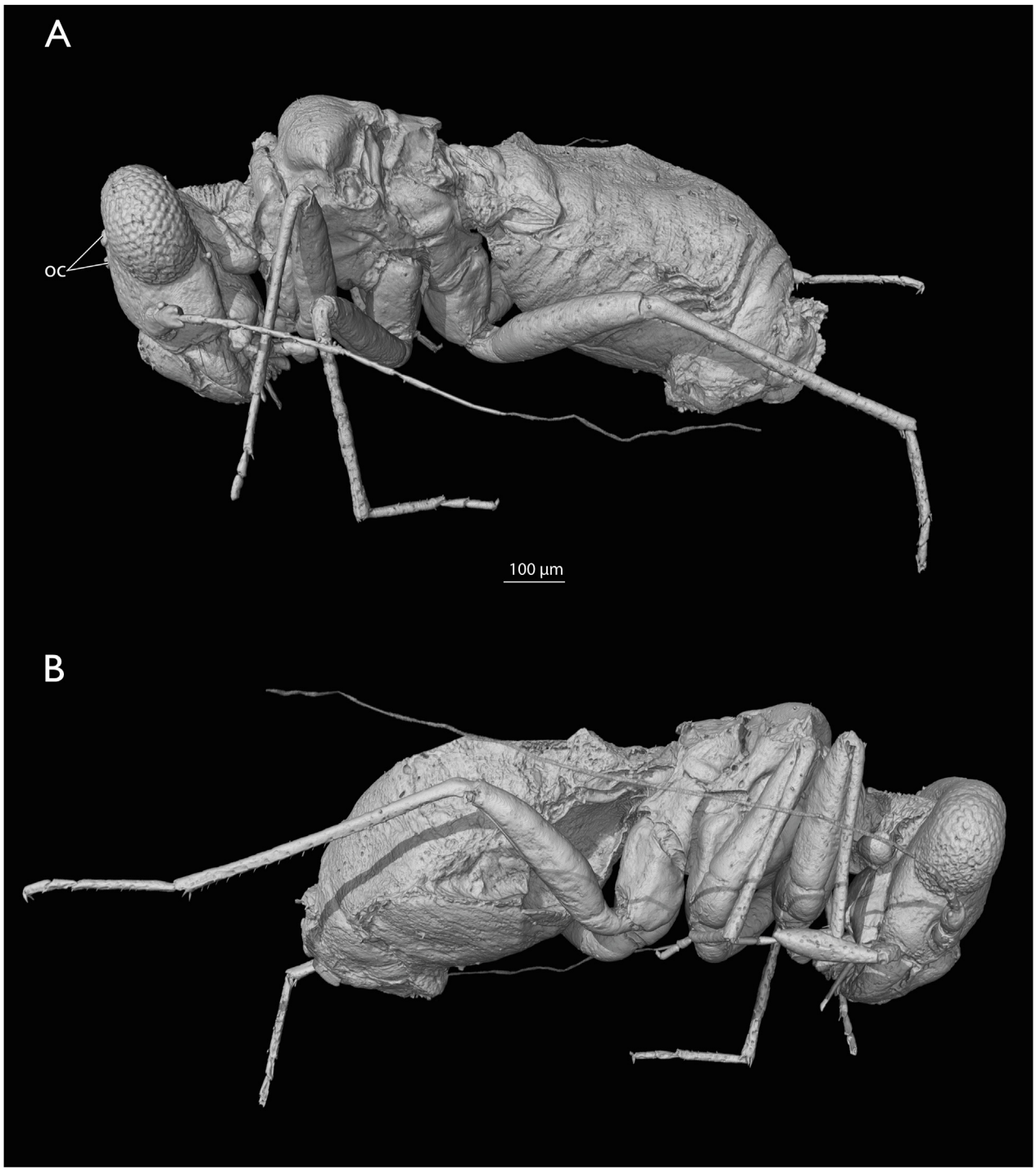

Fig. 3. 3D renders based on SR-µCT of the holotype (female?) of †*P. mili* **sp. nov.**, fore- and hindwings removed. **A** Habitus from left lateral view; **B** Habitus from right lateral view, same scale as A. Abbreviation: oc, ocelli.

Suborder Trogiomorpha Roesler, 1940.
Infraorder Psyllipsocetae Smithers, 1972.
Family Psyllipsocidae Kolbe, 1884.

I. Genus †***Annulipsyllipsocus*** Hakim, Azar, Maksoud, Huang & Azar, 2018.
A Kachin amber [Myanmar; Cretaceous, 99.6–93.5 Mya].
1 †***A. andreneli*** Hakim, Azar, Maksoud, Huang & Azar, 2018.
2 †***A. inexspectatus*** Hakim, Azar, Maksoud, Huang & Azar, 2018.

II Genus ***Psyllipsocus*** Selys-Longchamps, 1872.
[= †*Sinopsyllipsocus* Zhang, Nel, Azar & Wang, 2016; synonymy first proposed by Liang and Liu, 2021 (p. 86), see also Lienhard, 2023 (p. 75); type species: †*S. fushunensis* by monotypy].
[= †*Khatangia* Vishnyakova, 1975 **syn nov.**; type species: †*K. inclusa* by monotypy].
B Dominican amber [Miocene, 20.4–13.8 Mya].

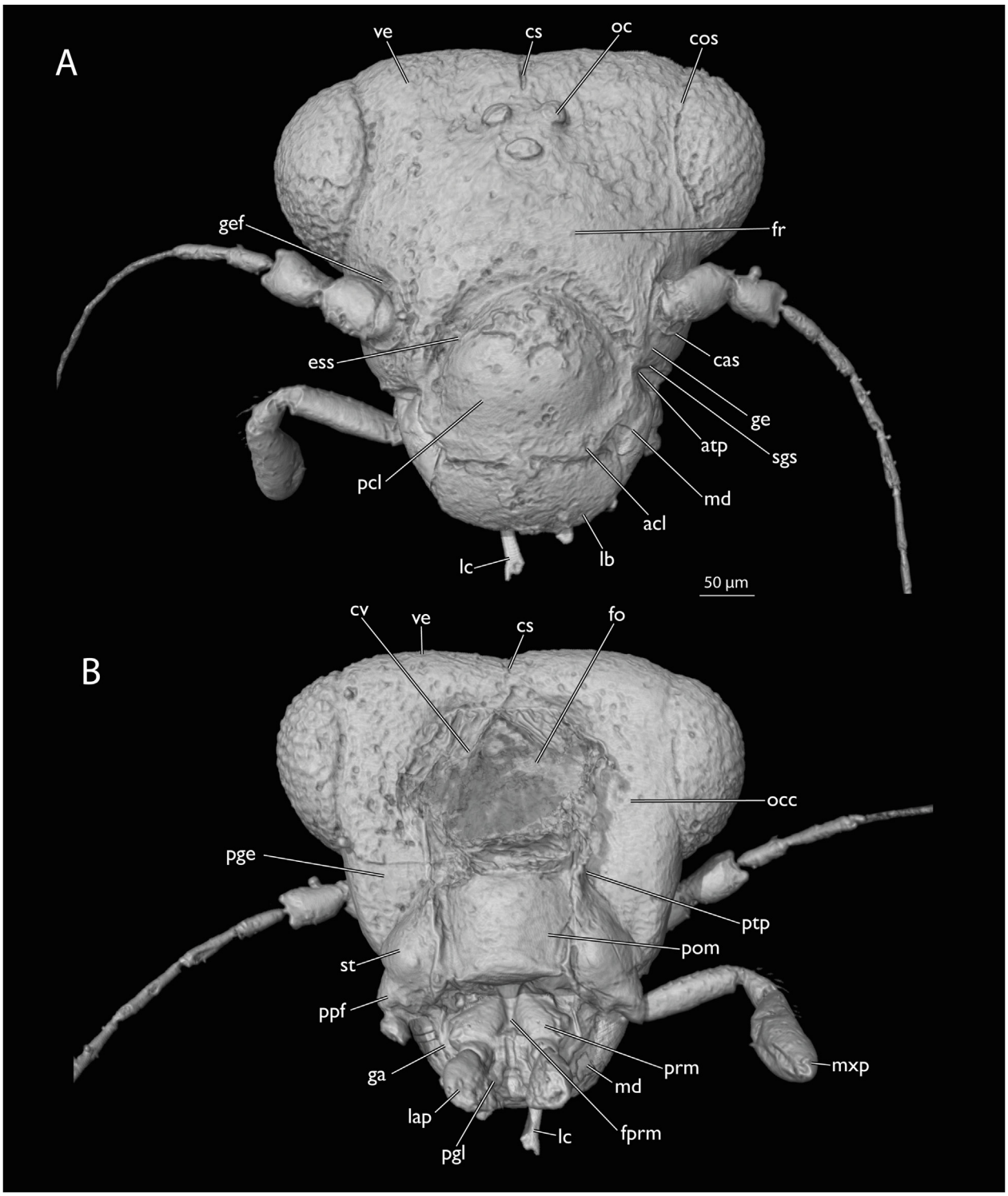

Fig. 4. 3D renders based on SR-µCT of the holotype (female?) of †*P. mili* **sp. nov. A** Details of head in anterior view; **B** Details of head in posterior view, same scale as B. Abbreviations: acl, anteclypeus; atp, anterior tentorial pit; cas, circumantennal sulcus; cos, circumocular sulcus; cs, coronal sulcus; cv, cervical membrane; ess, epistomal sulcus; fo, foramen occipitale; fprm, premental furrow; fr, frons; ga, galea; ge, gena; gef, genal fovea; lap, labial palp; lb, labrum; lc, lacinia; md, mandible; mxp, maxillary palp; oc, ocellus; occ, occiput; pcl, postclypeus; pge, postgena; pgl, paraglossa; pom, postmentum; ppf, palpifer; prm, prementum; ptp, posterior tentorial pit; sgs, subgenal sulcus; st, stipes; ve, vertex.

1 †***P.* sp. 1** [Note 1]**.**
2 †***P.* sp. 2** [Note 1]**.**
3 †***P.* sp. 3** [Note 1]**.**
4 †***P.* sp. 4** [Note 1]**.**

C Mexican amber [Mexico, Miocene, 23.0–16.0 Mya].

5 †***P.* sp. 5** [Note 2]**.**

D Fushun amber [China, Liaoning Province, Fushun City; Eocene, Ypresian, 53.0–50.0 Mya].

6 †***P. fushunensis*** (Zhang, Nel, Azar & Wang, 2016)

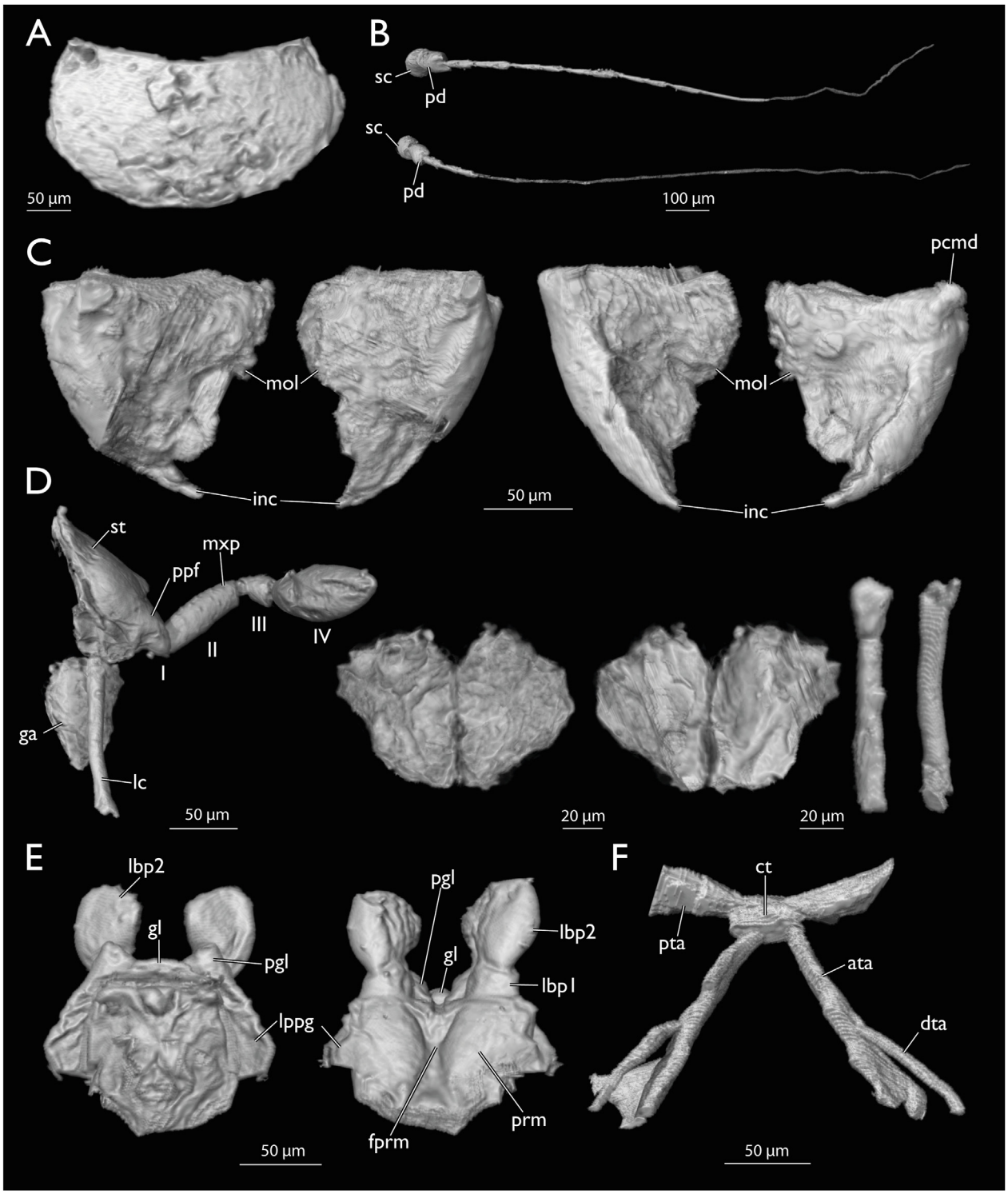

Fig. 5. 3D renders based on SR-µCT of the holotype (female?) of †*P. mili* **sp. nov. A** Details of labrum in anterior view; **B** Details of antennae; **C** Details of mandibles in anterior view (left) and posterior view (right); **D** Details of maxilla in posterior view (far left), galeae in anterior (left) view and posterior view (right), and laciniae in anterior view (far right); **E** Details of distal part of labium in anterior view (left) and posterior view (right); **F** Details of tentorium. Abbreviations: ata, anterior tentorial arm; ct, corpotentorium; dta, dorsal tentorial arm; fprm, premental furrow; ga, galea; gl, glossa; inc, incisivi; lbp1/2, lppg, prepalpiger lobe; first or second article of labial palp; mol, mola; mxp, maxillary palp; pcmd, posterior condyle of mandible; pd, pedicellus; pgl, paraglossa; ppf, palpifer; prm, prementum; pta, posterior tentorial arm; sc, scapus; st, stipes.

E Oise amber [France, Le Quesnoy; Eocene, Ypresian, 56.0–47.8 Mya].
7 †***P. eocenicus*** Nel, Prokop, De Ploeg & Millet, 2005.
F Taimyr amber [Russia; Cretaceous, 85.8–83.5 Mya].
8 †***P. inclusus*** (Vishnyakova, 1975) **comb. nov.**
G Kachin amber [Myanmar; Cretaceous, 99.6–93.5 Mya].
9 †***P. mili*** Weingardt, Liang & Yoshizawa **sp. nov.**

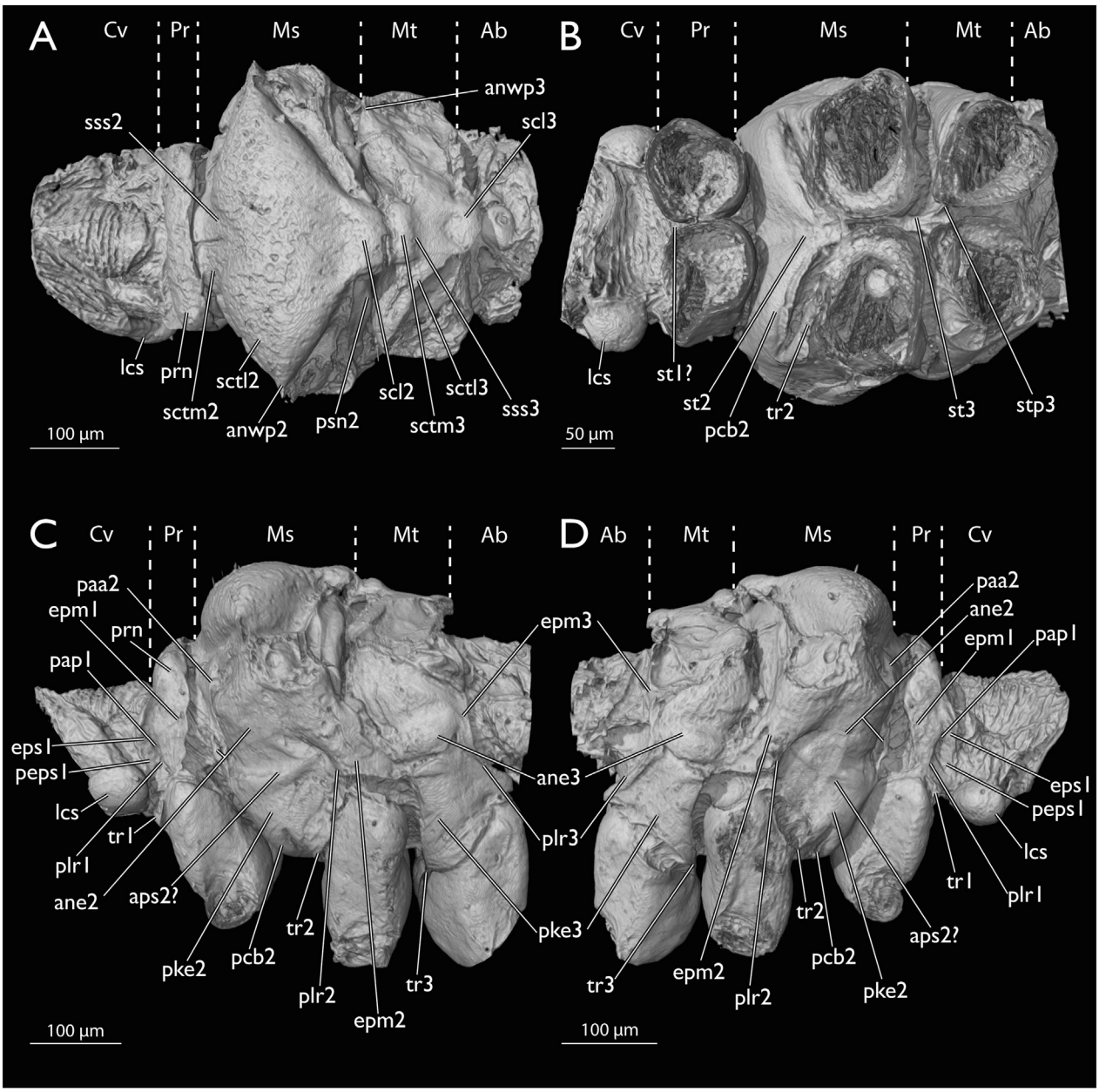

Fig. 6. 3D renders based on SR-µCT of the holotype (female?) of †*P. mili* **sp. nov. A** Details of thorax in dorsal view; **B** Details of thorax in ventral view. **C** Details of thorax in left lateral view. **D** Details of thorax in right lateral view. Sections: Cv, cervix; Pr, prothorax; Ms, mesothorax; Mt, metathorax; Ab, abdomen. Abbreviations: ane2/3, anepisternum of meso- or metathorax; anwp2/3, anterior notal wing process of meso- or metathorax; aps2, anapleural sulcus of mesothorax; epm1/2/3, epimeron of pro-, meso- or metathorax; eps1, proepisternum; lcs, laterocervical sclerite; paa2, prealar arm of mesothorax; pap1, pleural arm pit of prothorax; pcb2, precoxal bridge of mesothorax; peps1, preepisternum of prothorax; pke2/3, preepisternum + katepisternum of meso- or metathorax; plr1/2/3, pleural ridge of pro-, meso- or metathorax;, pronotum; psn2, postnotum of mesothorax; scl2/3, meso- or metascutellum; sctl2, lateral lobe of mesoscutum; sctm2/3, median lobe of meso- or metascutum; st1/2/3, eusternum of pro-, meso- or metathorax; sss2/3, scuto-scutellar suture of meso- or metathorax; stp3, process of metasternum; tr2/3, meso- or metatrochantin.

10 †***P. myanmarensis*** Jouault, Yoshizawa, Hakim, Huang & Nel, 2021.
11 †***P. yangi*** Liang & Liu, 2021.
12 †***P. yoshizawai*** Álvarez-Parra, Peñalver, Nel & Delclòs, 2020.

H Lebanese amber [Lebanon; Cretaceous, Barremian, 130.0–125.0 Mya].
13 †***P.* sp. 6** [Note 3].

Note 1. Four (undescribed?) species of *Psyllipsocus* were mentioned by Mockford (2011).

Note 2. Single undescribed species. Only a nymphal stage is known (Mockford, 1969).

Note 3. Misidentified by Grimaldi and Engel (2005) as member of Prionoglarididae. Systematic position later clarified by Mockford (2011) and Mockford et al. (2013). Possibly a member of an undescribed genus of Psyllipsocidae (Lienhard et al., 2022).

3.1.2. Taxon description

Genus *Psyllipsocus* Selys-Longchamps, 1872.

Type species: *Psyllipsocus ramburii* Selys-Longchamps, 1872, by

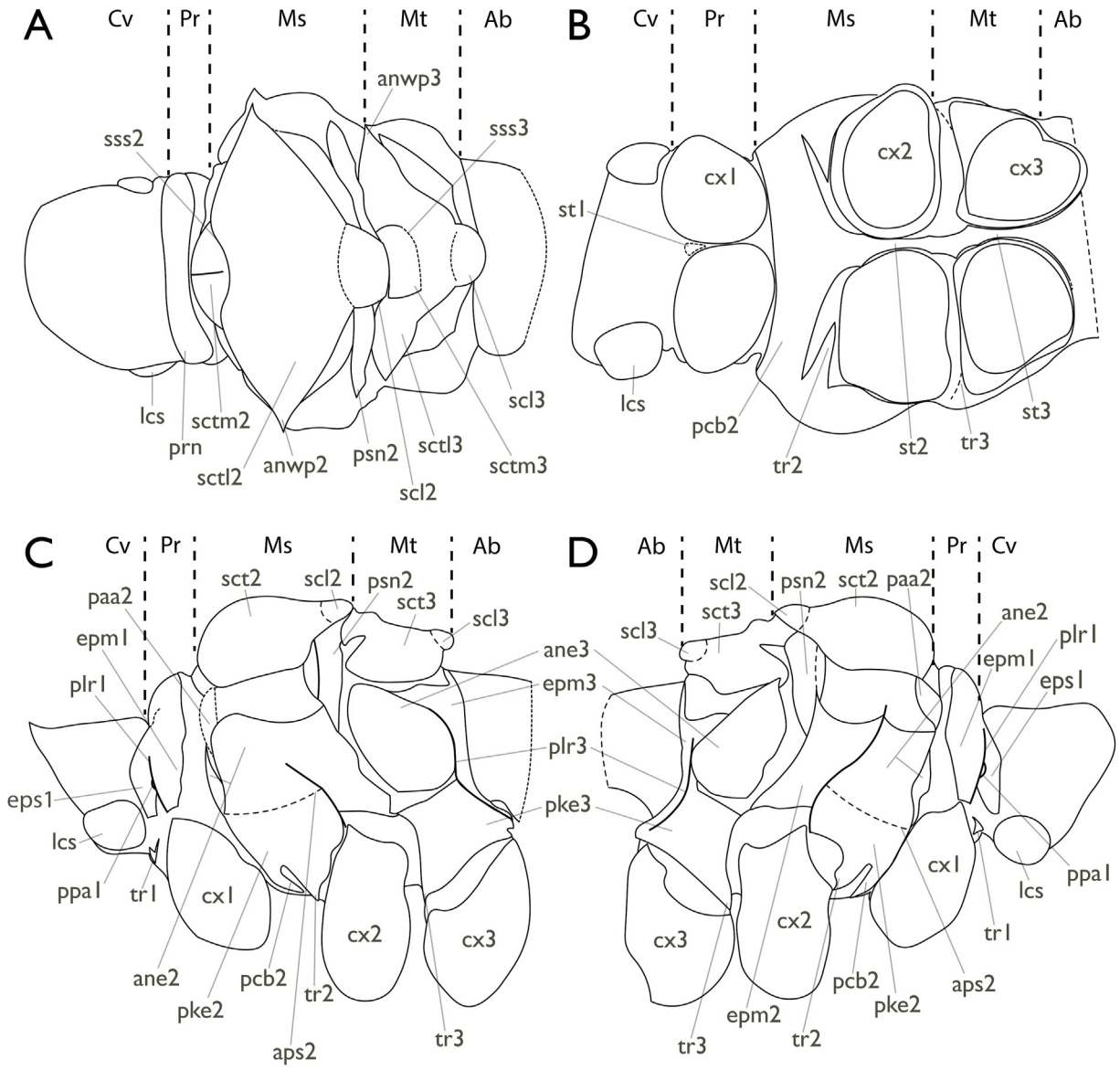

Fig. 7. Line drawings of the thorax of the holotype (female?) of †*P. mili* **sp. nov. A** Details of thorax in dorsal view; **B** Details of thorax in ventral view. **C** Details of thorax in left lateral view. **D** Details of thorax in right lateral view. Sections: Cv, cervix; Pr, prothorax; Ms, mesothorax; Mt, metathorax; Ab, abdomen. Abbreviations: ane2/3, anepisternum of meso- or metathorax; anwp2/3, anterior notal wing process of meso- or metathorax; aps2, anapleural sulcus of mesothorax; epm1/2/3, epimeron of pro-, meso- or metathorax; eps1, proepisternum; lcs, laterocervical sclerite; paa2, prealar arm of mesothorax; pap1, pleural arm pit of prothorax; pcb2, precoxal bridge of mesothorax; peps1, preepisternum of prothorax; pke2/3, preepisternum + katepisternum of meso- or metathorax; plr1/2/3, pleural ridge of pro-, meso- or metathorax;, pronotum; psn2, postnotum of mesothorax; scl2/3, meso- or metascutellum; sctl2, lateral lobe of mesoscutum; sctm2/3, median lobe of meso- or metascutum; st1/2/3, eusternum of pro-, meso- or metathorax; stp3, process of metasternum; tr2/3, meso- or metatrochantin.

original designation.

†***Psyllipsocus mili*** Weingardt, Liang & Yoshizawa **sp. nov** (Fig. 1–10).

The newly described species has been registered in ZooBank under https://zoobank.org/4196a57b-b635-4e8b-b463-b2245d50af9e. Description and species status is based on a comparison of four specimens from four different amber pieces.

Etymology. MW wants to honor the music group Mili and their incredible music and art. The name is inspired by the fairy tale "Liebe Mili" by Wilhelm Carl Grimm (1786–1859), translated into English as "Dear Mili".

Type material.

Holotype: **PMJ Pa 6101** stored in the Phyletisches Museum (previously in the research collection of MW as **BuA_MW_0002**, female?). Cybertype: Model 1, https://sketchfab.com/3d-models/psyllipsocus-mili-cybertype-holotype-7459e8dcd208424ca12168e36138aa0f. Model 2 (Thorax), https://sketchfab.com/3d-models/thorax-of-psyllipsocus-mili-female-69dc5a56fbc04c048bd902f19032facb.

Paratypes: **SMF Be 14667** (female) stored in the section amber research collection in the Senckenberg Research and Natural History Museum Frankfurt am Main (Hesse, Germany) **(**previously belonging to the research collection of MW under **BuA_MW_0003)**. **CAU-BA-LFY-24001** (male) stored in Hunan University of Science and Technology (Xiangtan, China). To be deposited in Entomological Museum, China Agricultural University (CAU) (Beijing, China). **CAU-BA-LFY-24002** (female) stored in Hunan University of Science and Technology (Xiangtan, China). To be deposited in

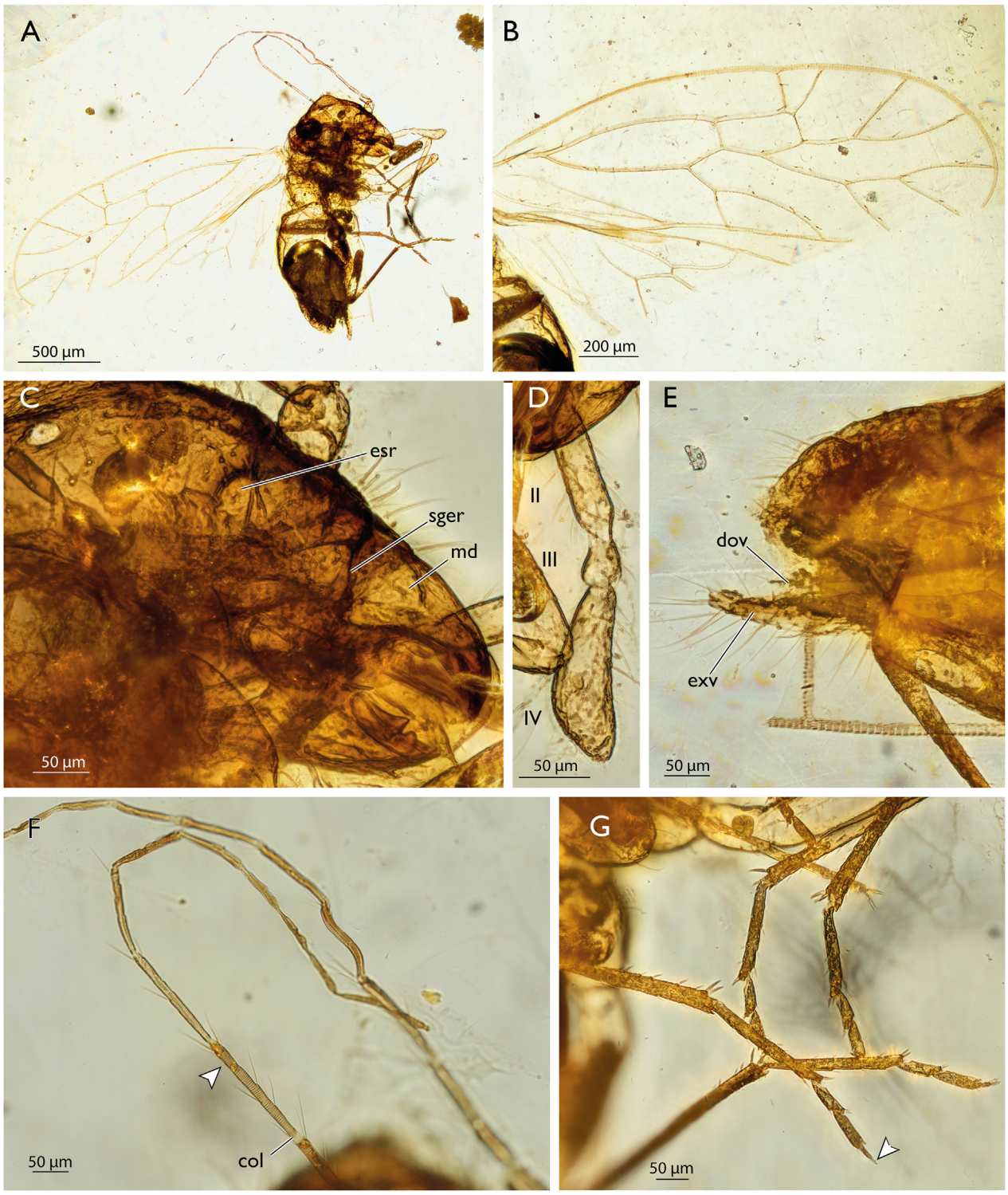

Fig. 8. Micrographs of paratype **SMF Be 14667** (female) of †*P. mili* **sp. nov. A** Habitus from lateral view; **B** Details of wing venation; **C** Details of head in caudolateral view; **D** Details of left maxillary palp; **E** Details of postabdomen and ovipositor. **F** Details of left and right antennal flagellum, arrow indicates secondary annulation. **G** Details of tarsi and claws, arrow indicates single preapical tooth. Abbreviations: col, collar of flagellomere; dov, dorsal valve; esr, epistomal ridge; exv, external valve; md, mandible; sger, subgenal ridge.

Entomological Museum, China Agricultural University (CAU) (Beijing, China).

Diagnosis. The new species can be unambiguously identified by the combination of the following features: (1) narrow quadrangular pterostigma, (2) secondary annulation of flagellomeres, (3) anterior curvature of R2+3 and R4+5 and wide distance between the tips of R1 and R2+3, (4) presence of subtriangular and small dorsal valve (v2), ventral valve (v1) absent, (5) hypandrium with two symmetrical lobes and two distally converging parameres.

Macropterous. Epistomal sulcus complete. Epistomal ridge wide.

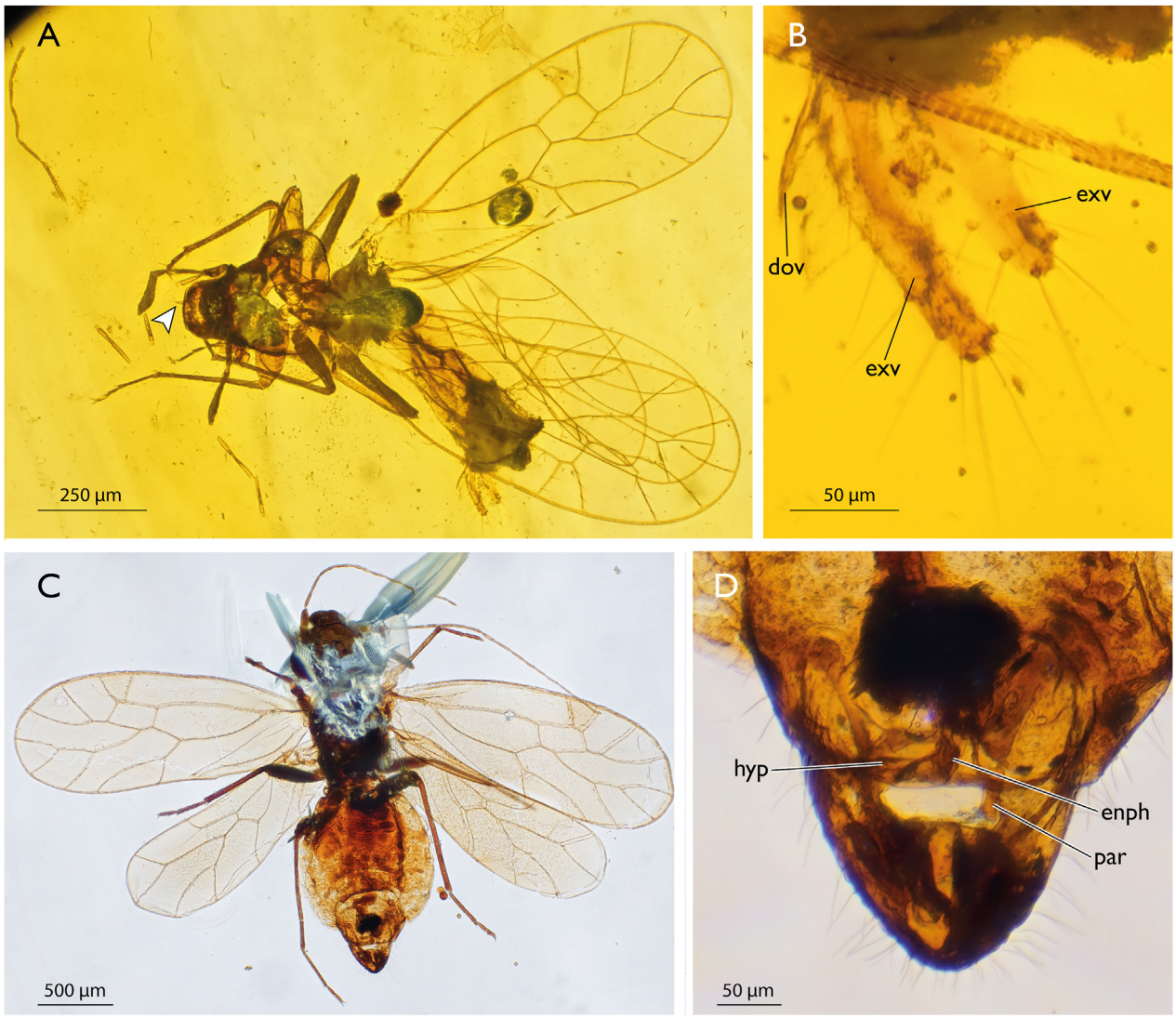

Fig. 9. Micrographs of paratype **CAU-BA-LFY-24002** (female) (A, B) and **CAU-BA-LFY-24001** (male) (C, D) of †*P. mili* **sp. nov. A** Habitus from dorsal view (female), arrow indicates lacinial tip; **B** Details of ovipositor; **C** Habitus from dorsal view (male); **D** Details of hypandrium–phallosome complex. Abbreviations: dov, dorsal valve; enph, endophallus; exv, external valve; hyp, hypandrium; par, paramere.

Clypeal region ventrally extended. Antennae filiform, longer than body, with 21 antennomeres (often fewer due to damage). Flagellomeres with secondary annulation. Lacinia with outer cusp bidentate and inner cusp as simple tooth. Maxillary palp with article 4 (mx4) wedge-shaped; palpomere 2 (mx2) without conical sensillum. Labial palp with two articles, the second flat and rounded. Large and strongly convex laterocervicalia present. Forewings hyaline with membrane mostly glabrous. Forewing veins with few setae placed in one row. Pterostigma not thickened, quadrangular and relatively narrow. In contrast to related species with a comparatively large distance between the tip of the veins R1 and R2+3 of the forewing. Radial cell hexagonal and complete in forewing. Tip of CuP and A1 reaching wing margin at a distance from each other. Hindwings glabrous. Tibiae of each leg with two thick apical spurs. Three tarsomeres present on each leg, first and second with two apical spurs. Claw with single preapical tooth. Pulvilli absent. Paraproctal spine absent. Sensorium inconspicuous. Subgenital plate rounded and unmodified. Ovipositor with long, cylindrical, and setose v3 and weakly developed subtriangular v2. v1 absent. Setae on v3 long. Hypandrium-phallosome complex with two symmetrical lobes and two distally converging parameres.

Description of holotype female (?). Based on the micrographs (Fig. 1), drawings (Fig. 7) and 3D-renders of the SR-µCT scan (Figs. 2–6). Additionally, a cybertype (3D-model, including the computer generated tomographic data used for constructing the model, of holotype) is available on Sketchfab (Model 1: https://sketchfab.com/3d-models/psyllipsocus-mili-cybertype-holotype-7459e8dcd208424ca12168e36138aa0f; Model 2: https://sketchfab.com/3d-models/thorax-of-psyllipsocus-mili-female-69dc5a56fbc04c048bd902f19032facb) and MorphoBank (https://www.morphobank.org/index.php/Projects/ProjectOverview/project_id/5274).

Coloration. Head dark brown. Compound eyes brown. Ocelli pale, with brownish tint. Membranous regions of thorax and abdomen light brown; sclerotized postcephalic regions dark brown; mostly less strongly pigmented as head but anterior portion of pronotum and mesonotum as dark. Legs almost uniformly brown, but somewhat less pigmented towards tarsal region. Both fore- and hindwings hyaline, only pterostigma slightly darker (Fig. 1).

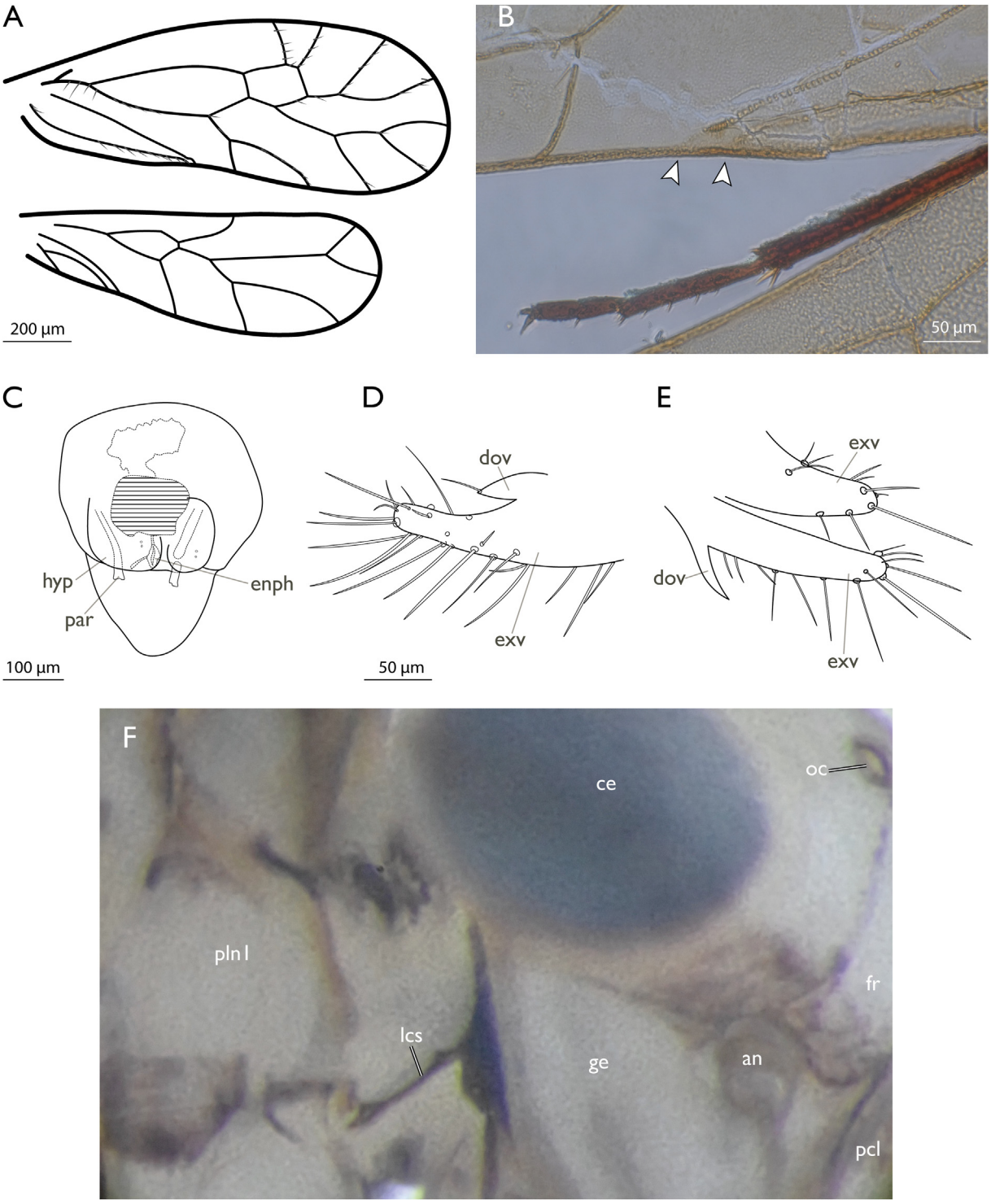

Fig. 10. Drawings if details of the paratypes of †*P. mili* **sp. nov.** (A–E) and micrograph of cervical region of *Stimulopalpus japonicus* (Troctomorpha: Amphientomidae) (F)**. A** Generalized wing scheme of all specimens combined; **B** Veins CuP and A1 near posterior forewing margin of paratype **CAU-BA-LFY-24001** (male); **C** Male genitalia of paratype **CAU-BA-LFY-24001**; **D** Ovipositor of paratype **SMF Be 14667**; **E** Ovipositor of paratype **CAU-BA-LFY-24002**, same scale as D; **F** Details of right side of cervix of *S. japonicus*. Abbreviations: an, antenna; ce, compound eye; dov, dorsal valve; enph, endophallus; exv, external valve; fr, frons; ge, gena; hyp, hypandrium; lcs, laterocervical sclerite; oc, ocellus; par, paramere; pcl, postclypeus; pln1, prothoracic pleural region.

Morphology. Head orthognathous, longer than wide, of scale-like shape, anteroposteriorly flattened (Fig. 2A–C, 3A, B). Median coronal sulcus (Fig. 2A–C, 4A, B, **cs**) present. Paired frontal sutures not visible. Epistomal sulcus (Fig. 4A, **ess**) completely developed with wide internal ridge (µCT scan). Compound eyes (Fig. 4A and B, **ce**) large, located slightly below dorsalmost vertexal margin. Vertex (Fig. 4A and B, **ve**) slightly elevated laterally, weakly concave medially; posteriorly narrow but rounded. Three large ocelli (lateral ocelli 30 µm, median ocellus 20 × 35 µm) (Fig. 3A and 4A, **oc**) located close to each other on flat surface, forming sub-equilateral

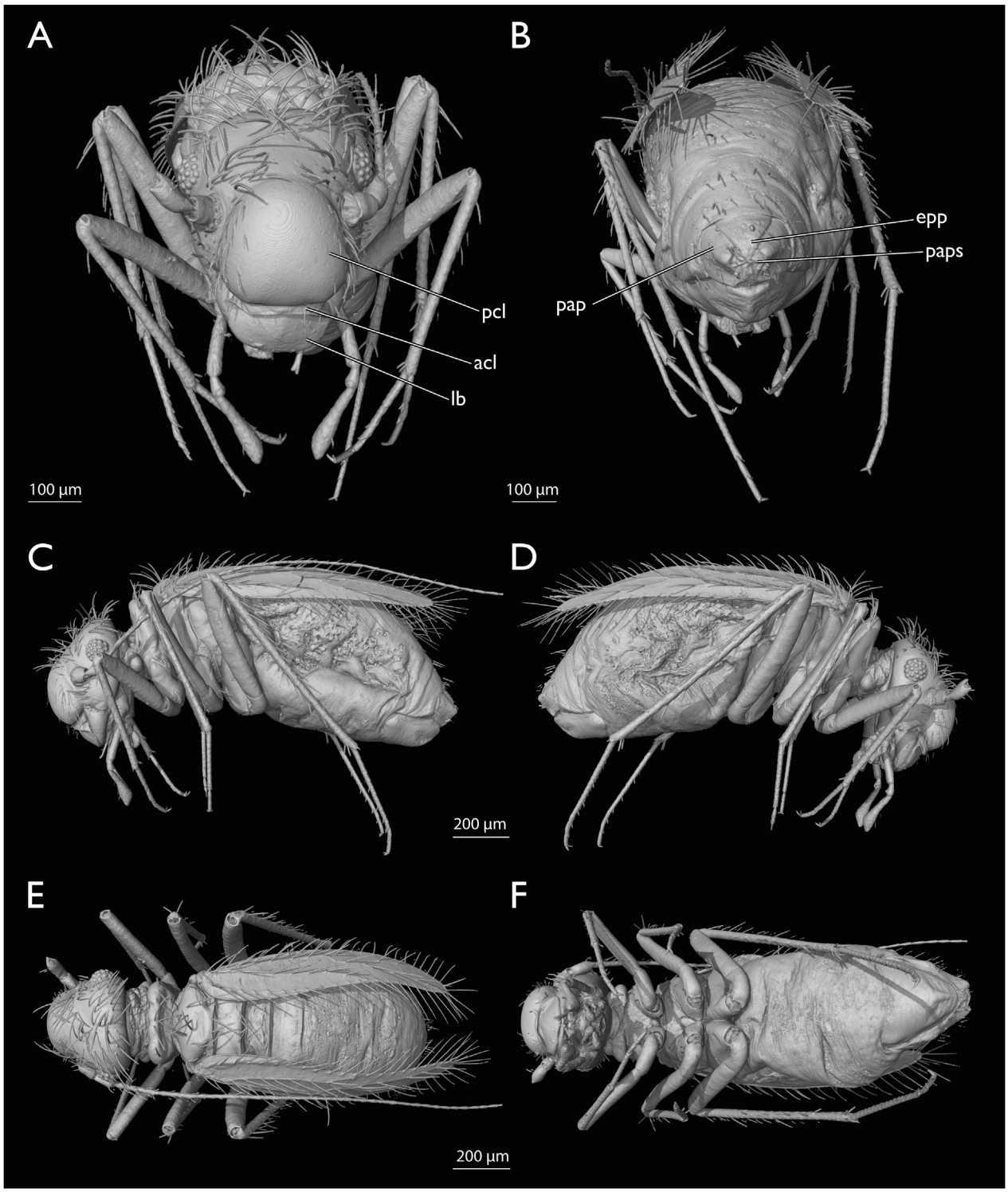

Fig. 11. 3D renders based on SR-µCT of *Dorypteryx domestica* (male), habitus. **A** Habitus in frontal view; **B** Habitus in caudal view; **C** Habitus in left lateral view; **D** Habitus in right lateral view, same scale as C; **E** Habitus in dorsal view; **F** Habitus in ventral view, same scale as E. Abbreviations: acl, anteclypeus; epp, epiproct; lb, labrum; pap, paraproct; paps, paraproctal spine; pcl, postclypeus.

triangle. Postclypeus (Fig. 1C and 4A, **pcl**) weakly convex, ventrally expanded; relatively small, approximately as long as frons. Anteclypeus (Fig. 4A, **acl**) present as short membranous strip, likely partly fused with postclypeus. Intraclypeal furrow not clearly recognizable but probably partly preserved. Tentorium recognizable in µCT scan but apparently enclosed by minute bubbles, thus appearing more massive than in related species; asymmetry likely caused by deformation. Anterior tentorial arms (Fig. 5F, **ata**) long and anteriorly twisted; invagination sites located at ventral margin of genae (Fig. 4A, **ge**) but anterior tentorial pits (µCT scan) small and not well visible externally (Fig. 4A, **atp**); anterior arms connected with corpotentorium (Fig. 5F, **ct**), distinctly separated from each

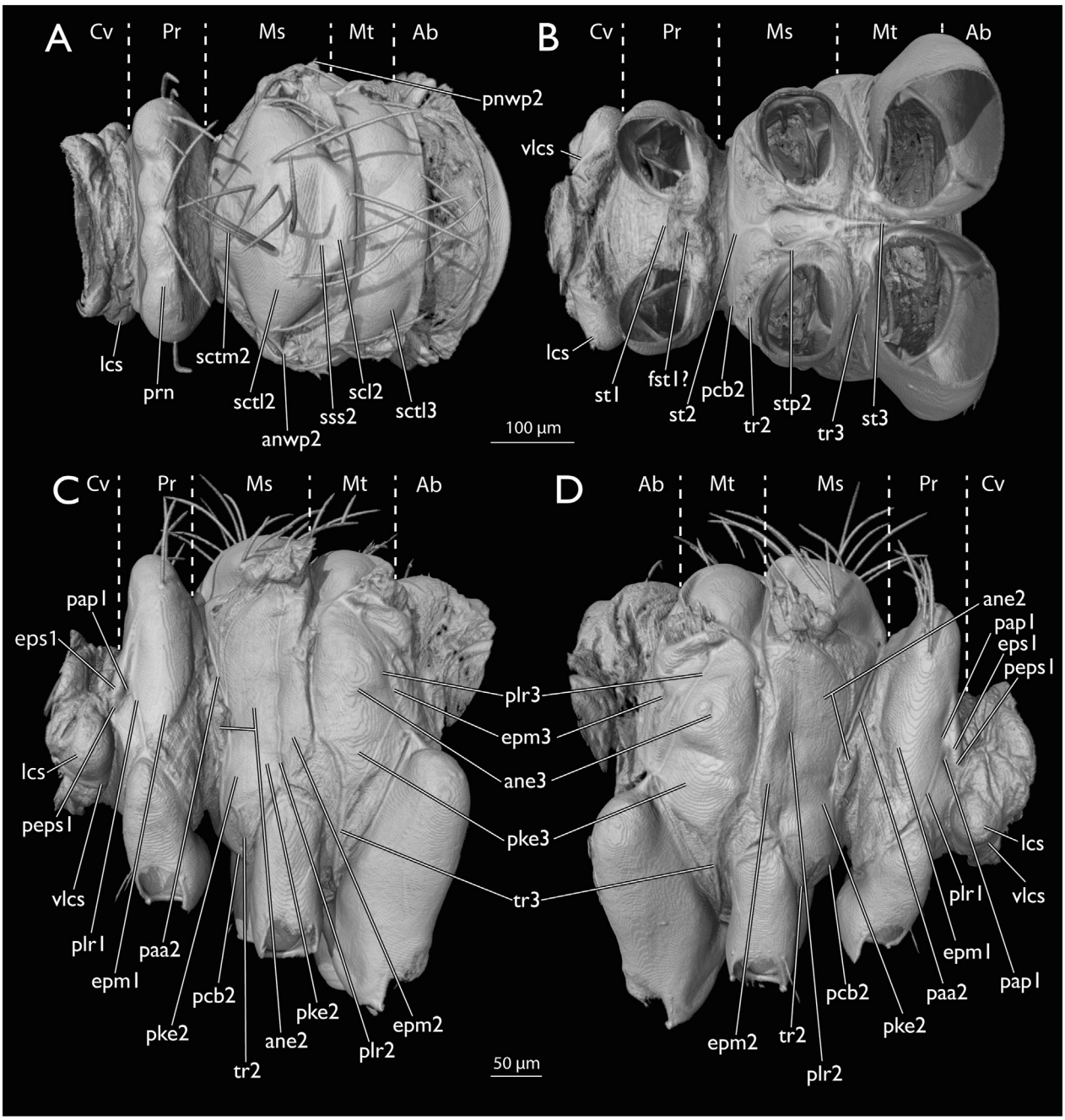

Fig. 12. 3D renders based on SR-µCT of *D. domestica* (male), thorax. **A** Details of thorax in dorsal view; **B** Details of thorax in ventral view, same scale A; **C** Details of thorax in left lateral view. **D** Details of thorax in right lateral view, same scale as C. Sections: Cv, cervix; Pr, prothorax; Ms, mesothorax; Mt, metathorax; Ab, abdomen. Abbreviations: ane2/3, anepisternum of meso- or metathorax; anwp2, anterior notal wing process of mesothorax; epm1/2/3, epimeron of pro-, meso- or metathorax; eps1, proepisternum; fst1?, furcasternum of prothorax; lcs, laterocervical sclerite; paa2, prealar arm of mesothorax; pap1, pit of prothoracic pleural arm; pcb2, precoxal bridge of mesothorax; peps1, preepisternum of prothorax; pke2/3, preepisternum + katepisternum of meso- or metathorax; plr1/2/3, pleural ridge of pro-, meso- or metathorax; pnwp2, posterior notal wing process of mesothorax; prn, pronotum; scl2, mesoscutellum; sctl2/3, lateral lobe of mesoscutum or metascutum; sctm2, median lobe of mesoscutum; sss2, scuto-scutellar suture of mesothorax; st1/2/3, eusternum of pro-, meso- or metathorax; stp2, process of mesosternum; tr2/3, meso- or metatrochantin; vlcs, ventral extension of laterocervical sclerite.

other. Dorsal tentorial arms (Fig. 5F, **dta**) originating on anterior 1/3 of anterior arms, ending shortly before reaching circumantennal ridge. Posterior tentorial arms (Fig. 5F, **pta**) strongly developed, longer than compact corpotentorium; slit-like posterior tentorial pits (Fig. 4B, **ptp**) immediately adjacent to dorsal margin of stipes. Occiput (Fig. 4B, **occ**) not separated by suture or ridge from anterior head capsule, ventrally continuous with postgenae (Fig. 4B, **pge**). Postocciput not preserved or not visible in µCt scan; occiput seemingly continuous with membranous cervical region (Fig. 3A and B), due to apparent absence of sclerotized postocciput. Head capsule of open type, with almost circular large foramen occipitale (Fig. 4B, **fo**). Labrum (Fig. 1C and 5A, **lb**) lobe-shaped, without ventral nodi or median notch, with distal margin smoothly rounded. Antennal insertion area located in shallow fovea of genal region (Fig. 4A, **gef**); dorsal line of fovea likely equivalent with border between frons and gena; antennifer not discernible. Antennae filiform, longer than body when complete, with long flagellum (Fig. 5B); circumantennal sulcus distinct (Fig. 4A, **cas**);

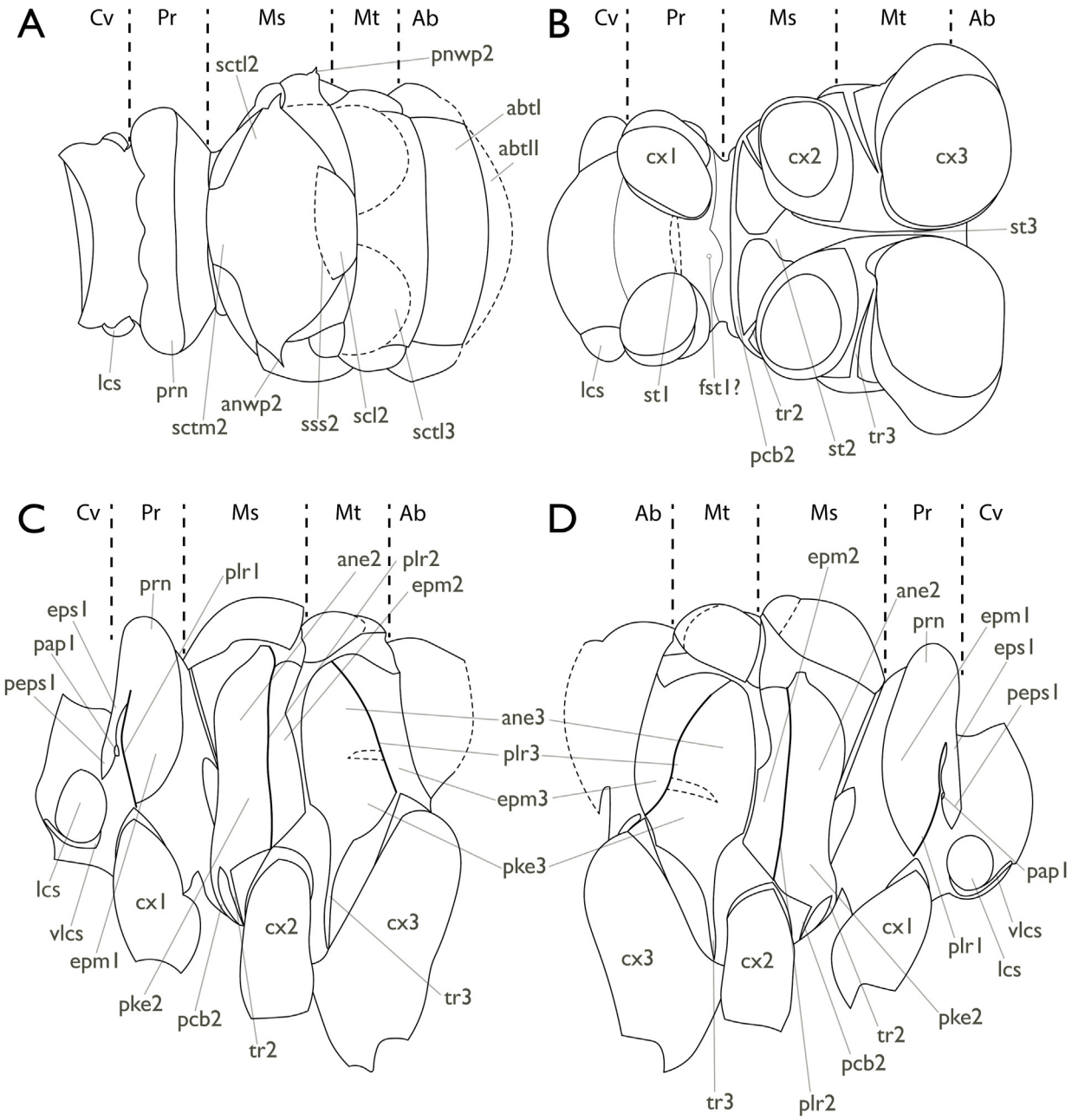

Fig. 13. Line drawings of *D. domestica* (male), thorax. **A** Details of thorax in dorsal view; **B** Details of thorax in ventral view. **C** Details of thorax in left lateral view. **D** Details of thorax in right lateral view. Sections: Cv, cervix; Pr, prothorax; Ms, mesothorax; Mt, metathorax; Ab, abdomen. Abbreviations: ane2/3, anepisternum of meso- or metathorax; anwp2, anterior notal wing process of mesothorax; epm1/2/3, epimeron of pro-, meso- or metathorax; eps1, proepisternum; fst1?, furcasternum of prothorax; lcs, laterocervical sclerite; paa2, prealar arm of mesothorax; pap1, pit of prothoracic pleural arm; pcb2, precoxal bridge of mesothorax; peps1, preepisternum of prothorax; pke2/3, preepisternum + katepisternum of meso- or metathorax; plr1/2/3, pleural ridge of pro-, meso- or metathorax; pnwp2, posterior notal wing process of mesothorax; prn, pronotum; scl2, mesoscutellum; sctl2/3, lateral lobe of mesoscutum or metascutum; sctm2, median lobe of mesoscutum; sss2, scuto-scutellar suture of mesothorax; st1/2/3, eusternum of pro-, meso- or metathorax; tr2/3, meso- or metatrochantin; vlcs, ventral extension of laterocervical sclerite.

right antenna with 21 preserved articles, left antenna with 20. Scape ca. 1.5x wider than pedicel; both ca. 2–3x as wide as flagellum. Flagellomeres narrow, annulated, with few setae; length and width decreasing distally. Rupture-facilitating device formed by enlarged membranous collars (best visible in paratype **SMF Be 14667**: Fig. 8F, **col**) at base of flagellomeres. Asymmetric mandibles (Fig. 5C, **md**) relatively long, with lateral margin evenly rounded; both apparently with two incisivi and distinct molar region; posterior side of mandibles shallowly concave, providing space for galeae. Maxillae without cardo, maxillary body thus only formed by stipes, together with distinct apical palpifer. Right maxillary palp (Fig. 5D, **mxp**) with four articles; terminal palpomere wedge-shaped; conical sensilla on second and fourth palpomere missing; P4 Index (Mockford, 2011) = 2.33; mx4 not extremely widened distally; left maxillary palp of specimen only with first palpomere preserved. Galeae flattened (Fig. 5D, **ga**), details of sclerotization not preserved. Apex of right lacinia (Fig. 5D, **lc**) distinctly recognizable; lateral cusp differentiated from broader and arched median cusp with anterior concavity; poorly preserved apex of left lacinia apparently more or less smoothly rounded. Postmentum

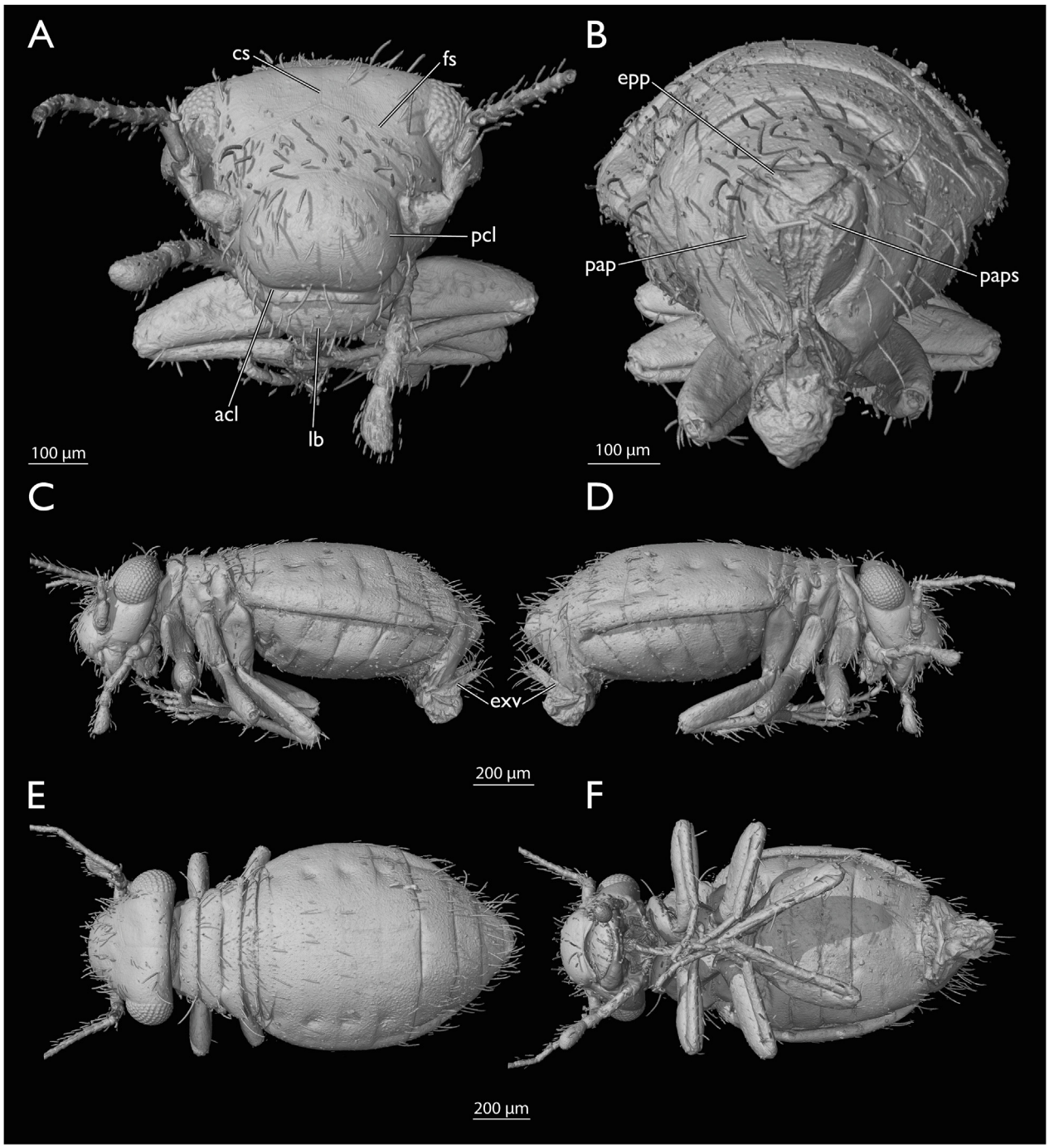

Fig. 14. 3D renders based on SR-µCT of *Cerobasis guestfalica* (female), habitus. **A** Habitus in frontal view; **B** Habitus in caudal view; **C** Habitus in left lateral view; **D** Habitus in right lateral view, same scale as C; **E** Habitus in dorsal view; **F** Habitus in ventral view, same scale as F. Abbreviations: acl, anteclypeus; cs, coronal sulcus; epp, epiproct; exv, external valve; fs, frontal suture; lb, labrum; pap, paraproct; paps, paraproctal spine; pcl, postclypeus.

(Fig. 4B, **pom**) forms ventral closure of head; apparently not differentiated into submentum and mentum. Prementum (Figs. 4B and 5E, **prm**) distinct, with two lateral prepalpiger lobes (Fig. 5E, **lppg**); median longitudinal furrow (Fig. 5E, **fprm**) separates symmetric premental halves; anteromedian lobe likely represents fused glossae (Fig. 5E, **gl**); flanked posterolaterally by subtriangular paraglossae (Fig. 5E, **pgl**). Labial palps (Fig. 5E, **lap**) with two palpomeres. First palpomere short and narrow, second flat, rounded and wide.

Laterocervicalia strongly enlarged and convex, placed below and sideways the widely exposed cervical membrane (Fig. 6A–D, 7A–D, **lcs**), reaching posterior head region. Pronotum (Fig. 6A–C, 7A, C, **prn**) small and short but distinctly visible from above. Pleural ridges of pro-, meso- and metathorax (Fig. 6C, D, 7C, D, **plr1, plr2, plr3**) distinct, nearly straight in former segments, but metapleural ridge strongly bent posterad, thus articulation with dorsal tip of coxa shifted posteriorly. Differentiation of propleuron into proepisternum (Fig. 6C, D, 7C, D, **eps1**) and proepimeron (Fig. 6C, D, 7,C, D, **epm1**) distinct; proepimeron approximately 1.5-times as wide as proepisternum, with irregular trapezoid shape with ventral side

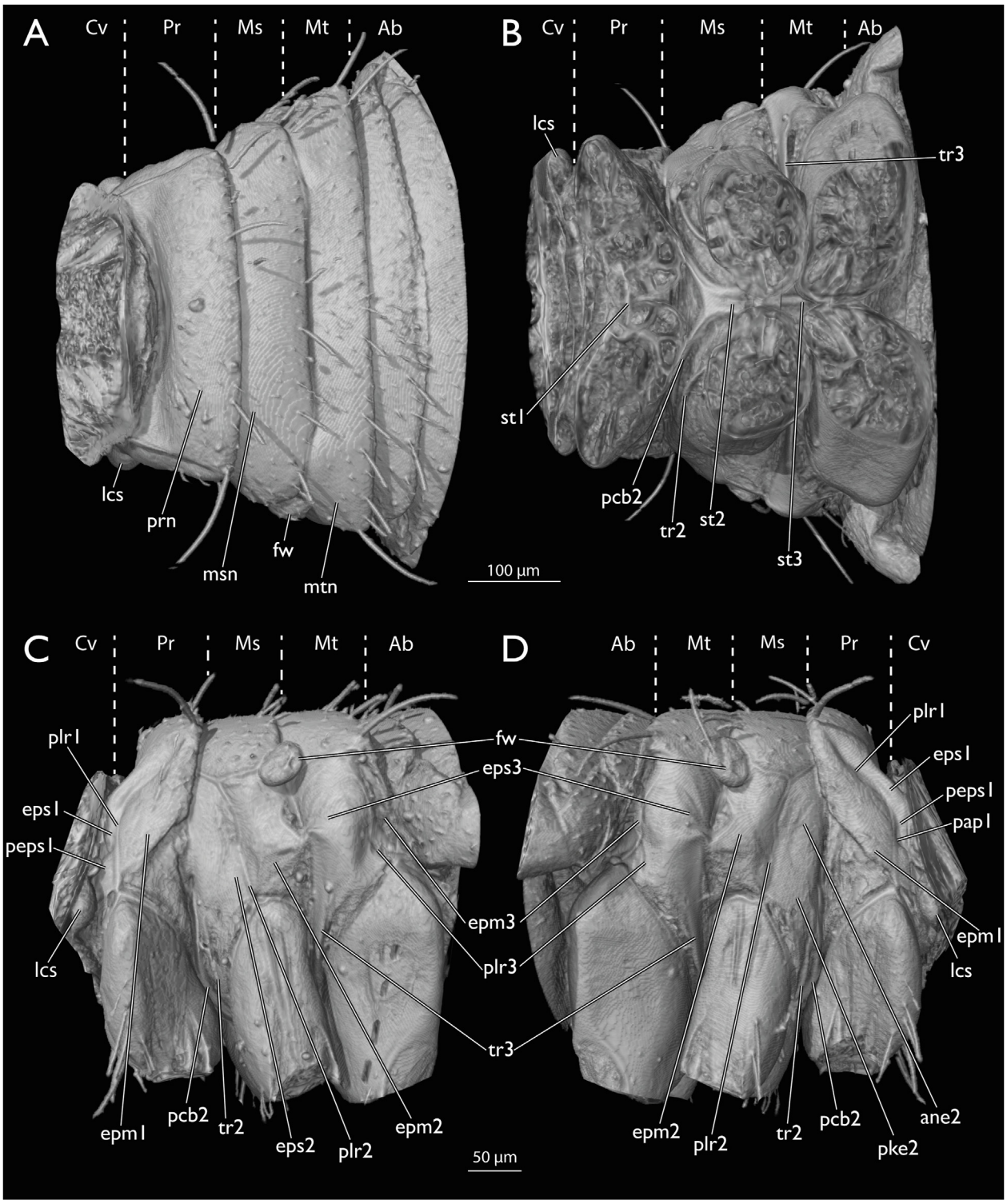

Fig. 15. 3D renders based on SR-µCT of *C. guestfalica* (female), thorax. **A** Details of thorax in dorsal view; **B** Details of thorax in ventral view, same scale as A. **C** Details of thorax in left lateral view. **D** Details of thorax in right lateral view, same scale as C. Sections: Cv, cervix; Pr, prothorax; Ms, mesothorax; Mt, metathorax; Ab, abdomen. Abbreviations: epm1/2/3, epimeron of pro-, meso- or metathorax; eps1/2/3, episternum of pro-, meso- or metathorax; fw, forewing; lcs, laterocervical sclerite; msn, mesonotum; mtn, metanotum; pap1, pit of pleural arm of prothorax; pcb2, precoxal bridge of mesothorax; peps1, preepisternum of prothorax; plr1/2/3, pleural ridge of pro-, meso- or metathorax; prn, pronotum; st1/2/3, eusternum of pro-, meso- or metathorax; tr2/3, meso- or metatrochantin.

shortest. Distinct preepisternal sclerite (Fig. 6C, D, 7C, D, **peps1**) short, likely fused with dorsal episternum, with its apicoventral sclerite distinctly articulating with enlarged and hemispherical laterocervicalia (Fig. 6A–D, 7A–D, **lcs**). Prothoracic trochantin (Fig. 6C, D, 7C, D, **tr1**) possibly represented by small triangular sclerite adjacent to procoxa anteroventrally. External proeusternum possibly represented by small triangular plate (Fig. 6B and 7B, **st1?**), but most of prosternal region uniformly membranous.

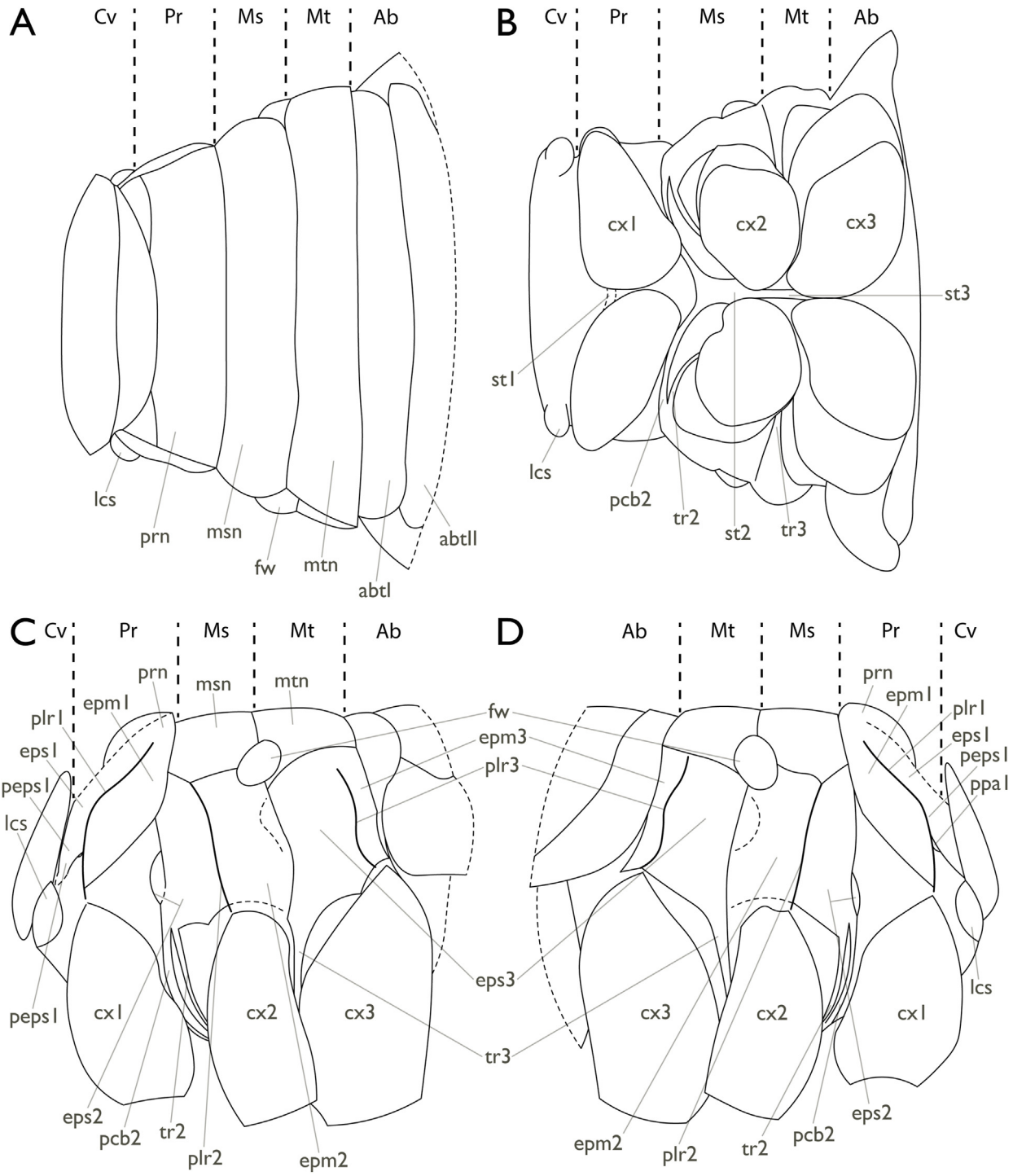

Fig. 16. Line drawings of the thorax of *C. guestfalica* (female), thorax. **A** Details of thorax in dorsal view; **B** Details of thorax in ventral view. **C** Details of thorax in left lateral view. **D** Details of thorax in right lateral view. Abbreviations: epm1/2/3, epimeron of pro-, meso- or metathorax; eps1/2/3, episternum of pro-, meso- or metathorax; fw, forewing; lcs, laterocervical sclerite; msn, mesonotum; mtn, metanotum; pap1, pit of pleural arm of prothorax; pcb2, precoxal bridge of mesothorax; peps1, preepisternum of prothorax; plr1/2/3, pleural ridge of pro-, meso- or metathorax; prn, pronotum; st1/2/3, eusternum of pro-, meso- or metathorax; tr2/3, meso- or metatrochantin.

Mesonotum largest dorsal thoracic element. Median lobe of scutum (Fig. 6A and 7A, **sctm2**), paired lateral lobes (Fig. 6A and 7A, **sctl2**), and scutellum (Fig. 6A and 7A, **scl2**) only weakly differentiated from each other; parapsidial sulci not visible; scutoscutellar suture (Fig. 6A and 7A, **sss2**) indistinct but present (Fig. 6C, D, 7C, D, **paa2**). Prealar arm present. Mesopleuron subdivided into wider and larger anterior anepisternal portion and smaller quadrangular posterior mesepimeron (Fig. 6C, D, 7C, D, **epm2**). Mesothoracic episternum clearly differentiated into dorsal anepisternum (Fig. 6C, D, 7C, D, **ane2**) and ventral preepisternum+katepisternum (Fig. 6C, D, 7C, D, **pke2**) by anapleural sulcus (Fig. 6C, D, 7C, D, **aps2**). Wide precoxal bridge (Fig. 6B–D, 7B–D, **pcb2**) placed anteriorly below preepisternum+katepisternum and narrow mesotrochantin posteriorly (Fig. 6B–D, 7B–D, **tr2**). Precoxal bridge of mesothorax

Fig. 17. Tree based on MP analysis. State transition was reconstructed and based on the character description and matrix in supplementary files S2 and S3. Full squares represent non-homoplasious apomorphies. Bremer support values (without implied weighting) included in supplementary file S8. Most important BS values: Trogiomorpha *s.l.* BS = 3, Atropetae BS = 3, Trogiidae BS = 1, Psoquillidae BS = 1, Lepidopsocidae BS = 2.

fused ventrally with mesosternal plate. Mesosternal plate (Fig. 6B and 7B, **st2**) large and triangular, located in front of mesocoxae; medially divided by longitudinal line or folded into two symmetric parts; lateral mesosternal portion bent towards median line, thus narrow membranous strip separating large triangular plate from smaller triangular region located close to anterior mesocoxal margin (Fig. 6B and 7B).

Metanotum smaller than mesonotum, with dorsal region appearing largely undifferentiated, likely due to poor preservation; small scutellum (Fig. 6A and 7A, **scl3**) separated from scutum by indistinctly visible scutoscutellar suture (Fig. 6A and 7A, **sss3**) as semicircular sclerite; metascutum divided into median lobe (Fig. 6A and 7A, **sctm3**) and paired lateral lobes (Fig. 6A and 7A, **sctl3**), but external parapsidial sulci not clearly visible. Anterior metapleural region clearly differentiated into ventral quadrangular sclerite formed by preepisternal and katepisternal fusion (Fig. 6C, D, 7,C, D, **pke3**), and slightly smaller dorsal anepisternum (Fig. 6C, D, 7C, D, **ane3**); both portions of anterior region separated by narrow strip-like membranous region; smaller posterior portion represented by narrow and bent Y-shaped metepimeron (Fig. 6C, D, 7C, D, **epm3**). Trochantins of meso- and metathorax not visible. Metasternum (Fig. 6B and 7B, **st3**) represented by longitudinal narrow sclerite in front of metacoxae; process formed by extension at contact zone with coxae (Fig. 6B and 7B, **stp3**) apparently functioning as ventral

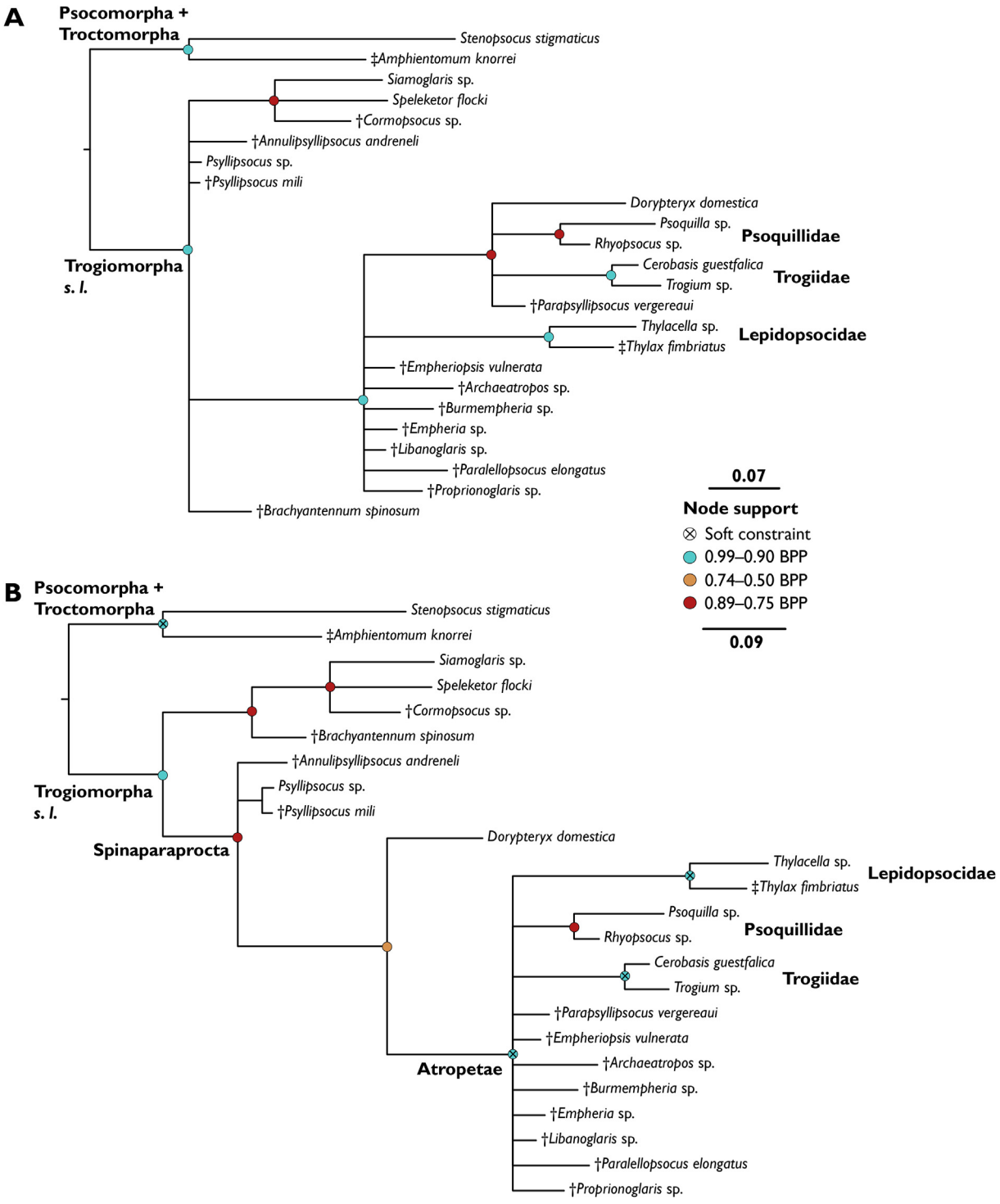

Fig. 18. Phylogenetic trees based on all 58 characters without (**A**) and with (**B**) soft constraints. Node support shows Bayesian Posterior Probability colored in color.

metacoxal articulation; metasternum widening again between posterior metacoxal portion (Fig. 6B and 7B). Meso- and metasternum apparently connected by longitudinal sclerotized strip (Fig. 6B and 7B). Thoracic endoskeletal structures not preserved.

Forewings (Fig. 1A, B, 10A) of macropterous specimen reaching beyond abdominal apex. Wings hyaline, only areas surrounding veins slightly pigmented, brownish. Fore wing venation of specimen symmetric. Microscopic setation of forewing margin not visible or absent. All veins of forewing with single row of setae except CuP, where setae are missing. Subcostal vein only faintly visible, relatively short, not reaching anterior wing margin, ending in wing membrane. Basiradial cell with four corners, moderately elongated. Radial cell hexagonal, with posterior vein (part of R1) of pterostigma shortest and with three subparallel sides. Distal region of R1 strongly bent anterad, thus forming almost right angle with proximal portion. Pterostigma trapezoid, with same degree of sclerotization as remaining forewing membrane, but slightly darker; base of pterostigma forming anterior vein of radial cell

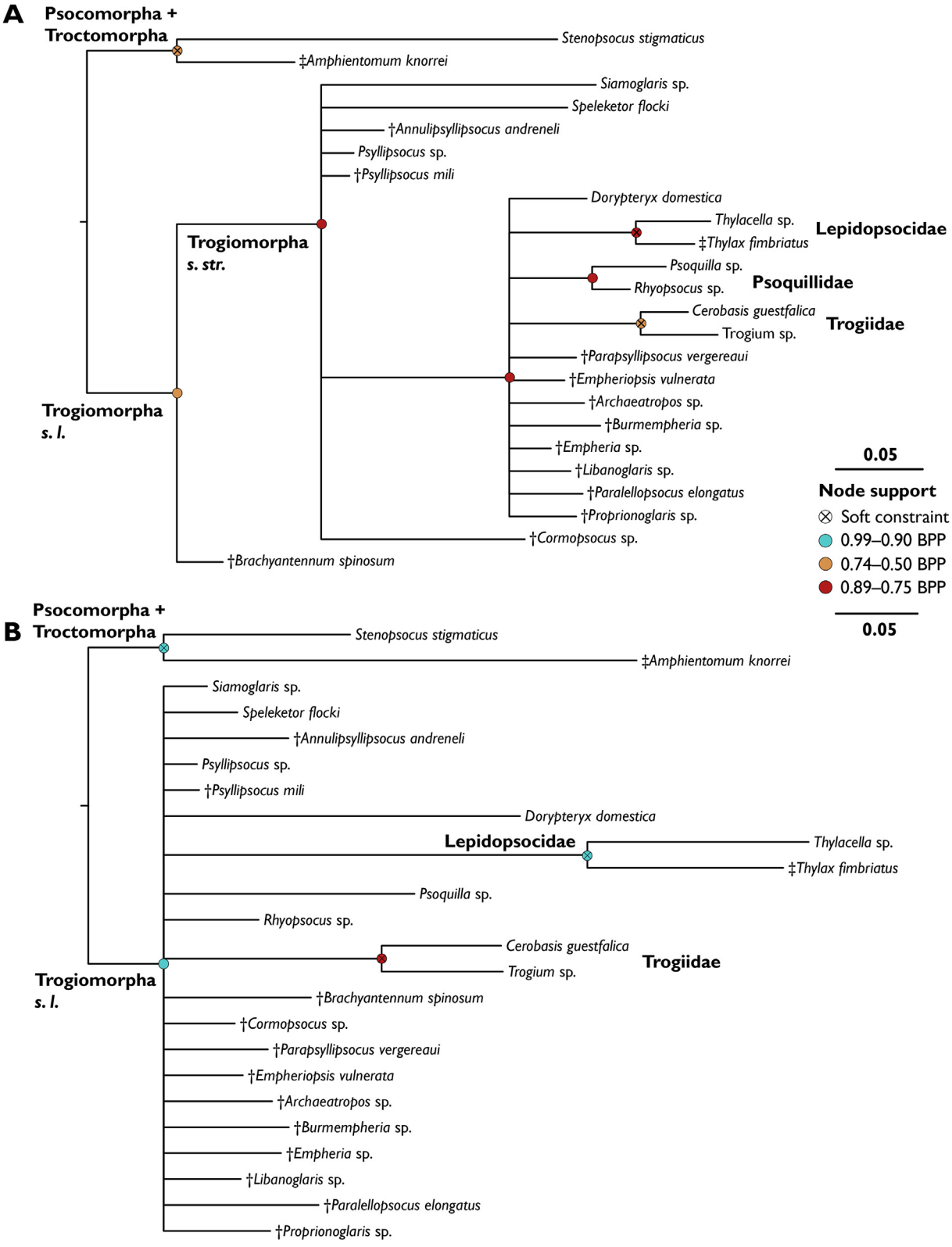

Fig. 19. Phylogenetic trees (both soft constrained) based on selection of characters: (**A**) only body characters (all wing characters constrained) and (**B**) only wing characters (all body characters constrained). Node support shows Bayesian Posterior Probability colored in color.

relatively short; anterior side of pterostigma also short, ca. 4-times as long as ventral vein (R1); middle portion of basal vein of pterostigma slightly curved, with two macrosetae; curvature of distal vein less distinct than that of basal vein; basal vein with four macrosetae and approximately as long as proximal vein; distal vein of pterostigma only slightly curved. Vein Rs forked. Both R2+3 and

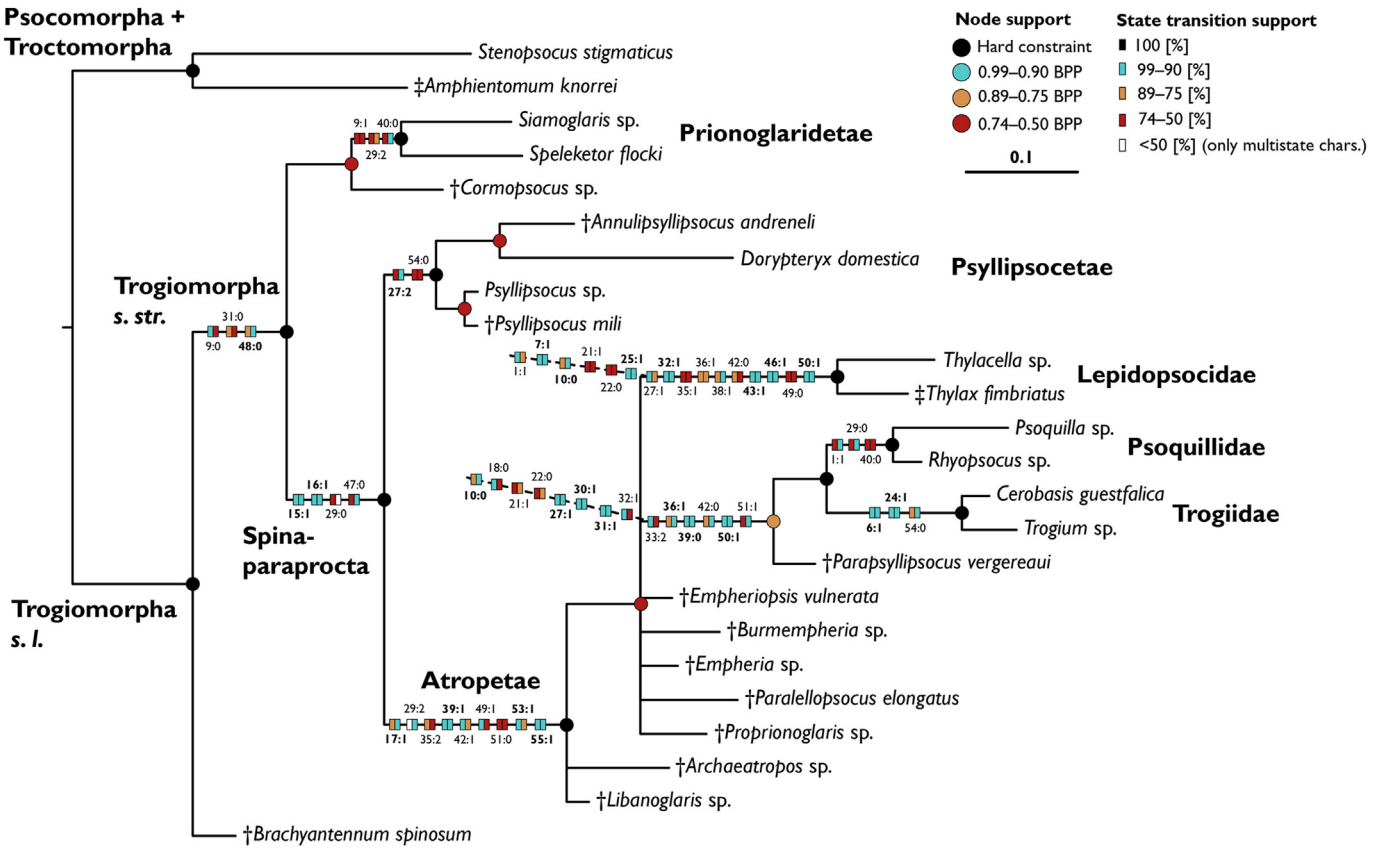

Fig. 20. Summary phylogram from the Bayesian phylogenetic analyses using constraints all major families and taxa above family level. The characters and states correspond to the ones of the matrix and description. Color code for Bayesian posterior probability for state transition. The non-homoplasious apomorphies (in bold) with high support (>90 %) are for: **Trogiomorpha (excl. †*Brachyantennum*)**: Absence of ctenidiobothria on first tarsomere of hindleg (48:0); **Atropetae**: Spur sensillum on mx2 present (17:1), Membranous region of forewing covered with many setae (or scales) (39:1), Paraproctal spine present (53:1), Female external valves long and thin (55:1). **Lepidopsocidae**: Distance of ocelli more distant, lateral ocellus closer to compound eye than to coronal sulcus (7:1), Forewing pointed apically (25:1), Hindwing pointed apically (43:1), Vein A unbranched in hindwing (46:1). **Psoquillidae** + **Trogiidae**: Cross vein r1-rs in forewing absent (30:1), Triangular pterostigma (31:1), Forewing membrane glabrous (39:0). **Trogiidae**: Ocelli absent (6:1), Forewings reduced in length (24:1).

R4+5 curved anterad apically. Tip of R2+3 and R1 widely separated. Cross vein between R1 and Rs present. Rs fused with M over short distance. M split into three subcomponents; M3 slightly bent posterad, with different angle than M1 and M2, also almost straight, in contrast to slightly curved M1 and M2. Base of CuA short. Areola postica subtriangular, with distal vein approximately three times longer than basal vein. CuP with equidistant rib-like structures; cuticle slightly thicker where tip of CuP meets wing margin. Tips of CuP and A1 separated, merging with wing margin with distance of ca. 40 μm. A1 very faint, ending at wing margin, close to posteriorly thickened cuticle. A2 absent. Retinaculum present, consisting of four curved spines (Fig. 10B).

Hindwings (Fig. 1A, B, 10A) glabrous. Proximal section of Sc short. Basiradial cell of similar shape as in forewing but shorter and more distinctly curved posterad. R1 reaches anterior wing margin. Rs and M forked, fused over short proximal distance. CuA weakly curved apically. CuP almost straight and only weakly bent apically. A1 strongly bent, reaches wing margin widely separated from CuP. A2 very short and straight, splits at common stem from A1.

Fore- and middle legs of similar size. Hindlegs distinctly elongated. Procoxae and mesocoxae laterally oriented, metacoxae posteriorly. Pearman's organ not visible (Fig. 1E). All tibiae equipped with two thick apical spurs. All legs with three tarsomeres (Fig. 1D and 3A, B). Claws with one distinct preapical tooth (Fig. 1D). Pulvilli or other attachment devices absent. Metafemora with deeply incised, distally widening membranous apical region (Fig. 2B); distal membranous regions of pro- and mesofemora only moderately incised.

Abdomen severely damaged and poorly preserved, especially posteroventral region; shape ovoid, but segmentation not clearly recognizable. Clunium unmodified (Fig. 2B, **cl**). Paraprocts (Fig. 2B, **pap**) semicircular; paraproctal spine absent; sensillum on paraproct not visible. Subgenital plate and genitalia not recognizable, but likely female.

Soft tissue not preserved, or indistinguishable from amber matrix in μCt scan.

Measurements (holotype) [length in mm]. Body: 1.40. Antenna: total: 1.26 (left), 1.40 (right). Scape: 0.06. Pedicel: 0.06. f1: 0.06. f2: 0.07. f3: 0.09. Head: 0.12. Cervix: 0.16. Thorax: 0.34 (without cervix). Abdomen: 0.78. Forewing: 1.35. Hindwing: 0.88. Hindleg: F: 0.32. T: 0.51. t1: 0.17. t2: 0.05. t3: 0.05.

Description of paratype female **SMF Be 14667**.

Fig. 8A–G, 10A, D.

Head with vestiture of long setae (Fig. 8A–C). Epistomal ridge preserved and wide (Fig. 8C, **esr**). Left antenna with 14 antennomeres, right antenna with 17 (Fig. 8A). Maxillary palpomeres without spur sensillum (Fig. 8D). Proximal Sc of forewing very short (Fig. 8B). Tibiae and first and second tarsomeres of each leg with two thick apical spurs (Fig. 8G). Ovipositor consisting of paired, long, and pilose external valves (3rd valvulae) (Fig. 8E and 10D, **exv**) and short triangular dorsal valves (Fig. 8E and 10D, **dov**). Dorsal valve with single seta on apex.

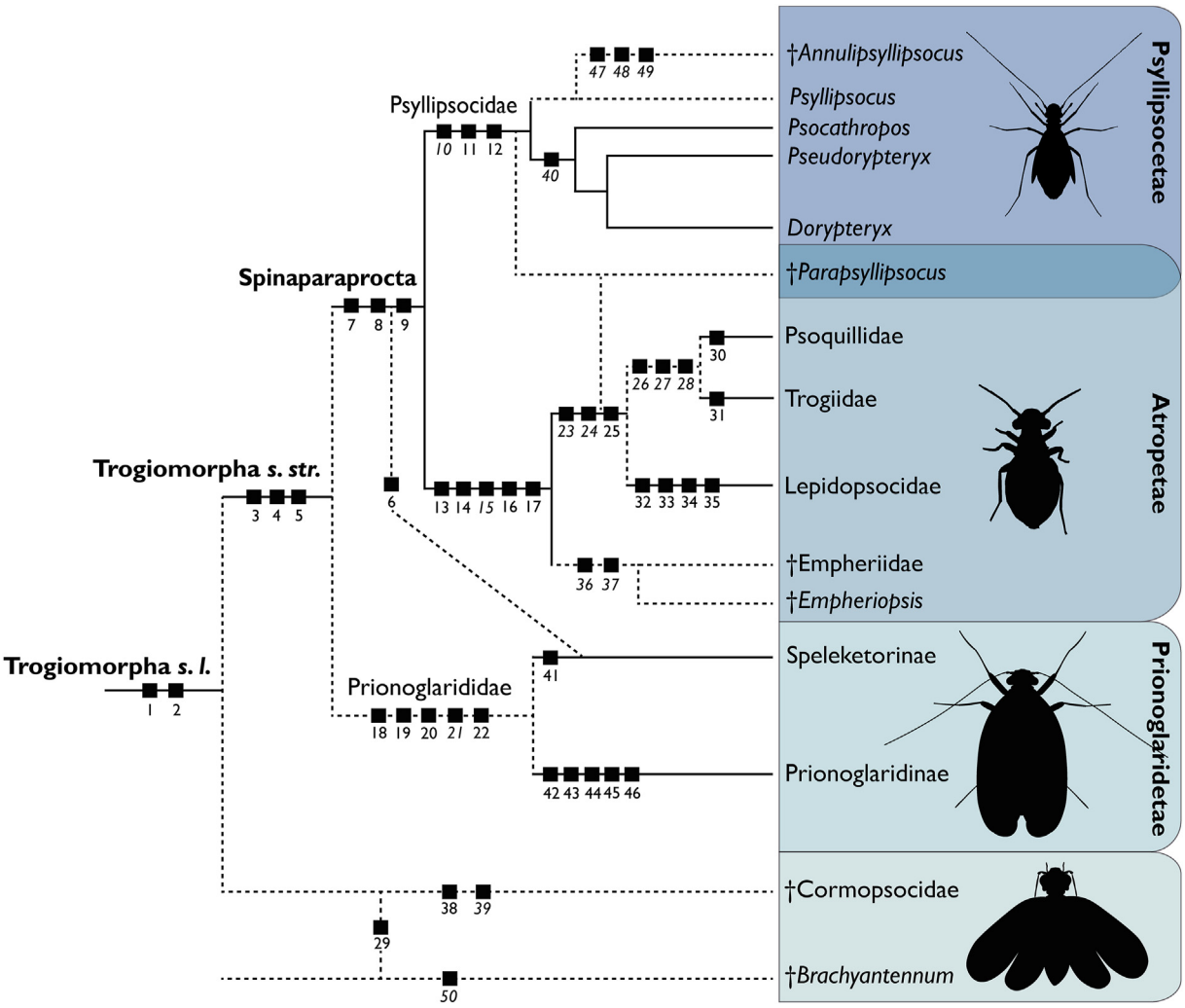

Fig. 21. Simplified phylogenetic tree showing the most plausible relationships in Trogiomorpha based on Yoshizawa et al. (2006), de Moya et al. (2021), Li et al. (2022), our analyses, and our critical discussion (see 4.1 and supplementary file S2). Solid lines indicate well supported monophyletic relationships. Dotted lines show unclear relationships (possible paraphyly). Homoplasious character states are marked in italics. Putative apomorphies (as square symbol): **Trogiomorpha *s.l.*:** (1) Strongly enlarged and convex laterocervical sclerites. (2) Short subgenital plate, covering basal portion of ovipositor. **Trogiomorpha *s. str.*:** (3) Partial intraclypeal fusion (?). (4) Enlarged v3, that are close to the ventral midline of abdomen. (5) v1 and v2 strongly reduced (reduction of both valves likely homoplasious throughout Trogiomorpha, as well developed, strongly sclerotized v1 and v2 are present in *Psyllipsocus stupendus* (Lienhard and García Aldrete, 2016)). **Speleketorinae** + **Spinaparaprocta:** (6) Spur sensillum on mx2 present. **Spinaparaprocta:** (7) Distally widened mx4. (8) Paraproctal (anal) spine present. (9). Phallosome opened anteriorly. **Psyllipsocetae:** (10) Reduced vein Sc in forewing (homoplasious). (11) Absence of a row of anteroventral spines on profemur (?). (12) Modified spermathecal sac with sclerotizations of spermathecal duct and presence of accessory vesicle. **Atropetae:** (13) Forewing M1+2 longer than M2. (14) Areola postica long, length exceeding half of maximum width of forewing. (15) Presence of pulvillus (groundplan?, homoplasious). (16) v3 elongated and partially joined together on midline by a membrane. (17) v1 completely reduced and v2 strongly reduced. **Prionoglaridetae:** (18) Reduced number of antennal flagellomeres (≤13). (19) Lacinia simplified or strongly reduced and virtually absent in adults. (20) Broad and rounded forewings. (21) Forewing veins glabrous (homoplasious). (22) Phallosome modified to cuticular sac with a pair of posterolateral processes. **Lepidopsocidae** + **(Psoquillidae** + **Trogiidae):** (23). Reduced proximal vein Sc in forewing (homoplasious). (24). Radial cell absent in forewing (homoplasious). (25) Modified spermathecal sac with one or two glandular accessory sacs. **Psoquillidae** + **Trogiidae:** (26) Forewing veins Rs and R1 not connected by cross vein (homoplasious). (27) Pretarsal claws lack preapical tooth (or teeth) (homoplasious). (28) Pulvillus apically widened (homoplasious?). †**Cormopsocidae** + †***Brachyantennum*:** (29) Simplified lacinial tip, lacking teeth, or cusps. **Psoquillidae:** (30) Accessory bodies situated at the opening of spermatheca. **Trogiidae:** (31) Forewing veins strongly reduced and always without veins, sometimes completely absent. **Lepidopsocidae:** (32) Body and wings covered with scales (only strongly setose in Thylacellinae). (33) Lateral ocelli distant from each other, closer to compound eye than to each other. (34) Forewing pointed. (35) Hindwing pointed. †**Empheriidae:** (36) Forewing veins setose (strongly homoplasious). (37) Forewing membrane setose (homoplasious). †**Cormopsocidae:** (38) Dorsally extended vertex. (39) Forewing veins glabrous (homoplasious). ***Psocathropos*** + **(*Pseudorypteryx* + *Dorypteryx*):** (40) Absence of spur sensillum on mx2 (homoplasious). **Speleketorinae:** (41). Presence of trichobothria on legs. **Prionoglaridinae:** (42) Paurometamorphosis of mouthparts and claws. (43) Postclypeus reduced and not bulging. (44) Complete reduction of water-vapor absorption apparatus. (45) Asymmetrical pretarsal claws. (46) Presence of membranous vesicle on inner side of claw. †***Annulipsyllipsocus*:** (47) Broad basiradial cell in forewing (homoplasious). (48) Broad radial cell in forewing (homoplasious). (49) Anteriorly bulging vein R1 in forewing (homoplasious). †***Brachyantennum*:** (50) Presence of ctenidiobothria on first mid- and hind-tarsomere (homoplasious?).

Measurements [length in mm]. Body: 1.43. Forewing: 1.83. Ovipositor: v2: 0.07. v3: 0.22.

Description of paratype female **CAU-BA-LFY-24002**.

Fig. 9A and B 10A, E.

Poorly preserved. Last maxillary palpomere very distinctly wedge-shaped (Fig. 9A). Galeae apparently preserved with sclerotized paramedial region (Fig. 9A). Tip of right lacinia with lateral cusp bidentate and inner cusp developed as simple acuminate tooth (Fig. 9A). Ovipositor long, with two distinct cylindrical valvulae and additional triangular lobe; rounded tip likely represents apices of both external valvulae (Fig. 9B and 10E, **exv**); triangular lobe ventrally connected with cylindrical lobes,

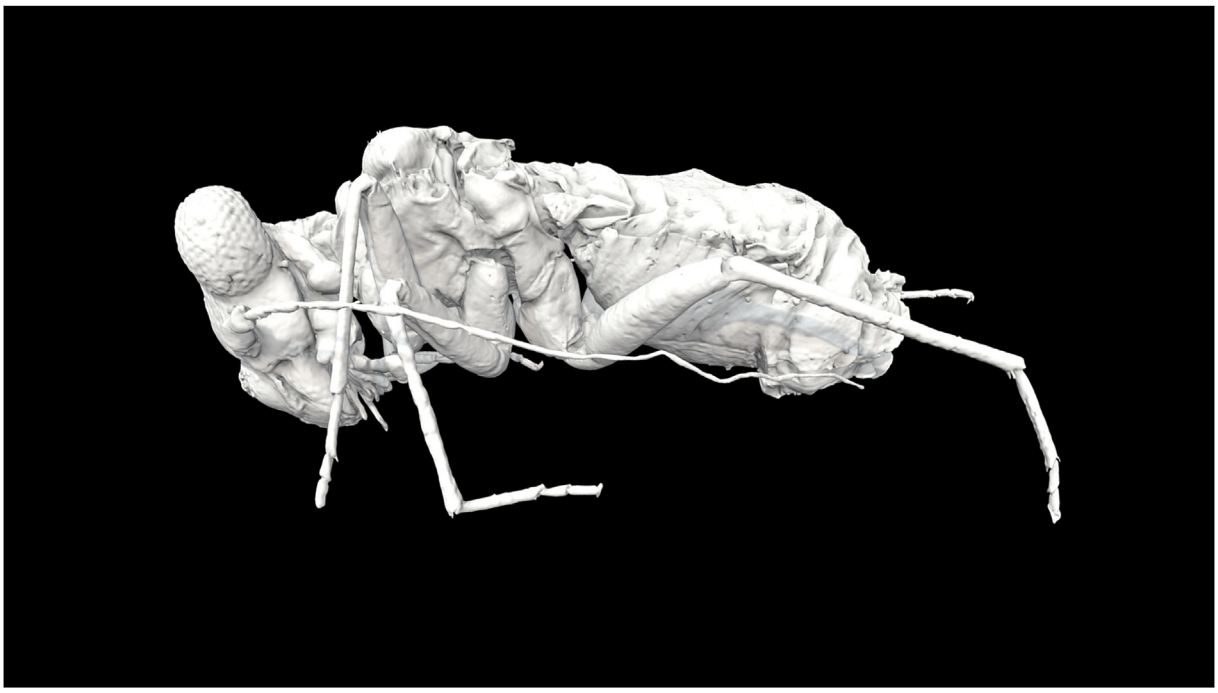

Model 1. 3D Model of holotype (= cybertype) of †*Psyllipsocus mili* **sp. nov.** https://sketchfab.com/3d-models/psyllipsocus-mili-cybertype-holotype-7459e8dcd208424ca12168e36138aa0f.

potentially homologous with dorsal valvula (Fig. 9B and 10E, **dov**).

Measurements [length in mm]. Body: 1.1 (body heavily damaged). Forewing: 1.2 Hindwing: 1.0. v2: 0.05. v3: 0.15.

Description of paratype male **CAU-BA-LFY-24001**.

Fig. 9C, D, 10A, B, D.

Large muscle M. clypeopalatalis (0ci1) possibly preserved, likely indicated by bands externally visible on postclypeus (Fig. 9C). Pterostigma slightly more pigmented (light brown) than in other specimens (Fig. 9C). Phallosome composed of pair of lateral parameres (Fig. 9D and 10C, **par**), slightly converging distally; widening at their distal tip and weakly turned outwards, ending with median notch at apex. Closely associated with lobe-shaped, quadrangular hypandrium (Fig. 9D and 10C, **hyp**); lateral sides apparently differentiated as ovoid projections from median furrow-like portion of hypandrium; median and lateral areas possibly representing phallic cradle. Endophallic tube (Fig. 9D and 10C, **enph**) present as complex oval structure; only apical portion of struts located outside of phallic cradle.

Measurements [length in mm]. Body: 1.55. Forewing: 1.4. Hindwing: 1.1.

3.1.3. *Key to extinct species of Psyllipsocidae*

Applicable to all presently described extinct species.

1. (A) Posterior forewing vein of pterostigmal cell distinct (distinctly quadrangular), ca. half as long as posterior vein (distal Sc vein). (B) Proximal pterostigmal vein (Sc) much shorter than distal pterostigmal vein. (C) Species known from Eocene French Oise amber … †***Psyllipsocus eocenicus*** **Nel, Prokop, De Ploeg & Millet, 2005**
   — (A) Posterior forewing vein of pterostigmal cell indistinct but present (indistinctly quadrangular), much shorter than posterior vein (distal Sc vein). (B) Proximal pterostigmal vein (Sc) much shorter than distal pterostigmal vein. (C) Species known from Eocene Chinese Fushun amber … †***Psyllipsocus fushunensis*** **(Zhang, Nel, Azar & Wang, 2016)**
   — (A) Posterior forewing vein of pterostigmal cell strongly reduced or missing (distinctly triangular). (B) Proximal pterostigmal vein (Sc) almost as long as distal pterostigmal vein. (C) Species known from Cretaceous Siberian Taimyr amber … †***Psyllipsocus inclusus*** **(Vishnyakova, 1975)**
   — (A) Pterostigma triangular or quadrangular. (B) Proximal pterostigmal vein (Sc) not nearly as long as distal pterostigmal vein. (C) Species known from Cretaceous Burmese amber … **2**
2. (A) Pterostigma triangular. (B) Radial cell distinctly broader than high. (C) Radial cell pentagonal … **3**
   — (A) Pterostigma quadrangular. (B) Radial cell either higher than wide or approximately as wide as high. (C) Radial cell hexagonal … **4**
3. (A) Fore- and hindwing without pigmentation. (B) Profemora cylindrical and not thickened. (C) Pretarsal claw with preapical tooth … †***Annulipsyllipsocus andreneli*** **Hakim, Azar, Maksoud, Huang & Azar, 2018**
   — (A) Fore-and hindwing with dark spot covering most of the surface. (B) Profemora thickened and enlarged. (C) Pretarsal claw without preapical tooth … †***Annulipsyllipsocus inexspectatus*** **Hakim, Azar, Maksoud, Huang & Azar, 2018**
4. (A) Flagellomeres without secondary annulation … **5**
   — (A) Flagellomeres with secondary annulation … **6**
5. (A) Distance between tip of M2 and M3 approximately the same as between M1 and M2 in forewing. (B) Hindwing R1 simply curved. (C) M2 in hindwing curved outwards towards tip … †***Psyllipsocus myanmarensis*** **Jouault, Yoshizawa, Hakim, Huang & Nel, 2021**
   — (A) Distance between tip of M2 and M3 approximately 25 % larger than between M1 and M2 in forewing. (B) Hindwing R1 with sigmoidal curvature. (C) M2 in hindwing curved inwards towards tip … †***Psyllipsocus yoshizawai*** **Álvarez-Parra, Peñalver, Nel & Delclòs, 2020**

Model 2. 3D Model of thorax of holotype (= cybertype) of †*Psyllipsocus mili* **sp. nov.** https://sketchfab.com/3d-models/thorax-of-psyllipsocus-mili-female-03617adde3f84f7594087868e9865889.

6. (A) mx2 with conical sensillum. (B) Pterostigma broader than high. (C) R2+3 and R4+5 in forewing almost straight or weakly curved … †***Psyllipsocus yangi*** **Liang & Liu, 2021**
   — (A) mx2 without conical sensillum. (B) Pterostigma higher than broad. (C) R2+3 and R4+5 in forewing distinctly curved anterad … †***Psyllipsocus mili*** **Weingardt, Liang & Yoshizawa**

3.2. Thoracic morphology of extant Trogiomorpha

3.2.1. Thoracic morphology and selected characters of D. domestica (Smithers, 1958) (Psyllipsocetae: Psyllipsocidae) and C. guestfalica (Kolbe, 1880) (Atropetae: Trogiidae)

For comparison, we examined two species of the suborder Trogiomorpha, one belonging to the same family as *Psyllipsocus* (*D. domestica*, Fig. 11A–F, Models 3, 4) and the other one to Trogiidae of the infraorder Atropetae (*C. guestfalica*, Fig. 14A–F, Models 5, 6).

Dorypteryx domestica **(**Smithers, 1958**) (Psyllipsocetae: Psyllipsocidae):** The laterocervicalia (Figs. 12 and 13, **lcs**) in *D. domestica* are strongly enlarged and convex. They are vertically oriented, with the largest distance between the dorsalmost and ventralmost point of this sclerite. A bar-shaped ventral extension extends further anterad where it probably articulates with the postoccipital condyles of the head (Figs. 12 and 13, **vlcs**). The membranous cervical region is strongly exposed and long. The pronotum (Figs. 12 and 13, **prn**) is rather simple and short. It is laterally continuous and fused with the pleural region. The propleural region consists of the anterior small episternum (Figs. 12 and 13, **eps1**) and the posterior epimeron, which is several times larger (Figs. 12 and 13, **epm1**). The episternum is ventrally separated from the trapezoid preepisternum (Figs. 12 and 13, **peps1**). The strongly developed pleural ridge (i.e. the corresponding internal sulcus) separates the epimeron from the episternal region (Figs. 12 and 13, **plr1**). The preepisternum articulates anteriorly with the laterocervical sclerite (Figs. 12 and 13). The pleural ridge forms the dorsal articulation of the procoxa. The procoxa is approximately as large as the mesocoxa but is located slightly more dorsally. The propleural region is otherwise membranous and allows flexible movements between the prothorax and head, and between the prothorax and pterothorax. The protrochantin is not visible in the 3D-renders but is likely present. The prosternum is mostly membranous and anteriorly continuous with the cervix. A small triangular area with laterally pointed arms possibly represents the proeusternum (Figs. 12 and 13, **st1**) and the ventral articulation of the procoxae. This sclerite is only very weakly sclerotized and appears almost membranous in the 3D-renders and μCT-scans. The prospinasternum is possibly externally visible as a slight membranous impression in the posterior prosternal region (Figs. 12 and 13, **fst1?**). The transition between pro- and mesothorax is a distinct waist-like constriction, and likely contributes to the high intrinsic flexibility of the prothorax.

The complex mesothorax is the largest thoracic segment. The scanned specimen is brachypterous with the forewings not extending beyond the abdominal apex. Even though the wings are reduced, the dorsal sclerotized region is only moderately simplified. The mesoscutum and entire mesonotum are hexagonal in dorsal view. The mesoscutum is almost uniform without any clearly delimited subregions. The anterior mesocutal lobe is almost rectangular but not distinctly separated from the rest of the mesoscutum by an external suture. Likewise, the lateral scutal lobes are not separated from the rest of the scutum. The anterior notal wing process is projecting from the lateralmost point of the lateral lobes. The posterior notal wing process is projecting from the posterior portion of the mesonotum at its lateralmost point and is located slightly below the anterior process. The scutellum is trapezoid and separated from the rest of the mesoscutum by the transverse scutoscutellar suture (Figs. 12 and 13, **sss2**). An anterolateral extension, the mesothoracic prealar arm (Figs. 12 and 13, **paa2**), runs ventrad until it reaches the mesanepisternum (Figs. 12 and 13, **ane2**). The presence or absence of the basalare and subalare cannot be assessed based on 3D renders. The anterior mesanepisternum (Figs. 12 and 13, **ane2**) is large and differentiated into a larger

Model 3. 3D Model of *Dorypteryx domestica*, male. https://sketchfab.com/3d-models/dorypteryx-domestica-male-3ab6a785e7784e70afd31a7bdeb03ab4.

posterior part and a small anterior region delimited by a thick external furrow. Ventrally the mesokatepisternum + mesopreepisternum (Figs. 12 and 13, **pke2**) are not clearly differentiated from the mesanepisternum and it is possible that both regions are fused. The mesotrochantin, present as a long and thin ventral extension of the mesokatepisternum + mesopreepisternum (Figs. 12 and 13, **tr2**), articulates ventrally with the mesocoxa. Anterior to the mesotrochantin the narrow precoxal bridge (Figs. 12 and 13, **pcb2**) splits from the area of the meskatepisternum+mesopreepisternum and merges with the mesothoracic eusternum. The mesepimeron (Figs. 12 and 13, **epm2**) is narrower than the mesanepisternum and is delimited from it by the pleural ridge and its corresponding external sulcus (Figs. 12 and 13, **plr2**). The ventral tip of the ridge articulates with the dorsal mesocoxal margin. The mesothoracic eusternum (Figs. 12 and 13, **st2**) is anteriorly triangular and strongly sclerotized. Posteriorly it articulates with the mesocoxae with short lateral processes (Figs. 12 and 13). Posterior to the mesocoxa it is strongly narrowed and directly continuous with the metasternum.

The metathorax is only slightly larger than the prothorax. The mesoscutum is divided by two large lateral semicircular elevations. A metascutellum is not developed. The metanepisternum is large (Figs. 12 and 13, **ane3**). An indistinct impression is present between this sclerite and the ventral metakatepisternum + metapreepisternum (Figs. 12 and 13, **pke3**). The narrow and long trochantin (Figs. 12 and 13, **tr3**) projects ventrally from the metakatepisternum+metapreepisternum and articulates with the basal margin of the metacoxa. The external sulcus corresponding with the pleural ridge (Figs. 12 and 13, **plr3**) delimits the anterior episternal regions from the metepimeron (Figs. 12 and 13, **epm3**). It is approximately Y-shaped and represents the posteriormost pleural thoracic sclerite. Ventrally, the pleural ridge (Figs. 12 and 13, **plr3**) articulates with the dorsal process of the metacoxa. The metathoracic eusternum (Figs. 12 and 13, **st3**) is very narrow and anteriorly confluent with the mesosternum. It apparently articulates with the dorsomedial metacoxal margin with a short process (Figs. 12 and 13), with the metasternum widening posterior to this configuration. The metacoxa have a pronounced posterior orientation.

Measurements [lengths in mm]: Body = 1.45. Forewing = 0.95.

Cerobasis. guestfalica **(**Kolbe, 1880**) (Atropetae: Trogiidae):** The latero-cervicalia (Figs. 15 and 16, **lcs**) are anteroposteriorly compressed and oval and a ventral bar-shaped extension is absent. They are smaller than in *D. domestica* or †*P. mili* **sp. nov.** The cervical region is shortened and not exposed. The specimen we examined is micropterous, with only scale-like forewings (Figs. 15 and 16, **fw**). The entire thorax is compressed, structurally simplified, with only few exposed membranous areas. All three segments have approximately the same size (length and width). All three coxal pairs are positioned at the same height. The pro-, meso-, and metanota (Figs. 15 and 16, **prn**, **msn**, **mtn**) are trapezoid, continuous with the corresponding sclerotized pleural regions, and not subdivided into different areas. The meso- and metascutellum are absent. The pleural ridges (Figs. 15 and 16, **plr1**, **plr2**, **plr3**) of all three segments are distinctly developed.

The preepisternum (Figs. 15 and 16, **peps1**) of the prothorax is not clearly differentiated. The oval and very narrow proepisternum (Figs. 15 and 16, **eps1**) apparently articulates with the laterocervical sclerite. The pleural ridge (Figs. 15 and 16, **plr1**) separates it from the larger proepimeron (Figs. 15 and 16; **epm1**). A protrochantin is not visible in the μCT-scan. The prosternum (Figs. 15 and 16, **st1**) is X-shaped and the anterior processes articulate with the procoxae. The prospinasternum is not visible in the 3D reconstruction.

The mesepisternal (mesanepisternum, mesokatepisternum, mesopreepisternum) (Figs. 15 and 16, **eps2**) elements are not differentiated as individual structures. A weakly developed pleural ridge (Figs. 15 and 16, **plr2**) separates this unit from the mesepimeron (Figs. 15 and 16, **epm2**). Ventrally the mesotrochantin (Figs. 15 and 16; **tr2**) is differentiated as a long and narrow process, visibly separated from the mesepisternal region. It articulates with the ventral margin of the mesocoxa. A narrow precoxal bridge (Figs. 15 and 16, **pcb2**) is present and merges ventrally with the

Model 4. 3D Model of thorax of *Dorypteryx domestica*, male. https://sketchfab.com/3d-models/thorax-of-dorypteryx-domestica-male-74ccf7438b844e34ae252ddf10f4cdbd.

mesothoracic eusternum. The subtriangular mesothoracic eusternum (Figs. 15 and 16, **st2**) is anteriorly continuous with the narrow precoxal bridges and posteriorly with the mesothoracic eusternum (Figs. 15 and 16, **st3**). The metapleural sclerites are apparently fused to the mesosternal elements, without a membrane separating them.

The metepisternal (metanepisternum, metakatepisternum, metapreepisternum) elements (Figs. 15 and 16, **eps3**) are not differentiated from each other and only separated by a weakly developed pleural ridge (Figs. 15 and 16, **plr3**) from the metepimeron (Figs. 15 and 16, **epm3**). The metatrochantin (Figs. 15 and 16, **tr3**) is similar to the mesotrochantin, ventrally extending from the ventral margin of the metepisternal region as a narrow and long sclerite. The metepimeron is very narrow and small. The metathoracic eusternum (Figs. 15 and 16, **st3**) is strip-like. The orientation of the metacoxa is only weakly shifted posteriorly.

Measurements [lengths in mm]: Body: 1.5. Forewing: 0.04.

3.3. Phylogenetic results

3.3.1. Parsimony analysis

This analysis (Fig. 17) used *Stenopsocus* as predefined outgroup (placed as 1st taxon in matrix). After the initial analysis the implied weighting function was used (K = 3.0). Trogiomorpha *s.l.* was monophyletic with †*Brachyantennum* as sister to the remaining Trogiomorpha. The next branch contained both members of Prionoglaridiidae and †*Cormopsocus*. Psyllipsocidae was not monophyletic, with *Dorypteryx* placed inside of Atropetae. The remaining psyllipsocids were also not a clade, with †*Annulipsyllipsocus* placed as the first branch, †*Psyllipsocus mili* as the second, and *Psyllipsocus* sp. as the third. *Psyllipsocus* sp. was placed as sister to the Atropetae. Each of the three extant atropetan families Trogiidae, Psoquillidae and Lepidopsocidae were monophyletic. Trogiidae was sister to the rest of Atropetae including *Dorypteryx*. †*P. vergereaui* was sister to Psoquillidae, which in turn was sister to *Dorypteryx*. All "empheriids" included in the analysis formed a clade with Lepidopsocidae, with this family placed as sister to †*Empheria*. The first branch of the larger clade containing the empheriids and Lepidopsocidae was formed by †*Archaeatropos*+†*Libanoglaris*. As the Bremer support values were calculated without implied weighting, the topology was slightly different, i.e. less resolved (see supplementary file S8).

The Bremer support values (see supplementary file S8) were 1 for most branches, but 3 for the branch containing †*Brachyantennum* and the remaining Trogiomorpha, as well as BS = 3 for all Atropetae incl. *Dorypteryx*, and 2 for the branch with the two members of Lepidopsocidae. The topology differed (see supplementary files S8) from the tree shown in Fig. 17, with a polytomy (BS = 1) at the base of Trogiomorpha not resolving the splitting events for †*Brachyantennum*, Prionoglaridetae and Psyllipsocidae, and a polytomy between the Trogiidae (BS = 1)+Psoquillidae (BS = 1)+†*Parapsyllipsocus*+*Dorypteryx* clade. Lepidopsocidae (BS = 3) formed a polytomy (BS = 1) with †*Empheriopsis* + †*Empheria* + †*Paralellopsocus*+†*Proprionoglaris* (supplementary file S8). Both polytomies placed as sister groups (BS = 1).

The state reconstruction yielded 20 non-homoplasious apomorphies (see Fig. 17; supplementary file S9). The loss of ctenidiobothria on the first tarsomere (char. 48:0) of the hindleg is an apomorphy of Trogiomorpha *s. str.* The distal widening of the fourth maxillary palpomere (char. 16:1) is an autapomorphy of Spinaparaprocta, and the presence of the paraproctal spine (char. 53:1) an autapomorphy of Atropetae. Trogiidae are supported by the autapomorphic reduction of ocelli (char. 6:1) and forewings (char. 24:1), and the Lepidopsocidae by the acuminate apices of the fore- and hindwings (chars. 25:1., 43:1). The remaining non-homoplasious apomorphies are presented in the supplementary file 9.

3.3.2. Bayesian analyses

We performed five Bayesian analyses: (1) Topology search without constraints, (2) topology search with soft constraints on taxa with reasonably well supported systematic placement (see Yoshizawa et al., 2006; de Moya et al., 2021), (3) unconstrained topology search with wing-only characters, (4) unconstrained

Model 5. 3D Model of *Cerobasis guestfalica*, female. https://sketchfab.com/3d-models/cerobasis-guestfalica-female-71774e9d301b408ab3d23a228dd4e496.

topology search with body-only characters, and (5) ancestral state estimation with hard constraints. Performance statistics for these are reported in Table 1; no pathologies in the performance of the analysis were detected. The estimated Γ distribution was not exponential in any of the analyses, hence with little probability density at 0, indicating that the inclusion of Γ in the model was justified.

The trees presented in Figs. 18 and 19 were rooted on the (*Stenopsocus*+*Amphientomum*) − Trogiomorpha *sensu lato* branch (outgroup rooting). Rooting could have been performed on †*Brachyantennum* or a possible (†*Brachyantennum* + (*Stenopsocus*+*Amphientomum*)) − Trogiomorpha split, but more outgroups are necessary to determine the character state polarity unambiguously and to confirm the monophyly of the ingroup. Regardless, †*Brachyantennum* is supported as distinct from the remainder of the Trogiomorpha in the MP analysis, which we used as criterion for rooting. In analysis with wing characters excluded (Fig. 19A) and for BI ancestral state estimation (Fig. 20), †*Brachyantennum* was placed as sister to the remainder of Trogiomorpha.

†*Cormopsocus*, which was unconstrained in all four topology search analyses, clustered with *Siamoglaris* and *Speleketor* in the analysis including all characters with and without soft constraints (Fig. 18A and B). Psyllipsocetae are never recovered as monophyletic, as *Dorypteryx* clusters with Atropetae (Figs. 18A and 19A), sister to Atropetae (Fig. 18B) or in an unresolved polytomy of Trogiomorpha (Fig. 19B). Together, these results indicate considerable phylogenetic instability for this widespread taxon. There was no support for monophyly of either †Archaeatropidae or †Empheriidae, which clustered in a basal atropetan polytomy (Fig. 18A, B, 19A) or in an unresolved polytomy of Trogiomorpha (Fig. 19B). Psoquillidae and Trogiidae were weakly supported as a clade together with †*P. vergereaui* and *D. domestica* (0.52 Bayesian probability, BPP; Fig. 18A), were part of the atropetan (Figs. 18B and 19A) or trogiomorphan polytomy (Fig. 19B). Extant atropetan families were well supported.

Table 1
Performance statistics from MrBayes, where, LnL_i = "cold" chain arithmetic mean log likelihood for runs 1 and 2, PSRF = average potential scale reduction factor (Gelman and Rubin, 1992), ESS_{avg} = average estimated sample size for combined runs (10 % burnin), ESS_{min} = minimum ESS as before, and ESS_{max} = maximum ESS as before. All analyses ran for 2 M MCMC generations.

Analysis	LnL_1	LnL_2	PSRF	ESS_{min}	ESS_{max}
1. Unconstrained	−4.71e+02	−4.93e+02	~1.00	3217	3602
2. Constrained	−4.73e+02	−4.93e+02	~1.00	3114	3602
3. Wing-only	−2.29e+02	−2.52e+02	~1.00	3292	3504
4. Body-only	−2.25e+02	−2.49e+02	~1.00	>2500	3602
5. Ancestral state	−4.75e+02	−4.91e+02	~1.00	33096	3602

3.3.3. Ancestral state estimation (BI)

Results from the Bayesian ancestral state estimation analysis are presented in Fig. 20. In total, we detected 57 state changes across the monitored nodes (white discs in Fig. 20; states at other nodes and terminal apomorphies not reported; expanded taxon sampling necessary to determine root node conditions). Unlike parsimony mapping, which provides absolute transitions, our results indicate the probability of the plesiomorphic and apomorphic states, shown in the left- and righthand boxes of each character (Fig. 20). Seven of the 14 characters newly defined here were supported as synapomorphies at differing branches of the tree (chars. 9, 10, 15, 21, 33, 48, 49). Of these, the loss of basitarsomeral ctenidiobothria of the hindleg (char. 48) was highly supported as an autapomorphy of Trogiomorpha *sensu stricto*, while at this node, the pterostigma shape (quadrangular, char. 31) was weakly supported, and antennomere count (>20, char. 9) destabilized. For the new character 15 (adult lacinial tip) the transitions from simple to bicuspid between the Trogiomorpha *s. str.* and Spinaparaprocta nodes were weakly supported for Atropetae, and also the absence of a preapical claw tooth (char. 49). The secondary antennal annulation (char. 10) and the fusion of the mesothoracic episternum (char. 21) were identified as results of convergency in Lepidopsocidae and

Model 6. 3D Model of thorax of *Cerobasis guestfalica*, female. https://sketchfab.com/3d-models/thorax-of-cerobasis-guestfalica-female-585d3276780a4a75939312f67c8cfd7d.

Psoquillidae+Trogiidae.

4. Discussion

4.1. Taxonomic placement of †*Psyllipsocus mili* sp. nov.

†*Psyllipsocus mili* **sp. nov.** is the fourth species of the genus *Psyllipsocus* Selys-Longchamps, 1872 and the sixth of the family Psyllipsocidae from Cretaceous Burmese amber (Hakim et al., 2018; Álvarez-Parra et al., 2020; Jouault et al., 2021; Liang and Liu, 2021). It differs from other valid Cretaceous species of Psyllipsocidae by the narrow and quadrangular pterostigma, the annulated flagellomeres, and the combination of an anterior curvature of R2+3 and R4+5, and the wide distance between the tips of R1 and R2+3. The shape of the radial cell seems to be only slightly variable and is always hexagonal. It resembles †*Psyllipsocus yangi* Liang & Liu, 2021 in the shape of the radial cell.

A robust phylogenetic placement of †*P. mili* is currently not possible due to the lack of a modern revision of the family Psyllipsocidae and the possible paraphyly of *Psyllipsocus* (discussion below). Bayesian phylogenetic inference with soft constraints recovered †*P. mili* generally in a polytomy with most of the psyllipsocids outside of Atropetae. It shares the typical wing venation of other *Psyllipsocus* species, including the shortened proximal Sc vein on the forewing (homoplasious character of Psyllipsocidae; Fig. 21), which makes the placement in the genus *Psyllipsocus* the currently best supported hypothesis.

The new species shares the annulated flagellomeres with the genus †*Annulipsyllipsocus* Hakim, Azar, Maksoud, Huang & Azar, 2018. However, it can be distinguished from it by the quadrangular pterostigma and the hexagonal radial cell. The wing venation of †*P. mili* is remarkably similar to that of a photographed specimen from Cretaceous Lebanese amber shown in Grimaldi and Engel (2005: fig. 8.6. bottom), which was erroneously placed in Prionoglarididae, and later assigned to Psyllipsocidae by Mockford (2011; see also Mockford et al., 2013). Especially the shape of the radial cell and pterostigma seem to match very closely with conditions observed in †*P. mili*. A formal species description of the psyllipsocid species from Lebanese amber (Grimaldi and Engel, 2005) is still lacking. It likely belongs to the genus *Psyllipsocus*, as indicated by the wing venation. This would extend the age of this genus further into the Cretaceous at approximately 125 Mya instead of the previously mentioned 100 Mya (Álvarez-Parra et al., 2020).

4.2. Character evolution in Trogiomorpha

A common problem in palaeontological studies is the assignment of new species based on diagnostic characters and not on apomorphies (e.g., Jouault et al., 2021; see also Fikáček et al., 2020). Since Hennig (1950), it has been recognized that new species should be placed into existing clades based on shared derived features, i.e., synapomorphies, and not on plesiomorphic (or highly homoplasious) characters that have a purely diagnostic value for previously described taxa. Moreover, prevailing problems of cladistic or phylogenetic analyses of fossil Psocodea are the lack of informative characters besides the wing venation (which we find to have limited signal in Trogiomorpha), setation, and the terminalia. For example, in a recent cladistic analysis of Trogiomorpha (Li et al., 2022), a total of 38 morphological characters for 18 taxa (with a focus on fossil taxa) were scored: 22 characters of wing venation (including setation) (58 %), 5 of setation (other body regions) (13 %), 4 of terminal segments (11 %) and only 7 characters of other body regions (18 %), e.g., attachment structures. More than 80 % of the phylogenetical signal resulted from characters of the wings, setation or terminalia, while all other body regions were almost entirely neglected. Álvarez-Parra et al. (2024) added one additional wing venation character to this matrix (Li et al., 2022) and changed the scoring of some characters. The matrix is also strongly biased towards venation and setation characters. In comparison, in a cladistic analysis of extant Psocomorpha (Yoshizawa, 2002), 68 characters were scored for 50 taxa: 22 features of wing venation (including setation) (32 %), 25 of the terminalia (37 %) and 21 of

other body regions (31 %). A larger number of characters and taxa and an improved balance of different character systems was achieved in this study. Well defined sclerites or structures, likely yield a stronger phylogenetic signal (e.g., thoracic sclerites with low levels of homoplasy, Yoshizawa and Johnson, 2014; and more information for Trogiomorpha, Fig. 18A) as compared to differences in wing venation and setation, which are obviously prone to homoplasy (see Yoshizawa and Johnson, 2014 for discussion of relative homoplasy of different characters in Psocodea). All this suggests that high-quality documentation of exoskeletal elements should have high priority in phylogenetic analyses of psocids (and other groups). Our 3D-reconstruction of †*P. mili* shows that SR-μ-CT was essential for documenting many skeletal elements that were neglected in previous taxonomic and systematic studies of fossils.

Another crucial problem with placing fossil psyllipsocids is the lack of a modern phylogenetic study for this family, including both extant and extinct taxa. As there are no properly evaluated synapomorphies shared by the four extant genera, it is not possible to place specimens based on derived character states. Mockford (1993) discussed the phylogeny of the Psyllipsocidae briefly and stated that *Dorypteryx* Aaron, 1883 and *Pseudorypteryx* García-Aldrete, 1984 are sister groups, supposedly forming a clade with *Psocathropos* Ribaga, 1899, which is in turn the sister group of the most species-rich genus *Psyllipsocus*. However, the extant species of *Psyllipsocus* show distinct differences in the morphology of the claws and genitalia, and also in the wing venation (Mockford, 2011; Lienhard and Ferreira, 2013, 2014; Lienhard et al., 2022). Therefore, it is conceivable that this genus is not monophyletic, as already discussed by Mockford (2011), who suggested that *Psyllipsocus* may be paraphyletic, a hypothesis that is not refuted by our Bayesian phylogenetic analyses (Fig. 18 and 19).

In contrast to Psyllipsocidae, a well-resolved molecular phylogeny for the major branching points exists for Psocodea (de Moya et al., 2021). However, it is noteworthy that several extinct key taxa cannot yet be reliably placed in this topology, i.e., †Cormopsocidae (Yoshizawa and Lienhard, 2020), †*Brachyantennum* Liang & Liu, 2022 (Zhang et al., 2022), and †*Concavapsocus* Wang, Li, Ren & Yao, 2019 (Wang et al., 2019). This is either due to the lack of morphological apomorphies that support these major clades, or to difficulties in observing them in fossils. As this reduces the amount of information available for phylogenetic modelling, it is important to study the morphological evolution and polarity of phylogenetically informative characters of Psocodea in detail. Reliable fossil placements achieved with such an approach will also minimize the risk of erroneously dating phylogenetic trees (see Fikáček et al., 2020). Consequently, a detailed discussion of characters is presented here, and character polarities are discussed. We present: (1) a statistical estimate of relationships based on the available data plus our new observations (Figs. 17–20, supplementary files S2 and S3), and (2) a cladogram (Fig. 21) that summarizes the most plausible phylogenetic hypotheses in Trogiomorpha. The cladogram is based on published morphological information and phylogenetic arguments (Mockford, 1993, 2011; Yoshizawa and Lienhard, 2020; Zhang et al., 2022), and also on previous phylogenetic analyses (Yoshizawa et al., 2006, 2019; Li et al., 2022).

4.2.1. Discussion of cephalic characters

The tentorium of the new species is apparently very similar to that of *Stenopsocus stigmaticus* (Imhoff & Labram, 1842) (Badonnel, 1934). The anterior arms fuse separately with the corpotentorium, which is likely a plesiomorphic condition in Psocomorpha. A fusion of both arms anterior to the corpotentorium was only observed in Epipsocetae (Yoshizawa, 2005). More taxa of Trogiomorpha and Troctomorpha have to be studied to confirm this interpretation. The subgenal sulcus is well developed above the mandibles in †*P. mili* like in other psocids (Yoshizawa, 2005). The compound eyes are of similar size as in other macropterous psyllipsocids and there is no obvious difference between the sexes. In many trogiomorphan psocids the distance between the ocelli is small (e.g., drawings in Günther, 1974; Li, 2002). This is in contrast to the condition in (some?) Lepidopsocidae, where they are widely separated (e.g., Li, 2002; Li et al., 2022), which is a potential apomorphy of this family (Li et al., 2022). The absence of the water-vapor absorption apparatus (Rudolph, 1982) and a strongly reduced, flat postclypeus in Prionoglaridinae are apomorphies of this subfamily (Lienhard, 2004). A putative apomorphy of the extinct family †Cormopsocidae excluding †*Brachyantennum* is the dorsally extended vertex (Yoshizawa and Lienhard, 2020; Hakim et al., 2021a, 2021b; Wang et al., 2021; Liang and Liu, 2022).

A conspicuous character of Psocodea is the large, convex postclypeus (except for Prionoglaridinae, see above). It is generally present as a dome-shaped convexity of the anterior wall of the head capsule. However, in Trogiomorpha it is shifted ventrad, compared to the condition in many Psocomorpha. The postclypeus is distinctly extended ventrad in the extinct †Cormopsocidae (Yoshizawa and Lienhard, 2020) and †Empheriidae (e.g., Li et al., 2020), and also in Prionoglarididae (e.g., Lienhard et al., 2010a, b; Azar et al., 2017), Psyllipsocidae (this study) and Atropetae (Li et al., 2022), as well as in the Troctomorpha (e.g., Li, 2002; Boudinot et al., 2024). This is in contrast to the condition in Psocomorpha, where it is only slightly extended ventrad (e.g., in Stenopsocidae, see figures in Badonnel, 1934; Liang and Liu, 2024) or where it does not surpass the ventral margin of the genae and is not extended along the oral region (e.g., in Psocidae, see drawings in Yoshizawa, 2005). The polarity of these states is yet unresolved and requires further study. Additionally, the anteclypeus is often not distinctly differentiated in Trogiomorpha (Yoshizawa, 2005), with the exception of †Cormopsocidae (Yoshizawa and Lienhard, 2020). It is likely that a partial fusion of the anteclypeus and postclypeus occurs in Trogiomorpha, resulting in a more distinct ventral extension (including to some extent in the †Cormopsocidae; see Yoshizawa and Lienhard, 2020). However, there are several species deeply nested within this group (excl. Prionoglarididae), where a distinct anteclypeus is visible (e.g., Lienhard and García Aldrete, 2016: fig. 1C). An anteclypeus is still recognizable in †Empheriidae, but it is sometimes only indistinctly separated from the much larger postclypeus (e.g., Li et al., 2020; MW pers. obs.). That a well differentiated anteclypeus is present in †Cormopsocidae suggests that a partial intraclypeal fusion is a possible autapomorphy of Trogiomorpha, possibly including the †Cormopsocidae, with several reversals in this group (homoplasy). That Hemiptera, Thysanoptera and †Permopsocida all share a distinct separation of the post- and anteclypeus (Beutel et al., 2014; Huang et al., 2016; Yoshizawa and Lienhard, 2016) clearly indicates that the intraclypeal fusion in trogiomorphans is apomorphic.

The presence of more than 20 antennomeres is common throughout Psyllipsocidae and Trogiomorpha, but it is currently unclear whether a high number of flagellomeres is plesiomorphic or apomorphic in Psocodea on the subordinal level. Prionoglaridinae have only 13 or less articles, and this low number likely represents an apomorphy of this family (Yoshizawa and Lienhard, 2020). At present, the evolutionary transformations of this character in Psocodea remains unclear. A well-known character of Psocodea is the secondary annulation of the flagellomeres. It was first described for Troctomorpha and was used as one of the defining features for this suborder (e.g., Roesler, 1944). Only later, this character state was observed in Trogiomorpha, i.e., Psyllipsocidae (New and Lienhard, 2007; Mockford, 2011; Hakim et al., 2018; Lienhard, 2023), Prionoglarididae (e.g., Weidner, 1972; New and Lienhard, 2007; Azar et al., 2017), †Empheriidae (e.g., Álvarez-

Parra et al., 2022), †Cormopsocidae (Yoshizawa and Lienhard, 2020; Liang and Liu, 2022), and †*Brachyantennum* (Zhang et al., 2022). Interestingly, no species of Psocomorpha with secondary annulation was described so far. That it occurs in the Trogiomorpha and Troctomorpha suggests that it is a groundplan apomorphy of Psocodea, even though this condition also occurs in some species of Thysanoptera (e.g., Mickoleit, 1963; Mound, 2009) and Heteroptera (Beutel et al., 2014). In any case, secondary reduction of the annulation occurred several times independently in Psocodea. The apparent absence in the last common ancestor of the Psocomorpha suggests that this is a potential autapomorphy of this group. However, as a reduction that occurred in different groups, the phylogenetic significance is limited.

Li et al. (2022) proposed the presence of antennal setation as an apomorphy for **Spinaparaprocta** (= Psyllipsocetae+Atropetae). In descriptions of "basal" trogiomorphans (i.e., †Cormopsocidae, Prionoglarididae) antennal setae are often not visible on photographs (e.g., Azar et al., 2017, but see Yoshizawa and Lienhard, 2020: fig. 2C: possible setae very short at apical end of flagellomere, but very unclear; also, Hakim et al., 2021a: fig. 2A: few, very short setae (?) apically on flagellomeres). However, it is likely that they are in fact present but were overlooked due to their small size or the poor preservation of the antenna, or an inadequate resolution of micrographs (see also Enderlein, 1909: high magnification needed to see pubescence of flagellomeres in *Prionoglaris* Enderlein, 1909). Seeger (1975: fig. 5) showed with histological sectioning that the flagellum of *Prionoglaris stygia* Enderlein, 1909 (Prionoglaridinae) bears a vestiture of short setae. The coding for this character in the matrix of Li et al. (2022) is therefore unreliable and was changed in our study.

The function of the annulation of the flagellomeres is presently not clarified. The presence of the antennal rupture-facilitating device (Seeger, 1975) and secondarily annulated flagellomeres appear to be often correlated. They both occur combined, i.e., in Trogiomorpha and Troctomorpha, or both are reduced in the same group, i.e., in Phthiraptera and Psocomorpha. However, exceptions occur, for instance the presence of a rupture-faciliating device in *Psyllipsocus ramburii* Selys-Longchamps, 1872 without secondary annulation (Seeger, 1975). It should also be noted that the annulation does not necessarily occur on all flagellomeres but might be restricted to a certain section of the flagellum, as for instance in †*Palaeosiamoglaris* Azar, Huang & Nel, 2017, where it is only found on the basal flagellomere (Azar et al., 2017). It is noteworthy that the flagellum and the membranous collar-like connection between the flagellomeres (Zhang et al., 2022: fig. 1E) in †*Brachyantennum* resembles the condition found in †*P. mili* and other members of Trogiomorpha (Seeger, 1975). However, as this state is likely a groundplan condition of Psocodea, it cannot be used to place †*Brachyantennum*. Seeger (1975) noted that after rupturing the flagellum and a subsequent molt, the size of the remaining flagellomeres increases and also the number of annuli. He pointed out that this weakens the diagnostic value of these characters (Seeger, 1975). The cuticle is distinctly less sclerotized at the annuli in the flagellomeres of species of Troctomorpha (Seeger, 1975), but it is unknown whether the same condition occurs in Trogiomorpha with secondary annulation. The secondary annulation likely increases the flexibility of the flagellomeres with an accordion-like mechanism, which can thus be extended, passively contracted, and bent. This possibly limits the damage to the remaining flagellomeres or decreases the number of lost flagellomeres when the flagellum ruptures. It could also help discarding flagellomeres in a more efficient way, as the flagellum can be bent more easily into an optimal angle to facilitate the rupture. This is in contrast to the condition found in Psocomorpha, where the flagellomeres are generally stiffer and only rarely bent in specimens entrapped in amber (MW pers. obs.), thus reducing the efficiency of the rupture-facilitating mechanism, leading to its complete reduction within the group (Seeger, 1975).

The labrum is a uniform lobe-like structure in †*P. mili*, without any visible ventral nodes or other external sclerotizations. A median notch is also lacking, similar to the condition found in *Amphientomum* (Boudinot et al., 2024) (and possibly other troctomorphans), but in contrast to its presence in *Stenopsocus* Hagen, 1866 or other psocomorphan taxa (Badonnel, 1934; Yoshizawa, 2005). A simple labrum as found in †*P. mili* is likely part of the groundplan of the entire order. Asymmetric mandibles are also possibly a groundplan feature of Psocodea, as it occurs in all three suborders (Pravdin, 1932; Badonnel, 1934; Yoshizawa, 2005; Boudinot et al., 2024).

The maxillae lack a cardo, likely due to a complete fusion with stipes (Yoshizawa and Saigusa, 2003). A distinct palpifer is delimited from the stipes by a sulcus, possibly with an internal ridge as in Psocomorpha (Yoshizawa, 2005; MW pers. obs.). The absence of the cardo as a separate element is a (groundplan?) apomorphy of Psocodea (Yoshizawa and Saigusa, 2003; Beutel et al., 2014). That the galeae are relatively flat and fit into the posterior concavity of the mandibles is a plesiomorphic condition in Psocomorpha (Yoshizawa, 2002, 2005), and might also represent a groundplan feature of Psocodea. The lacinial apex in †*P. mili* is bicuspid, with a bifid outer (lateral) cusp and a simple inner (median) acuminate cusp. A bicuspid lacinial tip also occurs in Prionoglaridetae (e.g., Lienhard et al., 2010a), Atropetae (Lienhard, 1998), †Empheriidae (Hakim et al., 2024, MW pers. obs.), Amphientometae (Mockford, 1967), Nanopsocetae (Lienhard, 1998), Archipsocetae, Homilopsocidea and Psocetae (Yoshizawa, 2002). However, some species of *Psyllipsocus* possess different lacinial tips (Mockford, 2011), which makes the interpretation of the polarity of this character difficult. All previously described laciniae of †Cormopsocidae (Yoshizawa and Lienhard, 2020; Wang et al., 2021) and †*Brachyantennum* (Zhang et al., 2022) are simple and lack distinct teeth or cusps. A bicuspid (and toothed) lacinia occurs in all three suborders, suggesting that it may have been present in their common ancestor. However, it is also conceivable that this condition evolved several times independently. Assuming that a bicuspid lacinial tip is plesiomorphic and belongs to the groundplan of Psocodea including the stem group implies that a simple tip is a synapomorphy of †Cormopsocidae + †*Brachyantennum* (possibly nested within †Cormopsocidae), and evolved independently in a similar fashion in other groups, such as Caeciliusetae (see Lienhard, 1998; Yoshizawa, 2005 for drawings of laciniae).

A transformation of the mandibles and lacinia occurs in the ontogeny of Prionoglaridinae, where both structures are distinctly simplified in adults compared to their equivalents in nymphs (Lienhard, 1988). This subfamily can be distinguished from other families of Psocodea based on these distinctive apomorphies. A less distinct metamorphosis of the lacinia also occurs in Speleketorinae, where the lacinial tip is simplified in adults (Mockford, 1984). This is a potential groundplan apomorphy of Prionoglarididae (Prionoglaridinae+Speleketorinae), even though most molecular data do not support the monophyly (Yoshizawa et al., 2019; de Moya et al., 2021; but see Yoshizawa et al., 2018 for monophyletic Prionoglarididae supported by using mitochondrial genomes), with Speleketorinae more closely related to Spinaparaprocta (= Psyllipsocetae+Atropetae).

The second maxillary palpomere often bears a conical or spur-like sensillum on its inner side. This was previously interpreted as an autapomorphy of Atropetae (Li et al., 2022), but several studies have revealed the presence of this sensillum in Psyllipsocidae (Liang and Liu, 2021; Lienhard, 2023) and Speleketorinae

(e.g., Mockford, 1984, 1993; Lienhard et al., 2010a). As the sensillum is often missing in species of *Psyllipsocus* (e.g., Mockford, 1993; Lienhard et al., 2022), it is apparent that the presence or absence is highly homoplasious, with multiple losses and possible regains. However, it was noted by Hallberg and Hansson (1999) that constraints related to the construction and function of sensilla have to be taken into consideration in this context. A possible synapomorphy of the three other extant genera of Psyllipsocidae, *Psocathropos*, *Dorypteryx* and *Pseudorypteryx*, is the reduction of the sensillum on maxillary palpomere 2, even though this condition also occurs in *Psyllipsocus*, likely as a result of convergency. When taking the current evidence into account, the presence of the spur sensillum on mx2 is arguably a synapomorphy of Speleketorinae+Psyllipsocetae+Atropetae, as it is missing in †Cormopsocidae, Prionoglaridinae (but see Jouault et al., 2021 for alternative evidence) and the two other suborders, Troctomorpha and Psocomorpha.

The morphology of the last maxillary palpomere was previously used in a comparative context in Psocodea (e.g., Yoshizawa, 2005). The ultimate segment is shaped like an apically tapering elongate tube in †Cormopsocidae (Yoshizawa and Lienhard, 2020; Li et al., 2022), in contrast to the hatchet- or wedge-shaped last palpomere of Psyllipsocetae (e.g., Jouault et al., 2021; Liang and Liu, 2021; this study, with exceptions, e.g., in Mockford, 2011: last palpomere broadened slightly before apical margin and then tapering distally) and Atropetae (e.g., Mockford, 1974, 1993; Lienhard, 1998; Li, 2002; Li et al., 2022; with exceptions, e.g., in *Lepinotus* Heyden, 1850 and †*Eolepinotus* Vishnyakova, 1975, see Lienhard, 1998; Vishnyakova, 1975 for illustrations of maxillary palps) including †Empheriidae (e.g., Cumming and Le Tirant, 2021; Li et al., 2022; Liang et al., 2022). It is also tubular in *P. stygia* (Lienhard, 1998), *Neotrogla* Lienhard, 2010 (Lienhard et al., 2010b) (in Prionoglarididdae distinctly elongated and thin), and †*Cormopsocus* Yoshizawa & Lienhard, 2020, which suggests that this character state is ancestral, possibly belonging to the groundplan of Psocodea. This is also supported by the condition found in many Psocomorpha and Troctomorpha (Mockford, 1993; Lienhard, 1998; Li, 2002), where the last palpomere is also long and tubular with a tapering apex. This suggests that the wedge- or hatchet-shaped last maxillary palpomere is a potential synapomorphy of Psylli-psocetae-+Atropetae. In the cladistic analysis of Li et al. (2022), this character state was also discussed as a potential apomorphy of this clade and would potentially represent the third known apomorphy of this unit, in addition to the presence of a paraproctal spine and an anteriorly open phallosome (Yoshizawa et al., 2006) (see discussion below). Moreover, this feature can be easily observed in fossil inclusions and is therefore additionally a useful diagnostic criterion for this group.

The labium in †*P. mili* consists of a trapezoid prementum with a posterior median furrow and lateral lobes, i.e., the prepalpiger lobes of Badonnel (1934), paired labial palps with two articles, the first short and truncated, the second plate-like, paired paraglossae that resemble subtriangular lobes, and a fused lobe-shaped median glossa (or at least a portion of the glossa). The labium is similar to that of *Echmepteryx madagascariensis* (Kolbe, 1885) (Yoshizawa, 2005). The labial morphology in Atropetae and Psyllipsocetae seems to be highly conserved, without distinct differences between both groups noted in the literature (Pravdin, 1932; Yoshizawa, 2005). As the species of Trogiomorpha use no silk and lack specialized silk glands (still present as ventral labial glands with different function) (Weber, 1938), the glossae are rather simple compared to taxa that use silk for shelters or depositing eggs, for instance in Caeciliusetae (Badonnel, 1967; Yoshizawa, 2005). However, some species of Psocomorpha that do not produce silk have similar glossae (Weber, 1938; von Kéler, 1966), making the interpretation of the evolution of these labial endite lobes and entangling function from phylogenetic constraints currently difficult. The presence of palps with two articles is a groundplan feature of Psocodea. A reduction to one occurs in several taxa of Troctomorpha and is generally found in Psocomorpha (Yoshizawa, 2005).

4.2.2. Thoracic characters

A swollen, strongly convex lateral cervical sclerite as described here for *Psyllipsocus*, is potentially a phylogenetically important feature. It is also present in †*Cormopsocus groehni* Yoshizawa & Lienhard, 2020 (Yoshizawa and Lienhard, 2020: fig. 2A), †*Palaeosiamoglaris inexpectata* Azar, Huang & Nel, 2017 (Azar et al., 2017: fig. 11A, B), †*Annulipsyllipsocus andreneli* Hakim, Azar, Maksoud, Huang & Azar, 2018 (Hakim et al., 2018: fig. 1A, B), †*Annulipsyllipsocus inexspectatus* Hakim, Azar, Maksoud, Huang & Azar, 2018 (Hakim et al., 2018: figs. 4A, 7B), †*Psyllipsocus yangi* Liang & Liu, 2021 (FL pers. obs.), †*Psyllipsocus yoshizawai* Álvarez-Parra, Peñalver, Nel & Delclòs, 2020 (Álvarez-Parra et al., 2020: fig. 1A), *Dorypteryx domestica* (Smithers, 1958) (this publication: Fig. 11C and D), †*Burmempheria raruschaetae* Li, Wang & Yao, 2020 (Hakim et al., 2023: fig. 5A, D), *Rhyopsocus bentonae* Sommermann, 1956 (see Sommermann, 1956: figs. 4, 6), and Cerobasis *guestfalica* (Kolbe, 1880) (this publication: Fig. 14C and D). The cervical region is strongly exposed in †*P. mili* and *D. domestica*, while it is largely concealed in *C. guestfalica*. The laterocervical sclerite is also larger in the former two species, likely increasing the moveability of the head.

The cervical sclerite is elongated and strip-like in many representatives of Psocomorpha (e.g., Badonnel, 1934; Yoshizawa, 2005; MW pers. obs.). In *Archipsocus nomas* Gurney, 1939 it resembles a club with a narrow strip-like anterior part and a hemispherical projection connected to its posterior side (Gurney, 1939), and a somewhat similar condition is found in *D. domestica* (Figs. 12 and 13). In *Stimulopalpus japonicus* Enderlein, 1906 (Troctomorpha: Amphientomidae) (Fig. 10E) the laterocervical sclerite is clearly strip-shaped, and also in *Embidopsocus* Hagen, 1866 (Crampton, 1926). The laterocervical sclerite of Trichodectidae is ovoid (Lyal, 1983), but not as distinctly spherical as in Trogiomorpha. The cervical sclerites of "mallophagans" (Crampton, 1926) are similar to those of embidopsocids and psocomorphans. The complete loss of the laterocervical sclerites is a shared derived feature of Anoplura and Rhynchophthirina (Weber, 1969; Lyal, 1983). In correlation with the piercing-sucking or burrowing-sucking mouthparts of both groups, the stability of the articulation of the head has to be maximized, correlated with a reduced movability. This is conform with the loss of the laterocervicalia in both groups.

In outgroups such as Sternorrhyncha (Hemiptera) and Thysanoptera, the laterocervicalia are strip-like to elongate-triangular (Crampton, 1926). This suggests that the similar condition found in most psocomorphans, in free-living troctomorphans, and also in "mallophagans" is plesiomorphic, whereas swollen, hemispherical cervical sclerites found in Trogiomorpha are apomorphic. This is also tentatively supported by the presence of a strip-like sclerite ventrolaterally inserted in the neck membrane of the extinct †Permopsocida (Yoshizawa and Lienhard, 2016: fig. 1b), the sister group of Condylognatha, confirming that swollen laterocervicalia might in fact represent a apomorphy of Trogiomorpha (including †Cormopsocidae), even though further confirmation is required. It is possible that the bar-shaped part of the laterocervicalia is still present to some extent in trogiomorphans, like for instance in *D. domestica* (Fig. 12C, D, 13C, D), but it is often not as distinct as in the other suborders. So far only female genital characters were proposed as apomorphies for this clade (Yoshizawa et al., 2006) and the secondary gain of the metathoracic basalar muscle IIItpm3 for extant members (Kawata et al., 2024). A larger taxon sampling,

more µCT scans or even light microscopic examinations, and additional anatomical data are required for a reliable clarification of this issue.

The thoracic sclerites in the holotype of †*P. mili* are exceptionally well preserved. It is possible to compare most sclerites with the corresponding structures of the two extant species of Trogiomorpha included in this study, and also of other psocids such as *Longivalvus nubilus* (Enderlein, 1906) (Psocomorpha: Psocidae) (Yoshizawa, 2005). For example, the anterior lobe of the mesonotal scutum is shorter and indented by a median furrow (possibly an artifact?) in †*P. mili*, while it is almost triangular and long in *L. nubilus*. The scutellum of the mesonotum in †*P. mili* is rectangular, differing from the subpentagonal and larger scutellum of *L. nubilus*. The anterior notal wing process is perpendicular to the longitudinal body axis in †*P. mili*, while it is directed anterad in *L. nubilus*. The scutal part bearing the posterior notal wing process is more distinctly separated from the rest of the scutum in †*P. mili* compared to *L. nubilus*. The anterior lobe of the metanotal scutum is protruding as a rectangular block from the remaining scutum in †*P. mili*, and it is larger than in *L. nubilus*. The shape of the metanotal scutellum is very similar in both species, a subpentagonal area only weakly delimited from the scutum by a faint scutoscutellar suture. The proepisternum of †*P. mili* is not divided into two portions on the ventral side as in *L. nubilus* and more similar to the episternum of *Ectopsocus* McLachlan, 1899 (Psocomorpha: Ectopsocidae) (Yoshizawa, 2005). The proepisternum and proepimeron are almost equally long in †*P. mili*, like for instance in *S. stigmaticus* (Badonnel, 1934), whereas the proepisternum is shorter in *Ectopsocus*. It is still unclear whether a clearly differentiated prothoracic preepisternal sclerite is present in †*P. mili*. The propleuron is otherwise mostly membranous, similar to the condition found in other psocids (Badonnel, 1934; Yoshizawa, 2005), likely resulting in a high movability of the head and flexibility in the neck region in "Psocoptera" on one hand, and also enhancing the flexibility between the prothorax and pterothorax. As the sclerites of the pro- and pterothorax do not touch each other (Badonnel, 1934; Yoshizawa, 2005; this study), the prothorax can likely be moved in all directions to a certain degree.

The entire thorax of *C. guestfalica* is very compact with few membranous regions, likely in correlation with the reduced wings. In contrast, the prothorax of †*P. mili* and *D. domestica* is very flexible due to a large posterior membranous region, enhancing the flexibility between this segment and the pterothorax. The prothoracic morphology is almost identical in †*P. mili, D. domestica* and *C. guestfalica*. The preepisternum and episternum are likely fused, and the ventral margin of this fused region articulates with the laterocervical sclerite in all three species. The pleural ridges of the pterothorax are more strongly developed in †*P. mili* and *D. domestica* than in *C. guestfalica*, correlated with the wing development. The mesonotum of †*P. mili* is very similar to the one of *D. domestica*, and the anterior lobe of the mesoscutum is more clearly delimited. It is strongly simplified in *C. guestfalica*, likely due to the reduction of the wings, with only micropterous forewings preserved.

A character of potential phylogenetic value is the width of the precoxal bridge of the mesothorax. It is wide in †*P. mili* but narrow in *D. domestica* and *C. guestfalica*. This feature was previously used by Yoshizawa (2002) in the context of the phylogeny of Psocomorpha, with character states of some non-psocomorphan psocids used for comparison. As character states were previously not specified, we define them here as follows: precoxal bridge either at most twice as wide as the mesotrochantin (= narrow precoxal bridge), or more than twice as wide (= broad precoxal bridge). Lepidopsocidae (Trogiomorpha), Pachytroctidae, Amphientomidae and Troctopsocidae (all three Troctomorpha) have a narrow precoxal bridge, whereas it is wide in Psocomorpha except for Epipsocetae and Psocetae (Yoshizawa, 2002). It was argued in that study that a wide bridge is an apomorphy, while a narrow condition is plesiomorphic in Psocodea. As the higher-level phylogeny of Psocomorpha is well resolved with transcriptomic and genomic data (de Moya et al., 2021), it is possible to use this updated tree for character comparison. As Epipsocetae and Psocetae are sister groups, the narrow condition of the bridge likely represents a synapomorphy of these two groups, whereas all other infraorders (Archipsocetae, Caeciliusetae, Homilopsocidea, Philotarsetae) have maintained the broad condition (Yoshizawa, 2002). However, it should be noted that the polarity of this character in the entire Psocodea is problematic. Previously, only a narrow bridge was observed in taxa outside of Psocomorpha (see above, Yoshizawa, 2002), and we could confirm that this condition also occurs in *D. domestica* and *C. guestfalica*. In contrast, †*P. mili,* and Prionoglaridinae and Speleketorinae (Kawata et al., 2022) have a broad bridge. The state is unknown in †*Brachyantennum*, †Cormopsocidae, and also in other species of *Psyllipsocus*. It is currently not possible to assess the character polarity unambiguously in Psocodea, except for Psocomorpha. Additional reliable observations are required with a representative taxon sampling. The most likely interpretation is presently that a broad mesothoracic precoxal bridge is plesiomorphic (possibly belonging to the groundplan?) of Psocodea, and a narrow bridge evolved independently (possibly three times?) in Psyllipsocidae and Atropetae, Troctomorpha, and Epi-psocetae + Psocetae (Yoshizawa, 2002), respectively. Interestingly, the morphology of thoracic sclerites, especially in the pleural region, can vary depending on the development of wings even within a single species, for instance in carabid beetles (Smith, 1964) or in the wildtype and mutants of *Drosophila melanogaster (*Meigen, 1830) (Fabian et al., 2016). Therefore, the differences in the thoracic elements between the three compared trogiomorphan taxa could possibly be correlated with wing polymorphism. These character complexes (wing development, thoracic sclerites, thoracic muscles, etc.) are obviously not independent from each other and should be critically assessed in phylogenetic analyses.

†*P. mili* apparently lacks Pearman's organ and it is also missing in some other members of Psyllipsocidae (Mockford, 1993). However, as the preservation of our fossil is not perfect, we cannot confirm the absence with certainty. Interestingly, the first tarsomeres of the middle- and hindlegs in †*Brachyantennum* are equipped with ctenidiobothria, a character previously rarely observed in Trogiomorpha, and arguably an apomorphy of the genus (Zhang et al., 2022). Similar structural specializations are present on the first tarsomere of the hindlegs in Amphientomidae (e.g., Boudinot et al., 2024), and on the same tarsomere on the mid- and hindlegs in psocomorphans (Zhang et al., 2022). Smithers (1972) suggested that ctenidiobothria may have evolved several times independently in Psocodea, but a formal analysis is necessary for a reliable interpretation. An autapomorphy of Speleketorinae is the presence of trichobothria on the legs (Lienhard, 2000, 2007; Lienhard et al., 2010b). Species of Speleketorini bear trichobothria ventrally on the femora and trochanters of all three pairs, whereas they are only inserted on the tibiae and tarsi of the middle and hind legs in Sensitibillini. Whereas the claws of the forelegs of nymphs of *P. stygia* display only a single preapical tooth, they bear an additional membranous vesicle on the inner side in adults (Lienhard, 1988). This developmental transformation of the claws, less distinct in the middle and hind legs, is unique within Psocodea. It is likely an apomorphy of the entire subfamily Prionoglaridinae, together with the asymmetry of the claws (Lienhard, 1988; Lienhard et al., 2010a).

A row of (articulated) spines on the anteroventral margin of the profemur occurs in Speleketorinae (Mockford, 1984; Lienhard, 2000) and the Amphientomidae (e.g., Boudinot et al., 2024), but

is absent in Prionoglaridinae (Lienhard, 1988; Lienhard et al., 2010a) and Psyllipsocidae (Mockford, 1984). The absence of these spines was previously suggested as a possible apomorphy of Psyllipsocidae (Mockford, 1984). However, an evaluation with a broader taxon sampling is necessary for a reliable evaluation of the polarity of this character.

Pulvilli or other pretarsal attachment structures (besides preapical cuticular teeth) are absent in Trogiomorpha except for Atropetae (Mockford, 1993; Lienhard, 1998), Prionoglaridinae (see discussion above), and some species of *Psyllipsocus* (Lienhard, 2023). Attachment structures on the claw also occur in psocomorphan taxa (Lienhard, 1998; Yoshizawa, 2002, 2005). The presence of a pulvillus is a putative apomorphy of Atropetae (see supplementary file S2), and the apical broadening of the pulvilli a possible snyapomorphy of Psoquillidae+Trogiidae (in contrast to Li et al., 2022 who proposed it as synapomorphy of Lepidopsocidae+-Psoquillidae+Trogiidae), even though the character state is apparently prone to homoplasy (see supplementary file S2). The attachment vesicles in Prionoglaridinae are structurally completely different (e.g., Lienhard, 1988, 2004) and have evolved independently. Reduction of the preapical tooth (or teeth) characterizes Psoquillidae+Trogiidae, a potential synapomorphy of the two families.

4.2.3. Wing characters

A character previously considered as important in psocodean systematics and taxonomy is the nodulus. The term is defined as the junction of the veins CuP and A1 on the posterior wing margin (Mockford, 1967; Smithers, 1972; Lienhard, 1998; Ogawa and Yoshizawa, 2017). Mockford (2011) confirmed that a nodulus is present in most extant macropterous *Psyllipsocus* species, and Vishnyakova (1975: p. 65) mentioned that it is present in all extant Prionoglarididae and Psyllipsocidae known by that time. In previous studies on Cretaceous psyllipsocids, it was assumed that a nodulus is developed (e.g., Hakim et al., 2018; Jouault et al., 2021). Yet, Ogawa and Yoshizawa (2017) demonstrated that it is absent in all extant trogiomorphan infraorders and that the veins CuP and A1 only terminate close to each other, but do not fuse at the wing margin.

This raises some questions on the evolutionary significance of the nodulus being absent or present in psocodean taxa. First of all, it was shown with high magnification SEM micrographs in a morphology-based phylogenetic study (Ogawa and Yoshizawa, 2017) that the in-flight wing-coupling mechanism has evolved once in the last common ancestor of all extant psocodeans. This means that the general configuration of this apparatus is homologous between the three suborders, but that structural details differ between them. In all extant psocodeans it consists of two components of the CuP vein of the forewing, the retainer and retinaculum, and the costal vein on the anterior hindwing margin, but the exact configuration of these components differs between the three suborders (Ogawa and Yoshizawa, 2017). Ogawa and Yoshizawa (2017) identified a specialized tip of the vein CuP with several rows of ribs in Troctomorpha, in fact the only unambiguous autapomorphy of this suborder (Ogawa and Yoshizawa, 2017). Additionally, a synapomorphy for Troctomorpha+Psocomorpha was found, a diagonal or vertical orientation of the ribs on the tip of the vein CuP (Ogawa and Yoshizawa, 2017). As the distance between the tip of CuP and A1 has no (obvious) functional implication for the in-flight wing-coupling apparatus, and therefore also the absence or presence of the "nodulus", there is probably only minimal selective pressure on this character if at all. Therefore, it is likely that the fusion of the veins CuP and A1 at the wing margin, i.e., the "nodulus", could have evolved several times independently within Psocodea. This is further supported by the simultaneous presence and absence of the "nodulus" in one single family, the Empheriidae (Baz and Ortuño, 2000; Li et al., 2022; Liang et al., 2022). On the other hand, a nodulus is described in all groups of Psocomorpha. Therefore, it is likely that this character state evolved in the last common ancestor of all Psocomorpha (Ogawa and Yoshizawa, 2017), and might represent an apomorphy of this clade.

The "nodulus" as currently defined, i.e., as a fusion of the tips of CuP and A1, is apparently of limited phylogenetic value, at least for Trogiomorpha, as the distance between the tips of the two veins is obviously variable. Besides this, the distance between CuP and A1 at the wing margin is functionally irrelevant for the in-flight wing-coupling mechanism. Vishnyakova (1975) described details of the wing-coupling apparatus of the forewing for †*P. inclusus* and observed that not only the tips of CuP and A1 reach the posterior wing margin separately, but also that the retinaculum is missing. As a retinaculum is developed in all macropterous psocodeans (Ogawa and Yoshizawa, 2017), its absence in this extinct species is uncertain. Even using high magnification light microscopy, the retinaculum in amber fossils is difficult to observe. In †*P. mili* the retinaculum is indistinct, but seems to consist of at least four curved spines (see Fig. 10B). Another technical problem is that high magnification is required to recognize whether both veins in question fuse with each other, for instance SEM micrographs (Ogawa and Yoshizawa, 2017). Additionally, the wings are often bent and not in an ideal position when a specimen gets entrapped in amber, which impedes the proper observations of these characters. It is currently unknown how the in-flight wing-interlocking works in psyllipsocids if a retinaculum is lacking.

The specific shape of the forewings is apomorphic for some clades in Trogiomorpha. Broad and rounded forewings are a potential apomorphy of Prionoglaridetae, even though their monophyly was previously questioned based on molecular data and is in conflict with a potential apomorphy (presence of a spur sensillum on mx2) supporting a possible clade comprising Speleketorinae + Psyllipsocetae+Atropetae. Additionally, glabrous veins of the forewing are a potential apomorphy of Prionoglarididae (Yoshizawa and Lienhard, 2020; Li et al., 2022), with independent evolution of this feature in †Cormopsocidae, also a potential apomorphy of this family (Yoshizawa and Lienhard, 2020). In Lepidopsocidae, the fore- and hindwings are apically pointed, while they are rounded in all other families, suggesting this as a unique apomorphy of this family (Li et al., 2022). Another potential autapomorphy of Lepidopsocidae is the vestiture of scales on their body and wings (Li et al., 2022). However, this interpretation remains ambiguous, as Thylacellinae, a subfamily of Lepidopsocidae, lacks scales (Enderlein, 1911; Smithers, 1972).

A strongly developed and curved Sc vein that is connected to R1 of the forewing is plesiomorphic in Psocodea. It is preserved in †Cormopsocidae (Yoshizawa and Lienhard, 2020), Prionoglarididae (e.g., Mockford, 1993; Lienhard, 1998) and †Empheriidae (e.g., Li et al., 2022). The reduction of Sc in the forewing is arguably an autapomorphy of Psyllipsocidae. Atropetae also have a partially reduced Sc vein of the forewing compared to the †Empheriidae. The condition differs between Atropetae and Psyllipsocetae, with a more strongly reduced Sc in the latter, never reaching the wing margin. Obviously, reduction of Sc is strongly prone to homoplasy. As it occurs in many psocopteran subgroups (Nanopsocetae, Amphientomidae, all Psocomorpha), it is of limited systematic value. The forewing Sc vein in Electrentomoidea is curved and connected to R1 (e.g., Mockford, 1967), but it is nevertheless reduced in size compared to the less derived state in “basal” trogiomorphans. A synapomorphy of †Empheriidae + Lepidopsocidae+Psoquillidae+Trogiidae is the consistently long M1+2 vein of the forewing, that is always longer than the vein M2 (Li et al., 2022). Additionally, an areola postica cell longer than half

of the maximum width of the forewing, is another apomorphy of Atropetae (Li et al., 2022).

Li et al. (2022) proposed two synapomorphies supporting a clade †Empheriidae+†Archaeatropidae: (1) forewing veins with setae, and (2) forewing membrane with setae. In the case of the first feature this interpretation is highly unlikely as wing veins with setae also occur in Psyllipsocidae (e.g., Liang and Liu, 2021; this study), Psoquillidae (García Aldrete, 2006), and also in Lepidopsocidae with setae transformed into scales. The second apomorphy is also questionable, as the forewing membrane is covered with scales in Lepidopsocidae and with setae in some species of Psoquillidae, e.g., *Eosilla denervosa* (Enderlein, 1912) (Smithers, 1972: .fig. 4.84). Additionally, some members of †Empheriidae and †Archaeatropidae have a glabrous forewing membrane, or only very few setae are present on the posterior basal portion or pterostigmal area, for instance in †*Libanoglaris mouawadi* Perrichot, Azar, Néraudeau & Nel, 2003 and †*Libanoglaris chehabi* Azar & Nel, 2004 (Cumming and Le Tirant, 2021: fig. 6G and H). The character definition is also too unspecific, as setae can occur on different regions of the wing membrane in different species, implying that the conditions are not homologous. Obviously, this character (or characters) is of limited phylogenetic value due to a high level of homoplasy. Currently, a convincing apomorphy of the synonymized family †Empheriidae (Li et al., 2022) is lacking, and there are open questions concerning the phylogenetic status of †Archaeatropidae and †Empheriidae (Álvarez-Parra et al., 2024; Hakim et al., 2024). Presently both families are only characterized by symplesiomorphies, such as the well-developed and curved basal Sc vein of the forewing and the shape of the forewing. Therefore, the monophyly is doubtful, and it is plausible to assume that both are paraphyletic assemblages in the stem group of Atropetae, with certain members of both groupings more closely related to Lepido-psocidae+-Psoquillidae+Trogiidae than to the other members of †Empheriidae or †Archaeatropidae. A similar conclusion was reached by Álvarez-Parra et al. (2024). This situation mirrors the one in Psyllipsocidae, where it is likely that *Psyllipsocus* is paraphyletic. A putative apomorphy of the wings suggesting a clade Psoquillidae+Trogiidae is the missing cross vein connecting the veins Rs and R1 (r1-rs) on the forewing (Li et al., 2022). However, as a reduction this character is likely of limited phylogenetic value.

Another reduction in the forewing venation is the lack of the radial cell, a potential synapomorphy of Lepido-psocidae+-Psoquillidae+Trogiidae (Li et al., 2022). However, like in the case of other venational characters, this character is also homoplasious as the radial cell is also missing in macropterous species of *P. ramburii* and *Psyllipsocus apache* Mockford, 2011 (Mockford, 2011). All members of Trogiidae have vestigial forewings or they are entirely lost (Smithers, 1972; Li et al., 2022). This is a potential apomorphy of this family (Li et al., 2022).

4.2.4. Characters of terminal abdominal segments

Characters of the terminal abdominal segments including genital structures of both sexes are highly informative for phylogenetic relationships in the Trogiomorpha (see Yoshizawa et al., 2006). The paraproctal or anal spines, paired cuticular outgrowths, generally converge towards the midline (see Models 3 and 5). They are surrounded by small sensilla and act as a sensory organ. This structure is present in some taxa of Psyllipsocidae (Mockford, 1993, 2011), and generally in †Empheriidae, Lepidopsocidae, Psoquillidae and Trogiidae (e.g., Mockford, 1993; Lienhard, 1998; Li, 2002; Li et al., 2022). As it is lacking in the “basal” trogiomorphan families (e.g., Mockford, 1993; Yoshizawa and Lienhard, 2020) and the two other suborders, the presence is most likely a synapomorphy of Psyllipsocetae+Atropetae (Yoshizawa et al., 2006), probably with several secondary reductions in Psyllipsocidae. This includes a single loss in the last common ancestor of *Psoc-athropos* + (*Pseudorypteryx*+*Dorypteryx*), a potential apomorphy of this unit. Due to its ubiquity in Psyllipsocetae+Atropetae, we consider this eponymous character as a synapomorphy of these two infraorders of a clade Spinaparaprocta.

Potential apomorphies of Psyllipsocidae also include features of the internal female genitalia. A modified spermatheca with sclerotizations of the spermathecal duct and the presence of an accessory vesicle, tentatively support the monophyly of Psyllipsocidae (Yoshizawa et al., 2006). In a modified form, with one or two glandular accessory sacs, this is a potential synapomorphy of Lepidopsocidae+Psoquillidae+Trogiidae, and possibly also Empheriidae (condition unknown) (Yoshizawa et al., 2006; Mockford, 2018). In Psoquillidae these accessory vesicles are shifted proximad to the opening of the spermatheca (Mockford, 1993; Yoshizawa et al., 2006), a convincing autapomorphy of this family. Currently, there are no data on the spermatheca of extinct members of Trogiomorpha. This impedes the reconstruction of the character evolution in the "basal" trogiomorphans.

A distinctive autapomorphy of Trogiomorpha *s.l.* is the shortened subgenital plate (Yoshizawa et al., 2006; Cheng and Yoshizawa, 2022; Li et al., 2022), covering only the basal portion of the ovipositor valves, or only the external v3 if the other valves are reduced. The external valve is consistently enlarged in all trogiomorphans, often correlated with a reduction or complete absence of the two other valve pairs (ventral valvulae v1 and dorsal valvulae v2). This condition is apomorphic for Trogiomorpha. It is currently unclear how the ovipositor valves or subgenital plate are composed in the extinct family †Cormopsocidae. However, apparently preserved parts of the terminalia (well-developed ventral and dorsal valves) of a putative female would place this family as sister group of all Trogiomorpha (see Hakim et al., 2021a). Contrasting evidence of a well-preserved ovipositor of a female specimen of †*Longiglabellus pedhyalinus* Wang, Li & Yao, 2021 (Wang et al., 2021), also belonging to †Cormopsocidae, suggests that only the shortened subgenital plate is an apomorphy uniting all trogiomorphans, and that the reduction of the ventral and dorsal valves occurred in the last common ancestor of Priono-glaretidae+-Psyllipsocetae+Atropetae, or in their stem group, and not at the "basal" node of Trogiomorpha. Wang et al. (2021) suggested an ovipositor with well-developed ventral and dorsal valves as an apomorphy of †Cormopsocidae. However, this is obviously a plesiomorphic condition, as an ovipositor with three pairs of well-developed valves very likely belongs to the groundplan of the entire Psocodea. In any case, the reconstruction of the evolution of these genital characters at the base of Trogiomorpha is still in a preliminary stage. Only the dorsal and external valve are present in Prionoglaridetae (Mockford, 2018; Cheng and Yoshizawa, 2022; Cheng et al., 2023), while all three pairs are generally developed in Psyllipsocetae (Mockford, 2018), with a tendency to reduce v1 and v2 in some taxa. The reduction of v1 and v2 might have happened several times independently in the Trogiomorpha, but the current taxon sampling is too limited to solve this problem. In Atropetae, v1 is seemingly entirely missing, while v2 is strongly reduced in combination with an elongated external valve pair v3 that are joined by a membrane in their midline (Yoshizawa et al., 2006; Mockford, 2018; Li et al., 2022). These features are potential autapomorphies of this infraorder.

The male genitalia of Psocodea consist of paired distal parameres, a median mesomere, a membranous endophallus, and a basal plate with a basal apodeme (Yoshizawa, 2005; Yoshizawa and Johnson, 2005). In some taxa of Trogiomorpha, the genitalia are strongly modified, for instance in Atropetae and Psyllipsocidae (Mockford, 2005, 2011; Yoshizawa et al., 2006; Mockford and García Aldrete, 2010). In Prionoglaridiidae, the phallosome is

present as a cuticular sac with posterolateral processes, a putative apomorphy of the family (Yoshizawa et al., 2006). As the male genitalia in Trogiomorpha are generally relatively well preserved in amber fossils, their investigation could help to solve some controversial phylogenetic issues in this group, for instance whether †Cormopsocidae are the sister group of the remaining Trogiomorpha. The psyllipsocid phallosome is highly complex and a cohesive theory of the homology and evolution of the different components in Psyllipsocidae is presently lacking (Mockford, 2011). Therefore, we propose homology hypotheses only for some elements that we could observe in the newly described fossil species. We have described the male genitalia of a fossil psyllipsocid in some detail for the first time, based on the comparatively well-preserved paratype specimen **CAU-BA-LFY-24001**. Similar to the condition in other described extant psyllipsocids, the phallosome is tightly connected to the hypandrial wall (Mockford, 2011: "hypandrium−phallosome complex") and bears external lateral parameres. The connection between the parameres and the other phallosome components, especially the endophallus, is not visible. The configuration differs from extant *Psyllipsocus* species (Mockford, 2011; Lienhard et al., 2022) by the presence of symmetric paired oval lobes, elements of the hypandrium, that cover the base of the parameres. Other species of *Psyllipsocus* have similar lobes (see Mockford, 2011), but they are not as large as in †*P. mili*.

4.3. Current concepts and questions concerning the systematic relationships of Trogiomorpha

The most recent phylogeny of Trogiomorpha was proposed by Yoshizawa et al. (2006), de Moya et al. (2021) and Li et al. (2022). The suborder is divided into the 3 extant infraorders Prionoglaridetae, Psyllipsocetae, and Atropetae, and the family †Cormopsocidae is placed as their (putative) sister group. We consider Trogiomorpha *sensu lato* as a clade containing all four previously mentioned taxa, and Trogiomorpha *sensu stricto* only comprising the three extant infraorders. The †Cormopsocidae includes the extinct genera †*Cormopsocus*; *Longiglabellus* Wang, Li & Yao, 2021; *Stimulopsocus* Liang & Liu, 2022, and possibly †*Brachyantennum*. The infraorder Prionoglaridetae includes Prionoglarididae, which is possibly paraphyletic (Yoshizawa et al., 2019; de Moya et al., 2021), with the two subfamilies Prionoglaridinae and Speleketorinae. Psyllipsocetae includes only Psyllipsocidae. The infraorder Atropetae includes the extinct empheriids and the three extant families Lepidopsocidae, Psoquillidae and Trogiidae. The monophyly of †Archaeatropidae (Baz and Ortuño, 2000; Cumming and Le Tirant, 2021) is still under debate (Li et al., 2022; Álvarez-Parra et al., 2024; Hakim et al., 2024; this study). We propose the taxon name **Spinaparaprocta** for the unranked group containing Atropetae+Psyllipsocetae. Its monophyly appears to be well supported (Yoshizawa et al., 2006; de Moya et al., 2021; Li et al., 2022), although further morphological and genomic data are necessary. The paraproctal (=anal) spine is a distinctive, putative autapomorphy of this clade (see Yoshizawa et al., 2006; Li et al., 2022; this study).

4.3.1. Parsimony analysis

Most branches had relatively low Bremer support values (Fig. 17, supplementary file S8), showing the scarcity of phylogenetic signal in our current morphological data for fossil Trogiomorpha. †*Brachyantennum* was placed as member of Trogiomorpha and with high statistical support inside of Trogiomorpha (BS = 3). †*Cormopsocus* was placed as sister to *Siamoglaris* Lienhard, 2004 (Prionoglaridinae), but this is likely due to insufficient signal in the data (BS = 1). Psyllipsocidae was split into four groups with †*Annulipsyllipsocus* placed as the first branch, and *Dorypteryx* inside of Atropetae (BS = 1). Atropetae had good statistical support (BS = 3) albeit with inclusion of the morphologically aberrant genus *Dorypteryx*. There was moderate (BS = 1 Trogiidae, BS = 1 Psoquillidae) to relatively high support (BS = 2 Lepidopsocidae) for the monophyly of each of the three extant families of Atropetae, in agreement with results of previous molecular phylogenetic studies (Yoshizawa et al., 2006; de Moya et al., 2021). †*Parapsyllipsocus* was placed in a clade containing Psoquillidae and *Dorypteryx* (Fig. 17), showing that this genus is likely closely related to the psoquilid psocids. Lepidopsocidae and †*Parapsyllipsocus* were nested within "†Empheriidae" (Fig. 17), but the branching pattern in this group is not well resolved (polytomy with BS = 1). In general, the branching pattern obtained in our parsimony analysis (Fig. 17) largely conform with results of previous analyses (Yoshizawa et al., 2006; de Moya et al., 2021; Li et al., 2022). Our morphological dataset likely suffered from a high degree of homoplasy and from missing character states ("?"), leading to a limited resolution of the tree (Fig. 17; supplementary file S8). This also shows clearly that the presently available morphological data for fossil Trogiomorpha are insufficient. Providing new observations for missing character states should be a focus in future studies on fossil psocids.

4.3.2. Bayesian inference

As analyses based on parsimony yielded a phylogeny with low resolution and support values, we additionally used Bayesian inference to assess the uncertainty in our data. The Bayesian analysis with body-only characters (wing characters constrained, Fig. 18A) placed †*Brachyantennum* as sister to Trogiomorpha incl. †Cormopsocidae (BI3: 0.81 BPP). The very low resolution using only wing characters (Fig. 18B) conforms with Yoshizawa and Johnson (2014) who demonstrated a high level of homoplasy for venation characters in Psocomorpha. This underlines the weaker phylogenetic signal in almost entirely wing venation-only matrices due to widespread homoplasy. Our analyses did not reveal the exact position of †*Cormopsocus*, as it was either nested within Prionoglaridetae (Fig. 18A, BI1: 0.65 BPP; Fig. 18B, BI2: 0.67 BPP), in a polytomy of Trogiomorphan taxa outside of Atropetae (Fig. 19A, BI3: 0.62 BPP), or in an almost entirely unresolved polytomy of all ingroup taxa (Fig. 19B, BI4: 0.94 BPP).

The placement of †*Brachyantennum* as sister to the rest of Trogiomorpha is likely, as this monotypic genus has ctenidiobothria on the first tarsomere of the mid- and hindlegs, a character state only present in Trocto- and Psocomorpha (and few atropetans) (see discussion above and SI1). The position of †*Brachyantennum* as sister to the remaining Trogiomorpha is also tentatively supported by our parsimony analysis (Fig. 17). The uncertain position of †*Cormopsocus* is apparently due to the lack of apomorphies linking this taxon with other groups (besides the extended vertex). As previously discussed, Psyllipsocetae might be non-monophyletic albeit with low statistical support in our analyses (Figs. 17−19). We were unable to resolve the deeper phylogeny of Atropetae in any of our analyses, except for the monophyly of its three extant families (Lepidopsocidae, Psoquillidae, Trogiidae) and the inclusion of †*Parapsyllipsocus* into a larger clade with Trogiidae and Psoquillidae (Figs. 17, 18A and 20). In contrast to our MP analysis (Fig. 17), the genera of the empheriids could not be resolved further except for their placement in Atropetae (Figs. 18, 19A and 20). Our analyses revealed the possible non-monophyly of Psyllipsocetae, and also of the empheriids, as well as a sister group relationship between †*Brachyantennum* and the rest of Trogiomorpha. However, it is obvious that more evidence is required for establishing a new family level taxon for †*Brachyantennum* (see also Zhang et al., 2022; Álvarez-Parra et al., 2024).

Possible paraphyly of †Empheriidae was a result in the parsimony analysis of Álvarez-Parra et al. (2024). As these authors

implemented hard constraints on the monophyly of the "†Empheriidae" in their Bayesian analysis, they were not able to confirm this family as a clade. Their analysis resulted in high support for a sister group relationship between the Psyllipsocidae and the extant atropetan clade Lepido-psocidae+(Psoquillidae+-Trogiidae), while the empheriids were placed as sister to this large clade (Álvarez-Parra et al., 2024: fig. 6B). The position of *Psyllipsocus* in the Atropetae (Álvarez-Parra et al., 2024) might have been an artifact due to the strong representation of venation characters in their analysis. The empheriids have apparently preserved more plesiomorphies in their venation compared to Psyllipsocidae or the remaining atropetan families. In contrast to the position of †*Brachyantennum* in our analyses, Álvarez-Parra et al. (2024) placed it within Trogiomorpha as sister to the Spinaparaprocta (parsimony analysis and Bayesian inference). As Álvarez-Parra et al. (2024) did not include any psocodean taxa outside of Trogiomorpha, i.e., no troctomorphan and psocomorphan outgroups, and only added one character ("anal vein in forewing") to the matrix of Li et al. (2022), the dataset is not suitable to clarify the position of this aberrant genus. Several characters of †*Brachyantennum* make a placement as sister to Spinaparaprocta unlikely, such as the presence of ctenidiobothria on tarsomeres of the mid- and hindlegs, well-developed Sc vein on the hindwing, and the absence of swollen, strongly convex laterocervical sclerites (holotype and one additional individual examined by FL). As ventral and dorsal valves are still present in many psyllipsocids (Mockford et al., 2013), it is possible that their reduction occurred several times independently (homoplasy) in Trogiomorpha *s. lat.*, which would reduce the significance of these character states as apomorphies for Trogiomorpha. The dorsal and ventral valves are possibly also reduced in †*Brachyantennum* (Zhang et al., 2022), but more specimens of this species and closely related taxa should be studied before making conclusion on the morphology of the ovipositor in this group. As it is not possible to dissect the genitalia of fossil psocids (except for virtual dissections in well-preserved specimens), it remains unclear whether the dorsal and ventral valves are only reduced in size or truly absent. †*Brachyantennum* and †*Cormopsocus* have preserved the maximum of plesiomorphic features of the wing venation in Psocodea. Therefore, this character system is insufficient for their phylogenetic placement if not used in combination with characters of other body regions.

Álvarez-Parra et al. (2024) supported the synonymization of †Archaeatropidae under †Empheriidae, citing the study by Li et al. (2022) and based on their own results (Álvarez-Parra et al., 2024: p. 193). However, this interpretation is not unambiguously supported by their data. Using parsimony analyses Álvarez-Parra et al. (2024) showed that †Empheriidae is possibly a paraphyletic group, making the synonymization of †Archaeatropidae taxonomically untenable. Following their argumentation, each empheriid clade would warrant family rank under Linnean taxonomy, making †Archaeatropidae (type genus †*Archaeatropos* Baz and Ortuño, 2001) valid again for the genus †*Archaeatropos* (and their putative sister genera). Our own results using Bayesian inference and parsimony analysis also suggest the possible paraphyly of the empheriids. The taxonomic status of †Archaeatropidae is therefore an unresolved question. A better resolved phylogeny of Trogiomorpha based on more well-documented morphological data is required.

4.3.3. Ancestral state estimation

Previous ancestral state reconstructions in Psocodea were used in the context of the morphological transitions in Psocomorpha (Yoshizawa and Johnson, 2014), changes in musculature of the female genitalia (Cheng and Yoshizawa, 2022), the mitochondrial genome arrangement in Psocodea (Yoshizawa et al., 2018), and ancestral hosts of mammalian lice (Johnson et al., 2022). In the present work, we estimated ancestral states for 58 characters across our Bayesian phylogeny. In total, we detected 63 character state transformations across the 9 constrained nodes excluding the outgroup and the basal split between Trogiomorpha and †*Brachyantennum* (Fig. 20). Of these, 20 had good statistical support (BPP $\geq$0.90). Future study with broader taxon sampling is necessary to establish the anatomical groundplan of the order.

Based on our estimates, the absence of ctenidiobothria on the tarsomeres is a potential non-homoplasious apomorphy of Trogiomorpha excluding †*Brachyantennum* (Fig. 20), indicating that the presence likely belongs to the groundplan of Psocodea. The presence of a paraproctal spine and a spur sensillum on the secondary maxillary palpomere were recovered as potential apomorphies of Atropetae (Fig. 20), but not as synapomorphies of Atro-petae+-Psyllipsocetae, as suggested by their presence in some psyllipsocids (Fig. 21). Presence of long and thin external valves (Fig. 20) was already previously inferred as an apomorphy of Atropetae (Yoshizawa et al., 2006). The presence of setae on the forewing membrane appears to be an apomorphy of Atropetae (Fig. 20). Apically pointed fore- and hindwings, an unbranched anal vein in the hindwing, and widely separated lateral ocelli are potential apomorphies of Lepidopsocidae (Fig. 20). Potentially apomorphic characters for the sister group relationship of Psoquillidae and Trogiidae are absence of a cross vein r1-rs in the forewing, a triangular pterostigma and a glabrous forewing membrane (Fig. 20). The reduced forewings and lack of ocelli were identified as apomorphies of Trogiidae (Fig. 20).

4.3.4. Problematic fossils

The phylogenetic placement of some fossils assigned to Trogiomorpha was not adequately evaluated previously (except for a study of Mockford et al., 2013). We attempt for the first time to synthetize the current knowledge on the evolution of the lineage (mostly based on Smithers, 1972; Yoshizawa et al., 2006; Mockford et al., 2013; Li et al., 2022) and provide arguments based on shared apomorphies (or their lack of) and also present the results of Bayesian analyses for a reliable phylogenetic interpretation of these controversial fossils (see summarizing Table 1).

Mockford et al. (2013) suggested a placement of †*Empheriopsis* Vishnyakova, 1975 in Trogiomorpha. We agree with that view as this genus can be reliably placed in a clade Psylli-psocetae-+Atropetae based on the shape of the last maxillary palpomere. The setose forewing membrane described by Vishnyakova (1975) tentatively suggests its placement in the empheriids, as this is a potential apomorphy of this family (Li et al., 2022). However, this character is strongly affected by homoplasy. Our phylogenetic analysis supports a position of this genus inside Atropetae (see Fig. 17–19).

Another controversial fossil genus is †*Parapsyllipsocus* Perrichot, Azar, Néraudeau & Nel, 2003. Previously placed as incertae sedis in Trogiomorpha with possible affinities to Psyllipsocidae (Perrichot et al., 2003; Mockford et al., 2013), this genus remains currently the least understood genus of this suborder concerning its phylogenetic placement. As the fossil specimen is poorly preserved, only few observed characters provide useful information. A distinctive feature is the very long areola postica cell, longer than half of the maximum width of the forewing. This character state was discussed as a possible autapomorphy of Atropetae (Li et al., 2022). Several venation characters differ strongly from conditions found in †Empheriidae and make a placement in this family unlikely according to Perrichot et al. (2003). Placing †*Parapsyllipsocus* in this group would imply far-reaching transformations of the wing venation in this genus. Alternatively, it could be a member of a clade Lepidopsocidae+Psoquillidae+Trogiidae, as suggested by the

proximal Sc vein not connecting with vein R1 in the forewing (Perrichot et al., 2003). The rounded apices of the forewings are incompatible with a placement in the crown group of Lepidopsocidae (Perrichot et al., 2003). The absence of the radial cell in the fossil is a potential synapomorphy with Lepido-psocidae+-Psoquillidae+Trogiidae (Li et al., 2022), making its placement into this clade or as member of the stem group likely. Until further informative characters are identified, we consider this as the best supported hypothesis as our Bayesian analyses (Fig. 18 and 19A) also support a placement inside Atropetae, but with uncertain affinities within this group.

The systematic position of further controversial species assigned to Psyllipsocidae remains unresolved or ambiguous. The Cretaceous Lebanese amber species †*Libanopsyllipsocus alexanderasnitsyni* Azar & Nel, 2011 was placed in the family by Azar and Nel (2011) based on three morphological characters. Two of these features are either diagnostic for Trogiomorpha, i.e., tubular hypopharyngeal filaments separated over their entire length, or Psyllipsocetae, i.e., presence of a nodulus (but see above for problematic aspects of this character). The third character, presence of Pearman's organ, excludes Pachytroctidae. The conclusions of Azar and Nel (2011) were challenged by Mockford et al. (2013), who demonstrated that their interpretations were not valid and do not support a placement in Psyllipsocidae. Furthermore, these authors could show that several diagnostic features of Pachytroctidae, i.e., characters of the wing venation and female terminalia with a T-shaped sclerite and gonapophyses (Azar and Nel, 2011 identified the holotype as male, even though it is obviously a female), suggest a position inside Pachytroctidae. This is also tentatively supported by the wide distance between the hindcoxae (Azar and Nel, 2011: fig. 1), which are generally adjacent or nearly adjacent in Psyllipsocidae (see Fig. 6B and 12B). Notably, the inner sides of the hindcoxae are not in contact with each other in the fossil, a prerequisite for a functioning Pearman's organ. The Pearman's organ is reduced or only present as a small cuticular bulge in Pachytroctidae (Mockford, 2018). The tentative assignment of †*L. alexanderasnitsyni* to Pachytroctidae (Mockford et al., 2013) appears plausible and is adopted here. At least any support for a position of this species inside Psyllipsocidae (Hakim et al., 2018) is lacking.

Zhang et al. (2016) erected a new genus of psyllipsocids, i.e., †*Sinopsyllipsocus,* based on the presence of a conical sensillum on the secondary maxillary palpomere (mx2), and the secondary annulation of flagellomeres. These character states also occur in extant (e.g., *Psyllipsocus siamensis* Lienhard & Yoshizawa, 2022; *Psyllipsocus sarawakensis* Lienhard & Yoshizawa, 2022 [secondary annulation of basalmost flagellomeres]) and extinct species (e.g., †*P. yangi*, †*P. mili*) of *Psyllipsocus*. Aside from this, the erection of a new genus would only be justified if the monophyly of *Psyllipsocus* excluding this new species would be clearly established. The monophyly of the genus *Psyllipsocus* is presently uncertain (Mockford, 2011; Lienhard et al., 2022). However, due to the lack of a modern revision and phylogenetic analyses based on molecular and morphological characters, we prefer to maintain it for now. Consequently, we consider the genus †*Sinopsyllipsocus* as a junior synonym of *Psyllipsocus* (proposed by Liang and Liu, 2021; see also Lienhard, 2023). This is also supported by the apomorphic presence of a long and low areola postica in the forewing in the extinct species. The combination for the species is:

†*Psyllipsocus fushunensis* (Zhang, Nel, Azar & Wang, 2016) **[combination first published by** Liang and Liu, 2021**: p.86]**

As the nodulus is neither a proper diagnostic nor an apomorphic character for *Psyllipsocus*, we assume that †*Khatangia* Vishnyakova, 1975, which lacks this feature, belongs to this genus. This is also suggested by the identical wing venation. A potential apomorphy of †*Khatangia* is the assumed absence of the retinaculum of the wing-coupling apparatus of the forewing (Vishnyakova, 1975). However, it is possible that this structure was overlooked by the authors due to insufficient magnification. Moreover, an autapomorphy would not be sufficient to establish the status as a separate genus, as *Psyllipsocus* would very likely be rendered paraphyletic (see Komarek and Beutel, 2006). A position outside of a clade *Psyllipsocus*, which would justify the status as a separate genus, is not supported by any evidence. Therefore, we treat †*Khatangia* as a junior synonym of *Psyllipsocus*. The new combination for the species is:

†*Psyllipsocus inclusus* (Vishnyakova, 1975) **comb. nov.**

The synonymizations of the genera †*Khatangia* and †*Sinopsyllipsocus* are based on a lack of phylogenetic evidence with respect to *Psyllipsocus*, i.e. the lack of shared apomorphies of this genus excluding the two extinct species. It cannot be excluded that new morphological data will reveal that they in fact belong to different genera than *Psyllipsocus*, but in light of current evidence, we think that treating both genera as synonyms of *Psyllipsocus* is favorable, due to the likely inflation of the number of fossil genera in Psyllipsocidae and also, the purely diagnostic way of looking at these fossil taxa. Both species do not even differ as strongly from "typical" species of *Psyllipsocus*, while species with strongly modified genitalia or attachment structures are still conveniently placed in *Psyllipsocus* (see Mockford, 2011; Lienhard and García Aldrete, 2016; Lienhard et al., 2022). This further indicates the need for a modern phylogeny (see also Lienhard et al., 2022) of Psyllipsocidae using both extant and extinct taxa, as well as morphological and molecular data.

Two venation characters are possibly apomorphic for both species assigned to the genus †*Annulipsyllipsocus*, even though they also occur in other related taxa: broad basiradial and radial cells of the forewing and an anteriorly bulging R1 vein of the radial cell. Nevertheless, a status as a separate genus is also doubtful in this case, as the two species might be more closely related to species of *Psyllipsocus* than to each other (possible synonymy of †*Annulipsyllipsocus* already suggested by Lienhard, 2023). Consequently, the status as a separate genus might render *Psyllipsocus* paraphyletic. The diagnostic characters for †*Annulipsyllipsocus* are annulated flagellomeres, a reduced number of antennomeres, and the previously discussed features of wing venation (Hakim et al., 2018). However, a secondary annulation of flagellomeres also occurs in extinct and extant *Psyllipsocus* species (Liang and Liu, 2021; Lienhard et al., 2022). A reduced number of antennal articles also occurs in †*Psyllipsocus myanmarensis* Jouault, Yoshizawa, Hakim, Huang & Nel, 2021. A triangular pterostigma and pentagonal radial cell without a bulging R1 also occurs in the extant *Psyllipsocus regiomontanus* Mockford, 2011. As the exact placement of the two species is presently unclear, we maintain the present status of †*Annulipsyllipsocus* until a reliable phylogenetic assessment is possible.

Another controversial fossil genus placed in Psyllipsocidae is †*Concavapsocus parallelus* Wang, Li, Ren & Yao, 2019. Considering the shape of the last maxillary palpomere, cylindrical with a tapering apex (Wang et al., 2019; MW pers. obs.), the placement in this family appears questionable. The shape of the lacinial apex also clearly differs from the condition found in Psyllipsocidae. The outer cusp of the apex is rather long (Wang et al., 2019), similar to the laciniae of Amphientometae, whereas it is shorter in Psyllipsocidae and distinctly higher than the inner tine. Wang et al. (2019) observed a putative paraproctal spine, which would suggest a placement in Atropetae+Psyllipsocetae (Spinaparaprocta). However, the position of this structure indicated in drawings (Wang et al., 2019) suggests that it is in fact a thick seta, not the paraproctal spine, which is generally inserted at the apical margin of the paraproct (see Fig. 11B and 14B). The well-developed valvulae v1

and v2 further indicate a placement outside of Spinaparaprocta (but three pairs of well-developed valvulae are present in many *Psyllipsocus*: Mockford, 2011, 2018). The fossil species †*Globopsocus aquilonius* Azar & Engel, 2008 (Azar and Engel, 2008a) is treated here as a species closely related to †*C. parallelus*. This was already indicated by Wang et al. (2019), and both species are very similar in some feature, for instance of the wing venation or genitalia. Therefore, it is possible that †*Concavapsocus* represents a junior synonym of †*Globopsocus*. We remove the genera †*Concavapsocus* and †*Globopsocus* from Psyllipsocidae and place them as **Psocodea incertae sedis** for the time being, as they do not share any apomorphies with any trogiomorphan clades or Spinaparaprocta in particular.

4.3.5. Unreliable characters used in taxonomy and systematics

As mentioned above and by other authors (e.g., Wang et al., 2019), the presence or absence of the nodulus is not a reliable character to assign specimens of Trogiomorpha to a genus, e.g., *Psyllipsocus*, or even to a family, e.g., †Empheriidae. It is recommendable to use a neutral descriptive approach concerning this feature in Trogiomorpha and to focus on the exact distance between both vein tips at the posterior forewing margin. Additionally, the in-flight wing-coupling system should be examined in more detail in future taxonomic and systematic studies on fossil psocid taxa, as this is apparently a phylogenetically valuable character complex, as shown by Ogawa and Yoshizawa (2017). Furthermore, a more consistent use of the established terminology (e.g., as defined by Lienhard, 1998) is needed for an adequate interpretation of the phenotypic evolution of fossil taxa. A consistent use of definitions and a homology-based approach in palaeontology is essential for solid phylogenetic and taxonomic conclusions. As the goal of phylogenetic systematics is to produce a natural system with monophyletic units, one cannot simply use diagnostic characters to place fossil specimens into a preexisting phylogenetic tree. Diagnostic characters are often plesiomorphies or can be prone to homoplasy, and not suitable for phylogenetic reconstruction as already shown by Hennig (1969, p. 25–26). Therefore, placing fossils into a phylogenetic system simply using diagnostic characters is scientifically unsound. A reliable phylogenetic assessment including fossils has to be based on a sound evaluation of morphological characters, using outgroup comparison for clarifying the polarity, i.e. for identifying synapomorphies (Hennig, 1969). Like in Fikáček et al. (2020), robust molecular phylogenies of extant taxa can be used as a framework. Using morphological matrices covering fossil terminals, reliable placements can be achieved using phylogenetic analyses (based on parsimony or Bayesian inference) with a fixed topology but the extinct taxa in question floating freely over the tree (Fikáček et al., 2020), as has also been done here.

4.3.6. A direct link between psocodean evolution and parasitism by mymarommatoid wasps?

As the mymarommatoid wasps, sister group of the extremely species-rich Chalcidoidea (Cruaud et al., 2023), are currently only known as parasites of eggs of trogiomorphan psocids, i.e., Lepidopsocidae (Honsberger et al., 2022), their fossil record and evolutionary origin are possibly closely linked to the origin of crown Psocodea. Trogiomorpha is the first suborder that splits from the remaining psocodeans at around 193 Mya (Early Jurassic), and the origin of crown Trogiomorpha is dated at around 168 Mya (Middle Jurassic) (de Moya et al., 2021). The dated origin of Trogiomorpha coincides with the origin of Mymarommatoidea almost perfectly, which is dated as 174 Mya (Middle Jurassic) (Cruaud et al., 2023; Ulmer et al., 2023). The dating analyses suggest a tight evolutionary link between both groups, in the case of Psocodea possibly restricted to crown Trogiomorpha. Additionally, the results of Cruaud et al. (2023) provide support for the accuracy of the dating analyses of de Moya et al. (2021), in contrast to the argumentation in Jouault et al. (2021). On the other hand, a mid-Cretaceous fossil belonging to the Homilopsocidea was described (Yoshizawa and Yamamoto, 2021), indicating an underestimation of lineage ages for the suborder Psocomorpha by de Moya et al. (2021). As Yoshizawa and Yamamoto (2021) pointed out, more described fossil psocodean taxa, as well as more detailed descriptions will yield improved dating analyses. A similar age for the origin of crown Psocodea (ca. 200 Mya, Early Jurassic) was assessed by Misof et al. (2014), in the first comprehensive phylogenetic analysis of Hexapoda based on transcriptomes. Crown Psocodea are therefore a younger clade than previously estimated (origin ca. 320 Mya, Carboniferous, e.g., Johnson et al., 2018). The origin of Psocodea, and their split from either Holometabola or Condylognatha, likely occurred in the Devonian ca. 400 Mya (Misof et al., 2014; Johnson et al., 2018). There is a conspicuous “taxonomic gap” for stem psocodeans, probably partially caused by preservation biases as psocids are relatively small and soft bodied. Presently no fossil can be unambiguously assigned to this grade (Mockford et al., 2013), with the possible exception of †*Zygopsocus permianus* Tillyard, 1935 (Nel et al., 2011) and a recently discovered incomplete fossil, showing Psocodea-like wing venation, from Middle Triassic deposits in Monte San Giorgio (Switzerland) (Montagna et al., 2024). The forewing venation of †*Westphalopsocus pumilio* Azar, Nel, Engel & Burgoin, 2013 (Nel et al., 2013) differs strongly from the condition found in the entire crown group of Psocodea and also in †*Zygopsocus*. The phylogenetic position remains therefore controversial. It is obviously of great importance to study well preserved adpression fossils of potential stem psocodeans, documenting and evaluating as many morphological features as possible. So far only the wing venation was studied, as it is often the best or even the only preserved character system of rock fossils (Nel et al., 2013). Presently only one described genus preserved as impression fossil from Jurassic limestone can be reliably assigned to crown Psocodea (Azar et al., 2008; Mockford et al., 2013). The discovery of new morphological characters could improve our understanding of the evolution of Psocodea distinctly.

4.4. Methodological considerations and future directions

While slide-mounting or simple observations of amber material usually show the inclusion only from two sides, the strength of μCT scanning and the resulting 3D models are the visualization of the entire body from all perspectives. This includes areas which are usually scarcely visible or not accessible at all, like the posterior head region, the thoracic sclerites, or the genitalia. The most obvious advantage is the non-destructive examination of inner structures. Therefore, the use of μCT and 3D modelling is highly recommendable for investigating extinct groups of Psocodea and other insects. This is especially important for palaeontology where morphology is the only source of phylogenetically relevant information. Using μCT, Richter et al. (2022) could reconstruct almost the complete head anatomy of a Cretaceous ant. Such exceptionally preserved specimens of Psocodea are not available so far. Therefore, searching for fossils of this group with preserved internal soft parts should have high priority. Internal features could contribute to phylogenetic reconstructions including extinct groups, and especially to the understanding of the evolution of the Psocodea. Our analyses based on Bayesian Inference could show that a phenomic approach (see Boudinot, 2019) is recommendable in palaeontology and systematic biology. Analyzing fossils (and extant) species using modern methods such as SR-μCT and 3D reconstructions can yield a larger amount of phenomic data compared to using only photomicrography and light microscopic

observations, and should be used in combination with these traditional methods.

As Psyllipsocidae have retained many ancestral features of Psocodea and Trogiomorpha, they are very useful for elucidating the groundplan of either group. It is important to put these observations into a wider phylogenetic context with other taxa in Trogiomorpha, i.e., †Cormopsocidae (Yoshizawa and Lienhard, 2020) and Prionoglarididae, families presumably also characterized by many retained plesiomorphic features. The groundplan of Psocodea including its stem group is currently largely unexplored and can only be inferred by carefully investigating the morphology of extant and extinct members of the group. Reconstructing the ancestral conditions in Psocodea in the widest sense can help to elucidate evolutionary events in three major clades of Neoptera, Condylognatha, Psocodea and Holometabola (Misof et al., 2014). The comparison of the groundplans of these major lineages (e.g. Peters et al., 2014: larval groundplan of Holometabola) will likely also help to clarify the hitherto ambiguous issue on the monophyly or paraphyly of Paraneoptera (Misof et al., 2014; Johnson et al., 2018).

A very promising recent approach in morphology and anatomy is ontology-based research (Dececchi et al., 2015; Porto et al., 2024). A well-known example is the "Hymenoptera Anatomy Ontology" (HAO, Yoder et al., 2010), which provides a comprehensive atlas on anatomical terms in Hymenoptera. An "ontology for the Anatomy of the Insect Skeleto-Muscular System" was published recently (AISM, Girón et al., 2023), but its scope is limited, as it does not include non-muscular soft tissues (e.g., nervous system, glands, and fat body). The development of an ontology of psocodean anatomy should have high priority as it will greatly facilitate anatomical studies. Moreover, this would also be very useful in the context of the general skeletomuscular ontology of hexapods (Girón et al., 2023) and also future ontologies for different insect orders and including various organs and types of soft tissues. Based on an ontology, phenomics-wide research (Girón et al., 2023; Porto et al., 2024) on Psocodea will become feasible and the morphological terminology standardized. It is likely that ontologies will also gain entry into arthropod palaeontology. Therefore, it will be important to standardize the terminology used for species descriptions of extinct and extant taxa, and also for the anatomical studies of both. We tried to follow the AISM (Girón et al., 2023) for terminology of cuticular structures as these are generally the best-preserved parts of a fossil insect. The consequent use of such an approach would certainly invigorate the investigation of Psocodea in future studies.

5. Conclusions

Our documentation of a Cretaceous *Psyllipsocus* enhances the morphological knowledge of extinct psocodeans with hitherto unknown precision. Synchrotron radiated μCT-scans combined with 3D-reconstructions can dramatically improve the documentation of amber fossils. Our critical discussion of different character systems and current taxonomic approaches revealed serious problems in the morphological and phylogenetic treatment of fossils of Trogiomorpha and other groups of Psocodea. Phylogenetic evaluations strictly based on synapomorphies, and appropriate analytical methods are necessary for a reliable phylogenetic reconstruction involving fossils and extant representatives of Psocodea and other groups. This should also result in a taxonomic approach aiming at a classification not based on intuition and/or diagnostic features, but reflecting phylogenetic relationships, exclusively containing monophyletic taxa. Moreover, a consistent terminology and homology assessments should have high priority. An ontology for Psocodea could greatly facilitate the investigation of the phylogeny and evolution of this neopteran key group.

CRediT authorship contribution statement

Michael Weingardt: Writing – review & editing, Writing – original draft, Visualization, Validation, Resources, Project administration, Methodology, Investigation, Funding acquisition, Data curation, Conceptualization. **Feiyang Liang:** Writing – review & editing, Writing – original draft, Visualization, Validation, Resources, Project administration, Methodology, Investigation, Funding acquisition, Data curation, Conceptualization. **Brendon E. Boudinot:** Writing – review & editing, Writing – original draft, Visualization, Validation, Supervision, Software, Resources, Methodology, Investigation, Funding acquisition, Formal analysis, Data curation. **Jörg U. Hammel:** Writing – review & editing, Writing – original draft, Software, Resources, Methodology. **Bernhard L. Bock:** Writing – review & editing, Writing – original draft, Visualization, Methodology. **Kazunori Yoshizawa:** Writing – review & editing, Writing – original draft, Visualization, Validation, Supervision, Resources, Methodology, Investigation, Funding acquisition. **Rolf G. Beutel:** Writing – review & editing, Writing – original draft, Validation, Supervision, Investigation.

Declaration of competing interest

The authors declare that they have no known competing financial interests or personal relationships that could have appeared to influence the work reported in this paper.

Acknowledgements

MW is supported by the Landesgraduiertenstipendium Jena (2023–). He is very grateful to Dr. Di Li for helping with initializing the contact with FL, which was essential for starting this project. We want to express our gratitude to Dr. Eva-Maria Sadowski (MfN Berlin) and Dr. David Ware (MfN Berlin) for permission to use their photography facility. We would also like to thank Prof. Alexey Polilov (Lomonosov Moscow State University), Prof. Alexander Rasnitsyn (RAS, Moscow) and Dr. Dmitry V. Vassilenko (RAS, Moscow), Anita Wagner (Fachbereichsbibliothek Biologie, Hamburg) for valuable literature. Additionally, MW would like to thank the Biodiversity Heritage Library for their invaluable online scans of taxonomic literature. BEB was supported by fellowships from the Alexander von Humboldt Stiftung and the Peter S. Buck program of the Smithsonian Institute. SR-μCT scanning was supported by the DESY project I-BAG-20210019 and project-20230517 “Lirum Larum Löffelstiel” funded to Hans Pohl at PETRA III at DESY (Hamburg, Germany), a member of the Helmholtz Association (HGF). This research was supported in part through the Maxwell computational resources operated at Deutsches Elektronen-Synchrotron DESY, Hamburg. We are also grateful to the International Amber Association (Gdańsk, Poland) for their FT-IR analysis of the two amber pieces. Lastly, we would like to thank Dr. Charles Lienhard and an anonymous reviewer for significantly improving our manuscript.

Appendix A. Supplementary data

Supplementary data to this article can be found online at https://doi.org/10.1016/j.asd.2025.101409.

References

Aaron, S.F., 1883. Description of new Psocidae in the collection of the American Entomological Society. Trans. Am. Entomol. Soc. proc. Entomol. Sect. Acad. Nat. Sci. 11, 37–40.

Akkari, N., Enghoff, H., Metscher, B.D., 2015. A new dimension in documenting new species: high-detail imaging for myriapod taxonomy and first 3D cybertype of a new millipede species (Diplopoda, Julida, Julidae). PLoS One 10, e0135243. https://doi.org/10.1371/journal.pone.0135243.

Álvarez-Parra, S., Nel, A., Perrichot, V., Jouault, C., 2024. Unravelling the mishmash: A new phylogeny for the family Empheriidae (Psocodea, Trogiomorpha) with a new genus and species from Cretaceous Charentese amber. Arthropod Syst. Phylo. 82, 183–199. https://doi.org/10.3897/asp.82.e114849.

Álvarez-Parra, S., Peñalver, E., Nel, A., Delclòs, X., 2020. The oldest representative of the extant barklice genus *Psyllipsocus* (Psocodea: Trogiomorpha: Psyllipsocidae) from the Cenomanian amber of Myanmar. Cretac. Res. 113, 1–9. https://doi.org/10.1016/j.cretres.2020.104480.

Álvarez-Parra, S., Peñalver, E., Nel, A., Delclòs, X., 2022. New barklice (Psocodea, Trogiomorpha) from Lower Cretaceous Spanish amber. Pap. Palaeontol. 8, e1436. https://doi.org/10.1002/spp2.1436.

Azar, D., Engel, M., 2008. A sphaeropsocid bark louse in Late Cretaceous amber from Siberia (Psocoptera: Sphaeropsocidae). Trans. Kansas Acad. Sci. 111, 141–146. https://doi.org/10.1660/0022-8443(2008)111[141:ASBLIL]2.0.CO;2.

Azar, D., Hajar, L., Indary, C., Nel, A., 2008. Paramesopsocidae, a new Mesozoic psocid family (Insecta: Psocodea "Psocoptera": Psocomorpha). Ann. Soc. Entomol. Fr. 44, 459–470. https://doi.org/10.1080/00379271.2008.10697581.

Azar, D., Huang, D.Y., El-Hajj, L., Cai, C.Y., Nel, A., Maksoud, S., 2017. New Prionoglaridae from Burmese amber (Psocodea: Trogiomorpha: Prionoglaridetae). Cretac. Res. 75, 146–156. https://doi.org/10.1016/j.cretres.2017.03.028.

Azar, D., Nel, A., 2004. Four new Psocoptera from Lebanese amber (Insecta: Psocomorpha: Trogiomorpha). Ann. Soc. Entomol. Fr. 40, 185–192. https://doi.org/10.1080/00379271.2004.10697415.

Azar, D., Nel, A., 2011. The oldest psyllipsocid booklice, in Lower Cretaceous amber from Lebanon (Psocodea, Trogiomorpha, Psocathropetae, Psyllipsocidae). ZooKeys 130, 153–165. https://doi.org/10.3897/zookeys.130.1430.

Badonnel, A., 1934. Recherches sur l'anatomie des Psoques. Bull. Biol. Fr. Belg. Suppl. 18, Paris, pp. 241.

Badonnel, A., 1967. Insectes Psocoptères. Faune de Madagascar 23, 1–235.

Baz, A., Ortuño, V.M., 2000. Archaeatropidae, a new family of Psocoptera from the Cretaceous amber of Alava, Northern Spain. Ann. Entomol. Soc. Am. 93, 367–373. https://doi.org/10.1603/0013-8746(2000)093[0367:AANFOP]2.0.CO;2.

Baz, A., Ortuño, V.M., 2001. New genera and species of empheriids (Psocoptera: Empheriidae) from the Cretaceous amber of Alava, northern Spain. Cretac. Res. 22, 575–584.

Beutel, R.G., Friedrich, F., Ge, S., Yang, X., 2014. Insect Morphology and Phylogeny. De Gruyter, Berlin, Germany, Boston, MA. https://doi.org/10.1515/9783110264043.

Boudinot, B.E., 2019. Toward phylomics in entomology: current systematic and evolutionary morphology. Insect Syst. Divers. 3, 1–4. https://doi.org/10.1093/isd/ixz019.

Boudinot, B.E., Bock, B.L., Weingardt, M., Tröger, D., Batelka, J., Li, D., Richter, A., Pohl, H., Moosdorf, O.T.D., Jandausch, K., Hammel, J.U., Beutel, R.G., 2024. Et latet et lucet: discoveries from the Phyletisches Museum amber and copal collection in Jena, Germany. Dtsch. Entomol. Z. 71, 111–176. https://doi.org/10.3897/dez.71.112433.

Boudinot, B.E., Richter, A., Katzke, J., Chaul, J.C.M., Keller, R.A., Economo, E.P., Beutel, R.G., Yamamoto, S., 2022. Evidence for the evolution of eusociality in stem ants and a systematic revision of †*Gerontoformica* (Hymenoptera: Formicidae). Zool. J. Linn. Soc. 195, 1355–1389. https://doi.org/10.1093/zoolinnean/zlab097.

Cheng, Z., Kamimura, Y., Ferreira, R.L., Lienhard, C., Yoshizawa, K., 2023. Acquisition of novel muscles enabled protruding and retracting mechanisms of female penis in sex-role reversed cave insects. R. Soc. Open Sci. 10. https://doi.org/10.1098/rsos.220471.

Cheng, Z., Yoshizawa, K., 2022. Exploration of the homology among the muscles associated with the female genitalia of the three suborders of Psocodea (Insecta). Arthropod Struct. Dev. 66, 101141. https://doi.org/10.1016/j.asd.2022.101141.

Crampton, G.C., 1926. A comparison of the neck and prothoracic sclerites throught the orders of insects from the standpoint of phylogeny. Trans. Am. Entomol. Soc. 52, 199–248.

Cruaud, A., Rasplus, J.Y., Zhang, J., Burks, R., Delvare, G., Fusu, L., Gumovsky, A., Huber, J.T., Janšta, P., Mitroiu, M.D., Noyes, J.S., van Noort, S., Baker, A., Böhmová, J., Baur, H., Blaimer, B.B., Brady, S.G., Bubeníková, K., Chartois, M., Copeland, R.S., Papilloud, N.D.S., Molin, A.D., Dominguez, C., Gebiola, M., Guerrieri, E., Kresslein, R.L., Krogmann, L., Lemmon, E., Murray, E.A., Nidelet, S., Nieves-Aldrey, J.L., Perry, R.K., Peters, R.S., Polaszek, A., Sauné, L., Torréns, J., Triapitsyn, S., Tselikh, E.V., Yoder, M., Lemmon, A.R., Wolley, J.B., Heraty, J.M., 2023. The Chalcidoidea bush of life: evolutionary history of a massive radiation of minute wasps. Cladistics 40, 34–63. https://doi.org/10.1111/cla.12561.

Cumming, R.T., Le Tirant, S., 2021. Review of the Cretaceous †Archaeatropidae and †Empheriidae and description of a new genus and species from Burmese amber (Psocoptera). Faunitaxys 9, 1–11.

de Moya, R.S., Yoshizawa, K., Walden, K.K.O., Sweet, A.D., Dietrich, C.H., Johnson, K.P., 2021. Phylogenomics of parasitic and nonparasitic lice (Insecta: Psocodea): combining sequence data and exploring compositional bias solutions in next generation data sets. Syst. Biol. 70, 719–738. https://doi.org/10.1093/sysbio/syaa075.

Dececchi, T.A., Balhoff, J.P., Lapp, H., Mabee, P.M., 2015. Toward synthetizing our knowledge of morphology: using ontologies and machine reasoning to extract presence/absence evolutionary phenotypes across studies. Syst. Biol. 64, 936–952. https://doi.org/10.1093/sysbio/syv031.

Enderlein, G., 1906. The scaly winged Copeognatha (Monograph of the Amphientomidae, Lepidopsocidae, and Lepidillidae in relation to their morphology and taxonomy). Spolia Zeylan. 4, 39–122.

Enderlein, G., 1909. Biospeologica. XI. Copeognathen (Erste Reihe). Arch. zool. exp. gen. 5, 533–539.

Enderlein, G., 1911. Die fossilen Copeognathen und ihre Phylogenie. Palaeontographica 58, 279–360.

Enderlein, G., 1912. Über einige hervorragende neue Copeognathen-Gattungen. Zool. Anz. 39, 298–306.

Engelkes, K., Friedrich, F., Hammel, J.U., Haas, A., 2018. A simple setup for episcopic microtomy and a digital image processing workflow to acquire high-quality volume data and 3D surface models of small vertebrates. Zoomorphology 137, 213–228. https://doi.org/10.1007/s00435-017-0386-3.

Fabian, B., Schneeberg, K., Beutel, R.G., 2016. Comparative thoracic anatomy of the wild type and wingless (wg1cn1) mutant of *Drosophila melanogaster* (Diptera). Arthropod Struct. Dev. 45, 611–636. https://doi.org/10.1016/j.asd.2016.10.007.

Fikáček, M., Beutel, R.G., Cai, C., Lawrence, J.F., Newton, A.F., Solodovnikov, A., Ślipiński, A., Thayer, M.K., Yamamoto, S., 2020. Reliable placement of beetle fossils via phylogenetic analyses—Triassic *Leehermania* as a case study (Staphylinidae or Myxophaga?). Syst. Entomol. 45, 175–187. https://doi.org/10.1111/syen.12386.

García Aldrete, A.N., 1984. The Trogiomorpha (Psocoptera), of Chamela, Jalisco, Mexico. Folia Entomol. Mex. 59, 25–69.

García Aldrete, A.N., 2006. New genera of Psocoptera (Insecta), from Mexico, Belize and Ecuador (Psoquillidae, Ptiloneuridae, Lachesillidae). Zootaxa 1319, 1–14. https://doi.org/10.11646/zootaxa.1319.1.1.

Gelman, A., Rubin, D.B., 1992. Inference from iterative simulation using multiple sequences. Stat. Sci. 7, 457–472.

Girón, J.C., Tarasov, S., Antonio, L., Montaña, G., Matentzoglu, N., Smith, A.D., Koch, M., Boudinot, B.E., Bouchard, P., Burks, R., Vogt, L., Yoder, M., Osumi-Sutherland, D., Friedrich, F., Beutel, R.G., Mikó, I., 2023. Formalizing invertebrate morphological data: a descriptive model for cuticle-based skeleto-muscular systems, an ontology for insect anatomy, and their potential applications in biodiversity research and informatics. Syst. Biol. 72, 1084–1100. https://doi.org/10.1093/sysbio/syad025.

Goloboff, P., 1994. NONA: a Tree Searching Program. Tucumán, Argentina.

Goloboff, P.A., Morales, M.E., 2023. TNT version 1.6, with a graphical interface for MacOS and Linux, including new routines in parallel. Cladistics 39, 144–153. https://doi.org/10.1111/cla.12524.

Greving, I., Wilde, F., Ogurreck, M., Herzen, J., Hammel, J.U., Hipp, A., Friedrich, F., Lottermoser, L., Dose, T., Burmester, H., Müller, M., Beckmann, F., 2014. P05 imaging beamline at PETRA III: first results. In: Stuart, R.S. (Ed.), 2014. Proceedings of SPIE 9212 – Development in X-Ray Tomography IX. https://doi.org/10.1117/12.2061768. San Diego, USA, 92120O-8.

Grimaldi, D.A., Engel, M.S., 2005. Evolution of the Insects. Cambridge University Press, Cambridge, USA.

Günther, K.K., 1974. Staubläuse, Psocoptera. Die Tierwelt Deutschlands 61. Gustav Fischer Verlag, Jena, Germany.

Gurney, A.B., 1939. Nomenclatorial notes on Corrodentia, with descriptions of two new species of *Archipsocus*. J. Wash. Acad. Sci. 29, 501–515.

Hagen, H.A., 1865. On some aberrant genera of Psocina. Entomol. Mon. Mag. 2, 148–162.

Hagen, H.A., 1866. Psocinorum et Embidinorum Synopsis synonymica. Verh. K.K. Zool.-Bot. Ges. Wien. 16, 201–222.

Haibel, A., Ogurreck, M., Beckmann, F., Dose, T., Wilde, F., Herzen, J., Müller, M., Schreyer, A., Nazmov, V., Simon, V., Last, A., Mohr, J., 2010. Micro- and nano-tomography at the GKSS imaging beamline at PETRA III. In: Stock, S.R. (Ed.), 2010. Proceedings of SPIE 7804 – Developments in X-Ray Tomography VII, San Diego, USA. https://doi.org/10.1117/12.860852, 78040B.

Hakim, M., Azar, D., Fu, Y.Z., Cai, C.Y., Huang, D.Y., 2021a. A new cormopsocid from mid-Cretaceous Burmese amber (Psocodea: Trogiomorpha: Cormopsocidae). Palaeoentomology 4, 178–185. https://doi.org/10.11646/palaeoentomology.4.2.7.

Hakim, M., Azar, D., Huang, D.Y., 2021b. A new species of Cormopsocidae from Burmese amber (Psocodea; Trogiomorpha). Palaeoentomology 4, 213–217. https://doi.org/10.11646/palaeoentomology.4.3.6.

Hakim, M., Azar, S., Maksoud, S., Huang, D.Y., Azar, D., 2018. New polymorphic psyllipsocids from Burmese amber (Psocodea: Psyllipsocidae). Cretac. Res. 84, 389–400. https://doi.org/10.1016/j.cretres.2017.11.027.

Hakim, M., Azar, D., Huang, D.Y., 2023. First record of fossil psocodeans in copula from mid-Cretaceous Burmese amber. Zootaxa 5396, 74–93. https://doi.org/10.11646/zootaxa.5396.1.13.

Hakim, M., Huang, D.Y., Azar, D., 2024. New genus of Empheriidae (Psocodea; Trogiomorpha) from mid-Cretaceous Burmese amber. Cretac. Res. 154, 105745. https://doi.org/10.1016/j.cretres.2023.105745.

Hallberg, E., Hansson, B.S., 1999. Arthropod sensilla: morphology and phylogenetic considerations. Microsc. Res. Tech. 47, 428–439. https://doi.org/10.1002/(SICI)

1097-0029(19991215)47:6<428::AID-JEMT6>3.0.CO;2-P.
Hennig, W., 1950. Grundzüge einer Theorie der phylogenetischen Systematik. Deutscher Zentralverlag, Berlin, Germany.
Hennig, W., 1966. Phylogenetic Systematics. University of Illinois Press, Urbana, USA.
Hennig, W., 1969. Stammesgeschichte der Insekten. Waldemar Kramer, Frankfurt a. M., Germany.
Heyden, C.H.G., 1850. Zwei neue deutsche Neuropteren-Gattungen. Stett. Ent. Zeit 11, 83–85.
Honsberger, D.N., Huber, J.T., Wright, M.G., 2022. A new *Mymaromma* sp. (Mymarommatoidea, Mymarommatidae) in Hawai'i and first host record for the superfamily. J. Hymenopt. Res. 89, 73–87. https://doi.org/10.3897/jhr.89.77931.
Hopkins, H., Johnson, K.P., Smith, V.S., 2024. Psocodea Species File. https://psocodea.speciesfile.org/.
Huang, D.Y., Bechly, G., Nel, P., Engel, M.S., Prokop, J., Azar, D., Cai, C.Y., van de Kamp, T., Staniczek, A.H., Garrouste, R., Krogmann, L., dos Santos Rolo, T., Baumbach, T., Ohlhoff, R., Shmakov, A.S., Bourgoin, T., Nel, A., 2016. New fossil insect order Permopsocida elucidates major radiation and evolution of suction feeding in hemimetabolous insects (Hexapoda: Acercaria). Sci. Rep. 6, 23004. https://doi.org/10.1038/srep23004.
Imhoff, L., Labram, J.D., 1842. Insekten der Schweiz, vol. 3. Basel.
Johnson, K.P., Dietrich, C.H., Friedrich, F., Beutel, R.G., Wipfler, B., Peters, R.S., Allen, J.M., Petersen, M., Donath, A., Walden, K.K.O., Kozlov, A.M., Podsiadlowski, L., Mayer, C., Meusemann, K., Vasilikopoulos, A., Waterhouse, R.M., Cameron, S.L., Weirauch, C., Swanson, D.R., Percy, D.M., Hardy, N.B., Terry, I., Liu, S., Zhou, X., Misof, B., Robertson, H.M., Yoshizawa, K., 2018. Phylogenomics and the evolution of hemipteroid insects. Proc. Natl. Acad. Sci. U.S.A. 115, 12775–12780. https://doi.org/10.1073/pnas.1815820115.
Johnson, K.P., Matthee, C., Doña, J., 2022. Phylogenomics reveals the origin of mammal lice out of Afrotheria. Nat. Ecol. Evol. 6, 1205–1210. https://doi.org/10.1038/s41559-022-01803-1.
Jouault, C., Yoshizawa, K., Hakim, M., Huang, D., Nel, A., 2021. New psocids (Psocodea: Prionoglarididae, Psyllipsocidae) from Cretaceous Burmese amber deposits. Cretac. Res. 126, 104890. https://doi.org/10.1016/j.cretres.2021.104890.
Kawata, A., Ogawa, N., Yoshizawa, K., 2022. Morphology and phylogenetic significance of the thoracic muscles in Psocodea (Insecta: Paraneoptera). J. Morphol. 283, 14. https://doi.org/10.1002/jmor.21492.
Kawata, A., Ogawa, N., Yoshizawa, K., 2024. Morphology of the pterothoracic musculature in Paraneoptera and its phylogenetic implication (Insecta: Neoptera). J. Morphol. 285, e21712. https://doi.org/10.1002/jmor.21712.
Kolbe, H.J., 1880. Monographie der deutschen Psociden mit besonderer Berücksichtigung der Fauna Westfalens. Jahres-Ber. Westfäl. Prov.-Vereins Wiss. 8, 73–142.
Kolbe, H.J., 1884. Der Entwicklungsgang der Psociden im Individuum und in der Zeit. Berl. Ent. Zeitschr. 28, 35–38.
Kolbe, H.J., 1885. Zur Kenntniss der Psociden-Fauna Madagaskars. Berl. Ent. Zeitschr. 29, 183–192.
Komarek, A., Beutel, R.G., 2006. Problems in taxonomy and suggestions for a standardized description of new insect taxa. Entomol. Probl. 36, 55–70.
Lewis, P.O., 2001. A likelihood approach to estimating phylogeny from discrete morphological character data. Syst. Biol. 50, 913–925.
Li, F., 2002. Psocoptera of China. Nat. Natural Sci. Found., Science Press, Beijing, China, xlvi + pp. 1976 (two volumes).
Li, S., Wang, Q., Ren, D., Yao, Y., 2020. New genus and species of Empheriidae (Psocodea: Trogiomorpha) from mid-Cretaceous amber of northern Myanmar. Cretac. Res. 110, 104421. https://doi.org/10.1016/j.cretres.2020.104421.
Li, S., Yoshizawa, K., Wang, Q., Ren, D., Bai, M., Yao, Y., 2022. New genus and species of Empheriidae (Insecta: Psocodea: Trogiomorpha) and their implication for the phylogeny of infraorder Atropetae. Front. Ecol. Evol. 10, 907903. https://doi.org/10.3389/fevo.2022.907903.
Liang, F., Li, S., Liu, X., Bai, M., Yao, Y., 2022. A new genus and species of the family Archaeatropidae (Psocodea: Trogiomorpha) from mid-Cretaceous amber of northern Myanmar. Cretac. Res. 138, 105233. https://doi.org/10.1016/j.cretres.2022.105233.
Liang, F., Liu, X., 2021. A new species of *Psyllipsocus* (Psocodea: Trogiomorpha: Psyllipsocidae) from the mid-Cretaceous amber of Myanmar. Zootaxa 5072, 81–87. https://doi.org/10.11646/zootaxa.5072.1.9.
Liang, F., Liu, X., 2022. A new genus and species of the family Cormopsocidae (Psocodea: Trogiomorpha) from mid-Cretaceous amber of Myanmar. Cretac. Res. 130, 105049. https://doi.org/10.1016/j.cretres.2021.105049.
Liang, F., Liu, X., 2024. Systematic revision and molecular phylogenetics refine the generic classification of the bark louse family Stenopsocidae (Insecta: Psocodea: Psocomorpha). Arthropod Syst. Phylog. 82, 433–446. https://doi.org/10.3897/asp.82.e114349.
Lienhard, C., 1988. Vorarbeiten zu einer Psocopteren-Fauna der Westpaläarktis. IV. Die Gattung *Prionoglaris* Enderlein (Psocoptera: Prionoglarididae). Mitt. Schweiz. Entomol. Ges. 61, 89–108.
Lienhard, C., 1998. Psocoptères euro-méditerranéens. Faune de France 83. Fédération Française des Sociétés de Sciences Naturelles, Paris.
Lienhard, C., 2000. A new genus of Prionoglarididae from a Namibian cave (Insecta: Psocoptera). Rev. Suisse Zool. 107, 871–882.
Lienhard, C., 2004. *Siamoglaris zebrina* gen. n., sp. n., the first representative of Prionoglarididae from the Oriental Region (Insecta: Psocoptera). Rev. Suisse Zool. 111, 865–875.
Lienhard, C., 2007. Description of a new African genus and a new tribe of Speleketorinae (Psocodea: 'Psocoptera': Prionoglarididae). Rev. Suisse Zool. 114, 441–469.
Lienhard, C., 2023. Nine new species of *Psyllipsocus* Selys-Longchamps, 1872 (Psocodea: 'Psocoptera': Psyllipsocidae) from Southeast Asia. Rev. Suisse Zool. 130, 59–76. https://doi.org/10.35929/RSZ.0088.
Lienhard, C., Carmo, T.O., Ferreira, R.L., 2010b. A new genus of Sensitibillini from Brazilian caves (Psocodea: 'Psocoptera': Prionoglarididae). Rev. Suisse Zool. 117, 611–635. https://doi.org/10.5962/bhl.part.117600.
Lienhard, C., Ferreira, R.L., 2013. Three new species of *Psyllipsocus* (Psocodea: 'Psocoptera': Psyllipsocidae) from Brazilian caves with description of a novel structure interpreted as a male accessory genital organ. Rev. Suisse Zool. 120, 421–443.
Lienhard, C., Ferreira, R.L., 2014. New species of *Psyllipsocus* from Brazilian caves (Psocodea: 'Psocoptera': Psyllipsocidae). Rev. Suisse Zool. 121, 211–246.
Lienhard, C., García Aldrete, A.N., 2016. An extraordinary new species of *Psyllipsocus* (Psocodea: 'Psocoptera': Psyllipsocidae) from the Biosphere Reserve Sierra de Huautla, Morelos, Mexico. Rev. Suisse Zool. 123, 105–112.
Lienhard, C., Holuša, O., Grafitti, G., 2010a. Two new cave-dwelling Prionoglarididae from Venezuela and Namibia (Psocodea: 'Psocoptera': Trogiomorpha). Rev. Suisse Zool. 117, 185–197. https://doi.org/10.5962/bhl.part.117780.
Lienhard, C., Smithers, C.N., 2002. Psocoptera (Insecta) – World Catalogue and Bibliography. Instrumenta Biodiversitatis V. Muséum d'Histoire naturelle, Geneva.
Lienhard, C., Yoshizawa, K., 2019. Authorities for family-group names of psocids (Insecta: Psocodea: 'Psocoptera'). Psocid News 21, 3–9.
Lienhard, C., Yoshizawa, K., Ghani, I.A., 2022. Oriental *Psyllipsocus* (Psocodea: 'Psocoptera': Psyllipsocidae): Checklist, new records and description of four new species from Southeast Asia. Insecta Matsumurana N. S. 78, 1–19.
Löns, H., 1911. Das Geheimnis der Bücherlaus. In: Der Zweckmäßige Meyer. Ein Schnurriges Buch, pp. 117–123. Sponholtz, Hannover, Germany.
Lyal, C.H.C., 1983. Taxonomy, Phylogeny and Host Relationships of the Trichodectidae (Phthiraptera: Ischnocera), vol. 1. University of London, Imperial College, UK. PhD thesis.
Lytaev, P., Hipp, A., Lottermoser, L., Herzen, J., Greving, I., Khokhriakov, I., Meyer-Loges, S., Plewka, J., Burmester, J., Caselle, M., Vogelgesang, M., Chilingaryan, S., Kopmann, A., Balzer, M., Schreyer, A., Beckmann, F., 2014. Characterization of the CCD and CMOS cameras for grating-based phase-contrast tomography. Proc. SPIE 9212, 921218. https://doi.org/10.1117/12.2061389.
McLachlan, R., 1899. *Ectopsocus briggsi*, a new genus and species of Psocidae found in England. Entomol. Mon. Mag. 35, 277–278.
Mickoleit, E., 1963. Untersuchungen zur Kopfmorphologie der Thysanopteren. Zool. Jahrb., Abt. Anat. Ontog. Tiere 81, 101–150.
Misof, B., Liu, S., Meusemann, K., Peters, R.S., Donath, A., Mayer, C., Frandsen, P.B., Ware, J., Flouri, T., Beutel, R.G., Niehuis, O., Petersen, M., Izquierdo-Carrasco, F., Wappler, T., Rust, J., Aberer, A.J., Aspöck, U., Aspöck, H., Bartel, D., Blanke, A., Berger, S., Böhm, A., Buckley, T.R., Calcott, B., Chen, J., Friedrich, F., Fukui, M., Fujita, M., Greve, C., Grobe, P., Gu, S., Huang, Y., Jermiin, L.S., Kawahara, A.Y., Krogmann, L., Kubiak, M., Lanfear, R., Letsch, H., Li, Y., Li, Z., Li, J., Lu, H., Machida, R., Mashimo, Y., Kapli, P., McKenna, D.D., Meng, G., Nakagaji, Y., Navarrete-Heredia, J.L., Ott, M., Ou, Y., Pass, G., Podsiadlowski, L., Pohl, H., von Reumont, B.M., Schütte, K., Sekiya, K., Shimizu, S., Slipinski, A., Stamatakis, A., Song, W., Su, X., Szucsich, N.U., Tan, M., Tan, X., Tang, M., Tang, J., Timelthaler, G., Tomizuka, S., Trautwein, M., Tong, X., Uchifune, T., Walzl, M.G., Wiegmann, B.M., Wilbrandt, J., Wipfler, B., Wong, T.K.F., Wu, Q., Wu, G., Xie, Y., Yang, S., Yang, Q., Yeates, D.K., Yoshizawa, K., Zhang, Q., Zhang, R., Zhang, W., Zhang, Y., Zhao, J., Zhou, C., Zhou, L., Ziesmann, T., Zou, S., Li, Y., Xu, X., Zhang, Y., Yang, H., Wang, J., Wang, J., Kjer, K.M., Zhou, X., 2014. Phylogenomics resolves the timing and pattern of insect evolution. Science 346, 763–767. https://doi.org/10.1126/science.1257570.
Mockford, E.L., 1967. The electrentomoid psocids (Psocoptera). Psyche 74, 118–165. https://doi.org/10.1155/1967/862560.
Mockford, E.L., 1969. Fossil insects of the order Psocoptera from tertiary amber of Chiapas, Mexico. J. Paleontol. 43, 1267–1273.
Mockford, E.L., 1974. The *Echmepteryx hageni* complex (Psocoptera: Lepidopsocidae) in Florida. Fla. Entomol. 57, 255–267.
Mockford, E.L., 1984. Two new species of *Speleketor* from southern California with comments on the taxonomic position of the genus (Psocoptera: Prionoglaridae). Southwest. Nat. 29, 169–179.
Mockford, E.L., 1993. North American Psocoptera (Insecta). Taylor & Francis Group, Boca Raton, Florida, USA.
Mockford, E.L., 2005. A new genus of perientomine psocids (Psocoptera: Lepidopsocidae) with a review of the perientomine genera. Trans. Am. Entomol. Soc. 131, 201–215.
Mockford, E.L., 2011. New species of *Psyllipsocus* (Psocoptera: Psyllipsocidae) from North and Middle America with a Key to the Species of the Region. Trans. Am. Entomol. Soc. 137, 15–47. https://doi.org/10.3157/061.137.0115.
Mockford, E.L., 2018. Biodiversity of Psocoptera. In: Foottit, R.G., Adler, P.A. (Eds.), Insect Biodiversity: Science and Society, II. John Wiley & Sons. https://doi.org/10.1002/9781118945582.ch16.
Mockford, E.L., García Aldrete, A.N., 2010. *Psoquilla infuscate* Badonnel (Psocoptera: Psoquillidae) in the Western Hemisphere with description of the male and brachypterous form. Zootaxa 2618, 61–68.
Mockford, E.L., Lienhard, C., Yoshizawa, K., 2013. Revised classification of 'Psocoptera' from Cretaceous amber, a reassessment of published information. Insecta Matsumurana N. S. 69, 1–26.

Montagna, M., Magoga, G., Stockar, R., Magnani, F., 2024. The contribution of the Middle Triassic fossil assemblage of Monte San Giorgio to insect evolution. Commun. Biol. 7, 1023. https://doi.org/10.1038/s42003-024-06678-5.
Mound, L.A., 2009. New taxa and new records of Australian Panchaetothripinae (Thysanoptera, Thripidae). Zootaxa 2292, 25–33. https://doi.org/10.11646/zootaxa.2292.1.3.
Nel, A., Prokop, J., De Ploëg, G., Miller, J., 2005. New Psocoptera (Insecta) from the lowermost Eocene amber of Oise, France. J. Syst. Palaeontol. 3, 371–391. https://doi.org/10.1017/S1477201905001598.
Nel, A., Prokop, J., Nel, P., Grandcolas, P., Huang, D.Y., Roques, P., Guilbert, E., Dostál, O., Szwedo, J., 2011. Traits and evolution of wing venation pattern in paraneopteran insects. J. Morphol. 273, 480–506.
Nel, A., Roques, P., Nel, P., Prokin, A.A., Bourgoin, T., Prokop, J., Szwedo, J., Azar, D., Desutter-Grandcolas, L., Wappler, T., Garrouste, R., Coty, D., Huang, D., Engel, M.S., Kirejtshuk, A.G., 2013. The earliest known holometabolous insects. Nature 503, 257–261. https://doi.org/10.1038/nature12629.
New, T.R., Lienhard, C., 2007. The Psocoptera of Tropical South East Asia. Fauna Malesiana Handbook 6. Brill, Leiden, Netherlands, Boston, USA. https://doi.org/10.1163/ej.9789004149021.i-290.
Nixon, K.C., 2002. WinClada, Version 1.00.08. Ithaca, New York, USA.
Ogawa, N., Yoshizawa, K., 2017. Origin and transformation of the in-flight wing-coupling structure in Psocodea (Insecta: Psocodea). J. Morphol. 279, 517–530. https://doi.org/10.1002/jmor.20785.
O'Leary, M.A., Kaufman, S.G., 2012. MorphoBank 3.0: Web application for morphological phylogenetics and taxonomy. http://www.morphobank.org.
Paleobiology, Database, 2024. The Paleobiology database: revealing the history of life. https://paleobiodb.org/#/.
Perrichot, V., Azar, D., Néraudeau, D., Nel, A., 2003. New Psocoptera in the Early Cretaceous amber of SW France and Lebanon (Insecta: Psocoptera: Trogiomorpha). Geol. Mag. 140, 669–683.
Peters, R.S., Meusemann, K., Petersen, M., Mayer, C., Wilbrandt, J., Ziesmann, T., Donath, A., Kjer, K.M., Aspöck, U., Aspöck, H., Aberer, A., Stamatakis, A., Friedrich, F., Hünefeld, F., Niehuis, O., Beutel, R.G., Misof, B., 2014. The evolutionary history of holometabolous insects inferred from transcriptome-based phylogeny and comprehensive morphological data. BMC Ecol. Evol.. 14, 52.
Pictet, F.J., 1854. In: Traité de Paléontologie ou Histoire naturelle des Animaux fossiles considérés dans leurs Rapports zoologiques et géologiques, second ed., vol. 2. Psocoptera, Paris.
Pohl, H., Wipfler, B., Grimaldi, D., Beckmann, F., Beutel, R.G., 2010. Reconstructing the anatomy of the 42-million-year-old fossil †*Mengea tertiaria* (Insecta, Strepsiptera). Naturwissenschaften 97, 855–859. https://doi.org/10.1007/s00114-010-0703-x.
Porto, D.S., Uyeda, J., Mikó, I., Tarasov, S., 2024. ontophylo: reconstructing the evolutionary dynamics of phenomes using new ontology-informed phylogenetic methods. Methods Ecol. Evol. https://doi.org/10.1111/2041-210X.14283.
Pravdin, T., 1932. Beiträge zur Kenntnis des Baues des Kopfes der Insekten. Zum Bau des Kopfes der Copeognathen. Zool. Zh. 11, 159–172.
Rambaut, A., 2010. FigTree v1.2.1. Institute of Evolutionary Biology. University of Edinburgh, Edinburgh. http://tree.bio.ed.ac.uk/software/figtree/.
Rambaut, A., Drummond, A.J., Xie, D., Baele, G., Suchard, M.A., 2018. Posterior summarization in Bayesian phylogenetics using Tracer 1.7. Syst. Biol. 67, 901–904.
Ribaga, C., 1899. Descrizione di un nuovo genere e di una nuova specie di Psocidi trovato in Italia. Riv. Patol. Vegetale 8, 156–159.
Richter, A., Boudinot, B., Yamamoto, S., Katzke, J., Beutel, R.G., 2022. The first reconstruction of the head anatomy of a Cretaceous insect, †*Gerontoformica gracilis* (Hymenoptera: Formicidae), and the early evolution of ants. Insect Syst. Divers. 6, 1–80. https://doi.org/10.1093/isd/ixac013.
Roesler, R., 1940. Neue und wenig bekannte Copeognathengattungen. I. Zool. Anz 129, 225–243.
Roesler, R., 1943. Über einige Copeognathengenera. Stett. Ent. Zeit. 104, 1–14.
Roesler, R., 1944. Die Gattungen der Copeognathen. Stett. Ent. Zeit. 105, 117–166.
Ronquist, F., Teslenko, M., Van Der Mark, P., Ayres, D.L., Darling, A., Höhna, S., Larget, B., Liu, L., Suchard, M.A., Huelsenbeck, J.P., 2012. MrBayes 3.2: efficient Bayesian phylogenetic inference and model choice across a large model space. Syst. Biol. 61, 539–542.
Rudolph, D., 1982. Occurrence, properties and biological implications of the active uptake of water vapour from the atmosphere in Psocoptera. J. Insect Physiol. 28, 111–121. https://doi.org/10.1016/0022-1910(82)90118-4.
Schindelin, J., Arganda-Carreras, I., Frise, E., Kaynig, V., Longair, M., Pietzsch, T., Preibisch, S., Rueden, C., Saalfeld, S., Schmid, B., Tinevez, J.Y., White, D.J., Hartenstein, V., Eliceiri, K., Tomancak, P., Cardona, A., 2012. Fiji: an open source platform for biological-image analysis. Nat. Methods 9, 671–675. https://doi.org/10.1038/nmeth.2019.
Seeger, W., 1975. Funktionsmorphologie an Spezialbildungen der Fühlergeißel von Psocoptera und anderen Paraneoptera (Insecta); Psocodea als monophyletische Gruppe. Z. Morphol. Tiere 81, 137–159. https://doi.org/10.1007/BF00301153.
Selys-Longchamps, M.E., 1872. Notes on two new genera of Psocidae. Entomol. Mon. Mag. 9, 145–146. https://doi.org/10.5962/bhl.part.4728.
Shi, G., Grimaldi, D.A., Harlow, G.E., Wang, J., Wang, J., Yang, M., Lei, W., Li, Q., Li, X., 2012. Age constraint on Burmese amber based on U-Pb dating of zircons. Cretac. Res. 37, 155–163. https://doi.org/10.1016/j.cretres.2012.03.014.
Smith, D.S., 1964. The structure and development of flightless Coleoptera: a light and electron microscopic study of the wings, thoracic exoskeleton and rudimentary flight musculature. J. Morphol. 114, 107–184. https://doi.org/10.1002/jmor.1051140106.
Smithers, C.N., 1958. A new genus and species of domestic psocid (Psocoptera) from Rhodesia. J. Entomol. Soc. South Afr. 21, 113–116.
Smithers, C.N., 1972. The classification and phylogeny of the Psocoptera. Aust. Mus. Mem. 14, 1–349. https://doi.org/10.3853/j.0067-1967.14.1972.424.
Solórzano-Kraemer, M.M., Perrichot, V., Soriano, C., Damgaard, J., 2014. Fossil water striders in Cretaceous French amber (Heteroptera: Gerromorpha: Mesoveliidae and Veliidae). Syst. Entomol. 39, 590–605. https://doi.org/10.1111/syen.12077.
Sommermann, K.M., 1956. Two new species of *Rhyopsocus* (Psocoptera) from the U.S.A., with notes on the bionomics of one household species. J. Wash. Acad. Sci. 46, 145–149.
Tillyard, R.J., 1935. Upper Permian Insects of New South Wales III. The order Copeognatha. Proc. Linn. Soc. N. S. W. 60, 265–279.
Ulmer, J.M., Janšta, P., Azar, D., Krogmann, L., 2023. At the dawn of megadiversity – Protoitidae, a new family of Chalcidoidea (Hymenoptera) from Lower Cretaceous Lebanese amber. J. Hymenopt. Res. 96, 879–924. https://doi.org/10.3897/jhr.96.105494.
Vishnyakova, V.N., 1975. Psocoptera in late-Cretaceous insect-bearing resins from the Taimyr. Entomol. Obozr. 54, 63–75.
von Kéler, S., 1966. Zur Mechanik der Nahrungsaufnahme bei Corrodentien. Z. Parasitenkd. 27, 64–79.
Wang, Q., Li, S., Ren, D., Yao, Y., 2021. New genus and species of †Cormopsocidae (Psocodea: Trogiomorpha) from mid-Cretaceous amber of northern Myanmar. Cretac. Res. 128, 104992. https://doi.org/10.1016/j.cretres.2021.104992.
Wang, R., Li, S., Ren, D., Yao, Y., 2019. New genus and species of the Psyllipsocidae (Psocodae: Trogiomorpha) from mid-Cretaceous Burmese amber. Cretac. Res. 104, 1–5. https://doi.org/10.1016/j.cretres.2019.07.008.
Weber, H., 1938. Beiträge zur Kenntnis der Überordnung Psocoidea. I. Die Labialdrüsen der Copeognathen. Zool. Jahrb., Abt. Anat. Ontog. Tiere 64, 243–286.
Weber, H., 1969. Die Elefantenlaus *Haematomyzus elefantis* Piaget 1869. Versuch einer konstruktionsmorphologischen Analyse. Zoologica. 116. E. Schweizerbart'sche Verlagsbuchhandlung, Stuttgart, Germany.
Weidner, H., 1972. 16. Copeognatha. Handbuch der Zoologie, IV. Band: Arthropoda – 2. Hälfte: Insecta, Berlin, Germany, pp. 94.
Wilde, F., Ogurreck, M., Greving, I., Hammel, J.U., Beckmann, F., Hipp, A., Lottermoser, L., Khokhriakov, I., Lytaev, P., Dose, T., Burmester, H., Müller, M., Schreyer, A., 2016. Micro-CT at the imaging beamline P05 at PETRA III. AIP Conf. Proc. 1741, 030035. https://doi.org/10.1063/1.4952858.
Yang, Z., 1994. Maximum likelihood phylogenetic estimation from DNA sequences with variable rates over sites: approximate methods. J. Mol. Evol. 39, 306–314.
Yoder, M.J., Mikó, I., Seltmann, K.C., Bertone, M.A., Deans, A.R., 2010. A gross ontology for Hymenoptera. PLoS One 5, e15991. https://doi.org/10.1371/journal.pone.
Yoshizawa, K., 2002. Phylogeny and higher classification of suborder Psocomorpha (Insecta: Psocodea: 'Psocoptera'). Zool. J. Linn. Soc. 136, 371–400. https://doi.org/10.1046/j.1096-3642.2002.00036.x.
Yoshizawa, K., 2005. Morphology of Psocomorpha (Psocodea: 'Psocoptera'). Insecta Matsumurana N. S. 62, 1–44.
Yoshizawa, K., Ferreira, R.L., Kamimura, Y., Lienhard, C., 2014. Female penis, male vagina, and their correlated evolution in a cave insect. Curr. Biol. 24, 1006–1010. https://doi.org/10.1016/j.cub.2014.03.022.
Yoshizawa, K., Ferreira, R.L., Lienhard, C., Kamimura, Y., 2019. Why did a female penis evolve in a small group of cave insects? Bioessays 41, 1900005. https://doi.org/10.1002/bies.201900005.
Yoshizawa, K., Johnson, K.P., 2005. Morphology of male genitalia in lice and their relatives and phylogenetic implications. Syst. Entomol. 31, 350–361. https://doi.org/10.1111/j.1365-3113.2005.00323.x.
Yoshizawa, K., Johnson, K.P., 2014. Phylogeny of the suborder Psocomorpha: congruence and incongruence between morphology and molecular data (Insecta: Psocodea: 'Psocoptera'). Zool. J. Linn. Soc. 171, 716–731. https://doi.org/10.1111/zoj.12157.
Yoshizawa, K., Johnson, K.P., Sweet, A.D., Yao, I., Ferreira, R.L., Cameron, S.L., 2018. Mitochondrial phylogenomics and genome rearrangements in the barklice (Insecta: Psocodea). Mol. Phylogenet. Evol. 119, 118–127. https://doi.org/10.1016/j.ympev.2017.10.014.
Yoshizawa, K., Lienhard, C., 2016. Bridging the gap between chewing and sucking in the hemipteroid insects: new insights from Cretaceous amber. Zootaxa 4079, 229–245. https://doi.org/10.11646/zootaxa.4079.2.5.
Yoshizawa, K., Lienhard, C., 2020. †Cormopsocidae: A new family of the suborder Trogiomorpha (Insecta: Psocodea) from Burmese amber. Entomol. Sci. 23, 208–215. https://doi.org/10.1111/ens.12414.
Yoshizawa, K., Lienhard, C., Johnson, K.P., 2006. Molecular systematics of the suborder Trogiomorpha (Insecta: Psocodea: 'Psocoptera'). Zool. J. Linn. Soc. 146, 287–299. https://doi.org/10.1111/j.1096-3642.2006.00207.x.
Yoshizawa, K., Saigusa, T., 2003. Reinterpretations of clypeus and maxilla in

Psocoptera, and their significance in phylogeny of Paraneoptera (Insecta: Neoptera). Acta Zool. 84, 33–40. https://doi.org/10.1046/j.1463-6395.2003.00127.x.
Yoshizawa, K., Yamamoto, S., 2021. The earliest fossil record of the suborder Psocomorpha (Insecta: Psocodea) from mid-Cretaceous Burmese amber with description of a new genus and species. Insecta Matsum. New Series 77, 1–15.
Zhang, Q.Q., Nel, A., Azar, D., Wang, B., 2016. New Chinese psocids from Eocene Fushun amber (Insecta: Psocodea). Alcheringa 40, 1–7. https://doi.org/10.1080/03115518.2016.1144952.
Zhang, X., Liang, F., Liu, X., 2022. A new genus and species of the suborder Trogiomorpha (Insecta, Psocodea) from mid-Cretaceous amber of Myanmar. Insects 13, 1064. https://doi.org/10.3390/insects13111064.